

## CHAPTER 1

# Complex Dynamics: Chaos, Fractals, the Mandelbrot Set, and More

RICH STANKEWITZ (text and applet design), JIM ROLF (applet coding and design)

### 1.1. Introduction

This chapter introduces *complex dynamics*, an area of mathematics that continues to inspire much ongoing research and experimentation. The goal of this chapter is not to give a comprehensive or step-by-step approach to this topic, but rather to get the reader engaged with the general notions, questions, and techniques of the area – but even more so, to encourage the reader to actively pose as well as pursue their own questions. To better understand the nature and purpose of this text, the reader should be sure to read the Introduction before proceeding.

Dynamics, in general, is the study of mathematical “systems” that change over time, i.e., *dynamical* systems. For example, consider a particular Newtonian model for the motion of the planets in our solar system. Here the mathematical “system” is a collection of variables corresponding to the location and velocity of each of the planets relative to the sun, and this system changes over time according to Newton’s laws of motion. Thus, as it turns out, one can describe the *process* by which the system evolves (i.e., the rules of how the system changes over time) by differential equations relating all the system variables to each other and to Newton’s laws of motion.

Many dynamical systems can be described similarly. Such examples include the population of bacteria in a petri dish, the weather in Muncie, IN (temperature, pressure, and wind velocity, to be more precise), the global temperature of the earth, and the flight of a paper airplane that you might toss across the room. The models for such dynamical systems all have a set of system variables, and some rule or set of equations that describes the process of how these variables change over time. The values of such variables at any particular moment in time  $t$  is called the *state* of the system at time  $t$ .

Knowing the *initial state* of the system (e.g., today’s location and velocity of each planet), we often try to analyze the equations which describe how the system variables change over time in order to the answer such questions as: What will the state of the system be tomorrow? next week? next year? 100 years from now? Will the system in

the long run settle into some sort of equilibrium? Will small changes or errors in our knowledge of the initial state only lead to small changes or errors in the system at some future time, or will such a small initial error lead to huge errors in the future? Such natural questions about one's ability to predict future states of a dynamical system have led to some very useful results of practical importance – and some very beautiful mathematics.

The famous physicist Richard P. Feynman has a quote regarding a common attitude towards the important question of a dynamical system's predictability, or lack thereof ([15], p. 9): “Physicists like to think that all you have to do is say, these are the conditions, now what happens next?” Unfortunately (or fortunately, depending on your perspective) there are many systems which we cannot adequately “solve” for the purposes of making useful predictions, and so “what happens next?”, a question taken to mean asking what happens well into the future, is simply a question that we cannot answer. Frequently this is due to an inability to find the right pattern, or to “solve” some differential equation. For these systems there is hope that someone in the future (maybe you!) will come along and find a clever way to solve such problems. With such solutions one can then predict the future of these systems and apply their predictions to the real world. But for a large class of systems there is no hope of *ever* being able to predict, with any *useful accuracy*, what such a system will behave like in the future. What's astounding is that, for these systems, it is not a matter of finding the right clever “solution”. In fact, we sometimes even have what we thought was a great solution, a formula even, but there is a problem with applying this formula to the real world.

The heart of this problem is that we have only solved a model, an approximation to the real world, and as an approximation we have to accept the fact that there will be some (hopefully small) error built into the setup of our model. The problem creeps in because of two issues that may arise in certain systems: (1) we can never pinpoint the initial conditions *exactly*, and (2) *any* approximation (or error) to the initial conditions leads to errors in our long term predictions so large that we cannot have any confidence at all in our application of our prediction to the real world. Such systems are called *chaotic*, a term you will explore and even be asked to *mathematically define* further into this text. Even though such systems do not allow for precise answers to some of the questions scientist like to ask, much can be gained from studying them.

In this chapter we will study certain so-called “simple” chaotic systems that can be analyzed using the tools of complex analysis. We do this because such systems are of interest in their own right, but also because it will lead to understanding fundamental principles of incredibly complicated systems, like those mentioned above. The dynamical systems we focus on are *discrete iterative* systems, which are in some sense the easiest kind of dynamical systems. For these, time is represented by a natural number  $n$ , and there is no need to solve a differential equation to determine the system's state down the road - one simply needs to repeatedly apply a function. Furthermore, the states of our systems are described not by a large number of variables (as are needed to

represent all the positions and velocities of the all the planets), but just a single complex variable. The system is then called iterative because the state  $z_n$  of the system at time  $n$  will evolve according to the rule  $z_{n+1} = f(z_n)$  where  $f$  is a complex valued function. Thus, given an initial state, computing the future state  $z_n$  is just a simple matter of computing the values  $z_1 = f(z_0)$ ,  $z_2 = f(z_1) = f(f(z_0))$ ,  $z_3 = f(z_2) = f(f(f(z_0)))$ , and so on. But don't be fooled, *predicting* the behavior of the sequence of states  $z_n$  (e.g., deciding if this sequence  $z_n$  converges or not), an altogether different problem, is by no means simple!

In this chapter we investigate several types of discrete iterative systems which make use of tools from complex function theory, including Newton's method, polynomial iteration, exponential iteration, and trigonometric iteration. We also consider what happens when such systems are perturbed by changing a parameter, thus leading us into what is called bifurcation theory. There are, however, many ways to perturb a system and in the concluding section we describe two such ways: perturbation with a pole and random dynamics. We begin, however, with perhaps the most familiar discrete dynamical system, Newton's method.

Although we are not studying the above mentioned "real world" dynamical systems directly, we should keep in mind that these systems exhibit many of the same behaviors as the systems we do study. In fact, much of the same phenomena we encounter here have direct analogs in flavor, if not in a strict mathematical sense, in the millions of dynamical systems you may encounter everyday.

### **How to use this chapter**

The sections of this chapter can, of course, be worked through in the order presented. However, one wishing to proceed to Section 1.3 more quickly may do so by skipping all of Section 1.2 with the exceptions of Sections 1.2.3 and 1.2.6. Also, Section 1.6 may be skipped by anyone not wishing to investigate the dynamics of transcendental entire maps. Reading the entire chapter and working on several additional exercises as well as large/small projects would suit a 3 credit hour 15 week semester reading course. However, one looking for a 2-3 week group or individual project for the end of the semester in an undergraduate complex variables course could pursue either A) Section 1.2 or B) Sections 1.2.3 and 1.2.6 together with Section 1.3.

Appendix A on page 407 contains a notation page, as well as a brief exposition of results from a standard undergraduate complex variables course. The reader should use it for reference as needed. Appendix B on page 420 contains a review, and perhaps, a brief introduction to a few new concepts related to the Riemann sphere. These concepts are very necessary for this chapter, and so the reader should expect to work through all of Appendix B; however, it is not necessary that it be completed in full before beginning this chapter. There are also three chapter appendices which begin on page 96 providing added information relevant to just this chapter.

This chapter will utilize the following applets which can be accessed at <http://rstantkewitz.iweb.bsu.edu/DynamicsApplets.htm>.

1. *Real Newton Method Applet* - is used to visualize the real-valued Newton's method.

2. *Complex Newton Method Applet* - is used to visualize the complex-valued Newton's method.

3. *Real Function Iterator Applet* - is used for iterating any real function, and seeing the orbit displayed as a numerical list and as points plotted on a number line.

4. *Complex Function Iterator Applet* - is used for iterating any complex function, and seeing the orbit displayed as a numerical list and as points plotted in the complex plane.

5. *Cubic Polynomial Complex Newton Method Applet* - is used for exploring the attracting basins for Newton's method applied to the family of cubic polynomials  $p_\rho(z) = z(z - 1)(z - \rho)$ .

6. *Global Complex Iteration Applet for Polynomials* - is used to draw the basin of infinity for any polynomial.

7. *Mandelbrot Set Builder Applet* - is used to illustrate how the Mandelbrot set is constructed.

8. *Parameter Plane and Julia Set Applet* - is used for investigating both the parameter plane and dynamic plane pictures for the families of functions  $z^2 + c$ ,  $z^d + c$ ,  $ce^z$ ,  $c \sin(z)$ ,  $c \cos(z)$ , and  $z^d + c/z^m$ .

## 1.2. Newton's Method

Solving equations, finding solutions to ordinary differential equations, finding eigenvalues of a matrix - all of these are very important mathematical procedures. However, each of these can be done *exactly*<sup>1</sup> only in very restrictive cases. When we come across a situation that is not one of these special cases, often the solution must be *approximated* via a numerical method, instead of computed *exactly*. And often, the numerical method is iterative in nature.

For example, consider the problem of finding a *root* of a complex valued function  $f(z)$ , i.e., a value  $\alpha$  such that  $f(\alpha) = 0$ . If the function is the quadratic  $f(z) = az^2 + bz + c$  where  $a \neq 0$ , then there are two roots given by the quadratic formula  $\alpha_\pm = (-b \pm \sqrt{b^2 - 4ac})/2a$ . If the function is a cubic or quartic polynomial, then there also exists formulas (or, more precisely, procedures) for *exactly* finding the roots. However, if  $f(z)$  is a quintic polynomial  $f(z) = az^5 + bz^4 + cz^3 + dz^2 + ez + h$ , then there is not, in general, a procedure that will *exactly* find any of its roots.<sup>2</sup> The same is true for many so-called transcendental functions such as  $h(z) = \cos z - z$  and  $g(z) = e^z - 4z$ .

---

<sup>1</sup>By computing a value *exactly* we usually mean being able to express the value in terms of standard mathematical operations and functions, e.g.,  $\sqrt{\cos(\pi/12)}$ .

<sup>2</sup>Note that any polynomial  $p(z)$  of degree  $n$  has, by the Fundamental Theorem of Algebra,  $n$  roots in the complex plane. However, this theorem does not help us to actually find them.

In such cases, one often must give up on finding *exact* roots and resort to *approximation* methods.

When considering real valued functions of a real variable, there are approximation methods for root finding based on the Intermediate Value Theorem, such as the bisection method. When considering a complex valued function  $f(z)$ , one can sometimes approximate a root of  $f$  using Rouché's Theorem (see [1], p. 294). Specifically, if  $f$  and  $g$  are analytic on and inside a simple closed curve  $C$  with  $|f| > |g|$  on  $C$ , then  $f$  and  $f + g$  have the same number of zeroes (counting multiplicities) inside  $C$ . Hence, if  $g$  can be chosen such that  $f + g$  has a known root inside of  $C$ , then so must  $f$ . However, even if  $f$  is a nice function (e.g., a polynomial), this can often be a difficult method to implement (and still hope to find good estimates). So we look for a better method. One of the best methods to apply in either situation (real or complex) is Newton's method. Often it allows one to approximate roots with extreme accuracy and extreme speed, if we have access to a computer. In this section we examine Newton's method for both real valued and complex valued functions, with the goal of understanding when it will succeed and when it will fail.

**1.2.1. Real Newton's Method.** If one seeks to find a root  $\alpha$  of a differentiable real valued function  $f(x)$  defined for a real variable  $x$ , then one can apply Newton's method as follows. We start with an initial guess  $x_0$  **close to**  $\alpha$  and define  $x_1 = x_0 - \frac{f(x_0)}{f'(x_0)}$ ,  $x_2 = x_1 - \frac{f(x_1)}{f'(x_1)}$ ,  $x_3 = x_2 - \frac{f(x_2)}{f'(x_2)}$ , and, in general,  $x_{n+1} = x_n - \frac{f(x_n)}{f'(x_n)}$ .

The geometric reasoning behind Newton's method, as illustrated in Figure 1.1, is as follows: Given an approximation  $x_0$  to the root  $\alpha$ , one considers a linear function  $\tilde{f}(x)$  which approximates the function  $f(x)$  near  $x_0$ . The best linear approximation in this case will be given by the first order approximation  $\tilde{f}(x) = f(x_0) + f'(x_0)(x - x_0)$  whose graph is the tangent line  $L$  to the graph of  $f(x)$  at the point  $x_0$ . The root of the approximating function  $\tilde{f}(x)$ , i.e., the  $x$ -intercept of  $L$ , is then the definition of  $x_1$ .

EXERCISE 1.1. Before going on, compute  $\tilde{f}(x)$  for  $f(x) = x^3 - 2x$  and  $x_0 = 2$  as in Figure 1.1. Then use  $\tilde{f}(x)$  to find the equation of the tangent line  $L$  and also check that  $x_1$ , given by the above formula, is the  $x$ -intercept of  $L$ . **Try it out!**

EXERCISE 1.2. Verify that for general  $f(x)$  the formula given for  $\tilde{f}(x)$  has a root at  $x_1$  as defined above. **Try it out!**

In general (as illustrated in Figure 1.1), we *expect* that this root  $x_1$  of  $\tilde{f}(x)$  will be a better approximation to  $\alpha$ , the sought after root of  $f(x)$ , than the initial guess  $x_0$ . This process is repeated now using  $x_1$  as the initial guess to generate a new, hopefully improved, approximation  $x_2$ . We then iterate this process, i.e., apply this procedure over and over again, to generate successive approximations  $x_n$ , for  $n = 0, 1, 2, \dots$ . For various reasons it will be useful for us to express this process in terms of iteration of the following function.

DEFINITION 1.3. The function  $F(x) = x - \frac{f(x)}{f'(x)}$  is called the *Newton Map* for  $f$ .

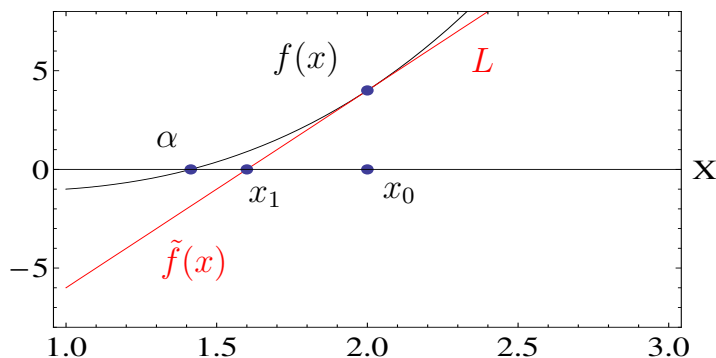


FIGURE 1.1. An illustration of the first step in Newton’s method where  $f(x) = x^3 - 2x$  and  $x_0 = 2$ . Newton’s method can be succinctly described as “from  $x_0$  move to the graph of  $f(x)$ , slide along the tangent until you hit the  $x$ -axis, and then repeat”.

Thus, the *orbit*, i.e., sequence of iterates  $F(x_0), F(F(x_0)), F(F(F(x_0))), \dots$ , is the same as the sequence  $x_n$  generated above, and it will be proven that  $x_n$  converges to the sought after root  $\alpha$  whenever our original guess  $x_0$  is “close enough” to  $\alpha$  (see Proposition 1.21). Of course, this issue of what does it mean to be “close enough” is very important. We will come back to this later (see Remark 1.24), but we first explore this method with some examples.

EXAMPLE 1.4. Consider  $f(x) = x^2 - 3x + 2 = (x - 1)(x - 2)$ , which clearly has roots at 1 and at 2. Let’s apply Newton’s method to see how it works. We first compute the Newton Map for  $f$  which is  $F(x) = x - \frac{x^2 - 3x + 2}{2x - 3} = \frac{x^2 - 2}{2x - 3}$ . If we make an initial guess  $x_0 = 0.5$ , then using your calculator (do this now) you can compute  $x_1 = F(x_0) = 0.875, x_2 = F(F(x_0)) = F(x_1) = 0.9875$ , and  $x_3 = F(F(F(x_0))) = F(x_2) = 0.99984756$ . Since using the calculator is drudgery and computers are so efficient at such tasks, we have created a *Real Newton Method Applet* for you to use. Use this now to confirm the calculations above and then, by taking many iterates of the Newton map using this applet, convince yourself that with the *initial value* (a term we use interchangeably with the terms *seed value* and *starting point*)  $x_0 = 0.5$ , we have  $x_n \rightarrow 1$ . **Try it out!**

Now use the *Real Newton Method Applet* to determine the behavior using an initial guess  $x_0 = 3$ . **Try it out!**

What you learned above is that some initial guesses for  $x_0$  find the root 1 (i.e., have the corresponding  $x_n$  limit to 1) while other initial guesses find the root 2. This begs the question: Given an initial guess  $x_0$ , how do we know which root it will find?

EXPLORATION 1.5. Make an intelligent prediction about which seed values for  $x_0$  in Example 1.4 will find the root 1 and which will find the root 2. Are there any seed values for which Newton's method fails to find either root? Experiment with the *Real Newton Method Applet* to test your prediction. **Try it out!**

EXPLORATION 1.6. Using the function  $f(x) = x(x-1)(x+1)$  determine the Newton Map for  $f$  and then analyze Newton's method using different initial guesses for  $x_0$  in the *Real Newton Method Applet*. Describe (as best as you can) the set of seed values for  $x_0$  which find the root -1, and then do the same for for the roots 0, and 1. **Try it out!**

**1.2.2. Global Picture of Real Newton Method Dynamics.** Identifying how the orbits of *all* seed values behave, as you attempted in Explorations 1.5 and 1.6, is what we mean by looking at the *global* dynamics of Newton's method. In some cases, this can be done without too much work, but in other cases, it turns out to be very complicated. In order to help with one labor intensive approach to this problem, use the **Graph basins of attraction** feature in the *Real Newton Method Applet* to display by using different colors which initial guesses will "find" which roots of  $f(x)$  when Newton's method is applied.

EXERCISE 1.7. For each of Explorations 1.5 and 1.6, use the *Real Newton Method Applet* to get a one picture snapshot of what the dynamics of Newton's method are for *all* starting values. **Try it out!**

What you see when using the *Real Newton Method Applet* with  $f(x) = (x-1)(x-2)$  is, perhaps, what one might expect. The initial values which are closer to the root at 1 will find 1, and the initial values which are closer to the root at 2 will find 2. One should also check that Newton's method fails when the initial value  $x_0 = 1.5$  is used. *Analytically* we see this in the formula because  $f'(1.5) = 0$  leads to a zero in the denominator when one attempts to calculate  $x_1$ . *Geometrically* we see this by noting that the tangent line at  $x_0 = 1.5$  becomes horizontal, never crosses the  $x$ -axis, and thus leaves  $x_1$  undefined. We can also understand this *dynamically*, at least in a heuristic way. The point 1.5 separates those points which are pulled or attracted to 1 and those points which are attracted to 2, and so by an informal use of symmetry, it would *seem* that something must fail to work out at exactly  $x_0 = 1.5$ .

Though this reasoning is informal, it does seem to capture an important idea at play here. As a rule, we encourage the reader to often make use of and even create your own heuristic ideas to explain or describe mathematics. Sometimes it's hard to be formal with all of your mathematical ideas. But don't let that stop you from thinking of and sharing great mathematical thoughts, even if you can't make them precise or formal. Some of the best mathematics, if not all mathematics, starts off as raw unformed ideas with no foundation whatsoever in formalism. Later, one can (and should) try to be formal with their ideas.

The case when  $f(x) = x(x - 1)(x + 1)$  is much different from the quadratic case. It is not simply that a seed for Newton's method will find the root it is nearest to. For example,  $x_0 = 0.55$  will find the root at  $-1$ , even though it is closer to both the roots at  $0$  and  $1$ . Indeed, in this case the set of initial guesses on the real line is divided into intricate regions of points that find the various roots. In fact, if you zoom in near the point  $x = 0.4472135951871958$  you will see a cascade of ever shrinking and alternating colored intervals of blue and turquoise (see Figure 1.2). It turns out, in fact, that this pattern goes on forever (see Small Project 1.8). Use the **Zoom** feature of the *Real Newton Method Applet* to observe this.

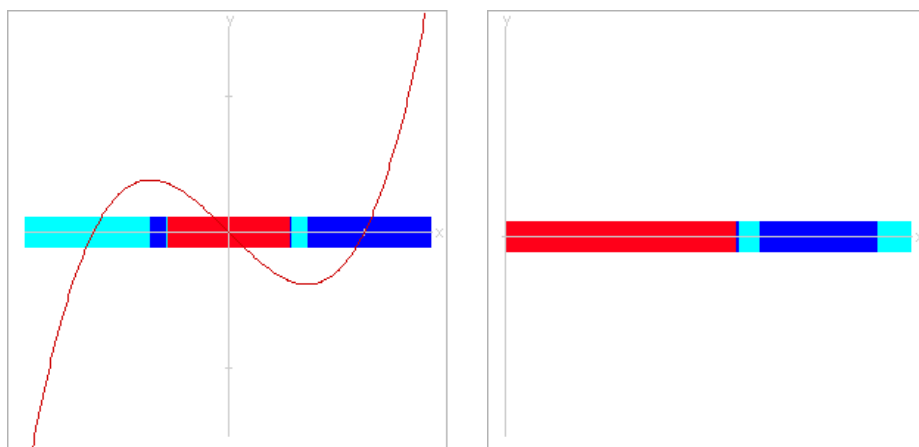


FIGURE 1.2. On the left is a cascade of intervals in the global picture of Newton method dynamics for  $f(x) = x(x - 1)(x + 1)$ , and on the right is a magnification centered at  $x = 0.4472135951871958$ .

**SMALL PROJECT 1.8.** Prove the existence of the infinite cascade of ever shrinking and alternating colored intervals of blue and turquoise found in Figure 1.2. Hint: First use the applet to understand what each of these colored intervals means dynamically, and then try to give a proof for what you witness in the applet.

So we see that Newton's method gets really complicated to understand globally when we switch from a quadratic to a cubic, specifically from  $f(x) = (x - 1)(x - 2)$  to  $f(x) = x(x - 1)(x + 1)$ . This begs the questions: Why? How? Is there a way to know when a system will necessarily be simple or complicated ahead of time?

Answers will come from taking the advice of Jacques Hadamard who once said, "The shortest path between two truths in the real domain passes through the complex domain." So let's look at Newton's method applied to complex valued functions of a complex variable. There are many wonderful theorems and structures at our disposal when we consider complex analytic maps instead of mere real valued differentiable maps. Let's take advantage of some of these.



Before we investigate Newton's method applied to complex valued functions, however, we first take some time to develop some important concepts that we'll need, not just to understand Newton's method, but also any kind of iterative dynamics.

**1.2.3. Orbits, Examples, and Fixed Points.** The general questions we consider in iterative dynamical systems concern describing and predicting what we shall call *orbits*. Let  $g$  be a function mapping its domain set  $\text{domain}(g)$  into itself,<sup>3</sup> which we take to be a subset of the Riemann sphere<sup>4</sup>  $\overline{\mathbb{C}}$ . We then denote the  $n$ th iterate of  $g$  by  $g^n$ . Thus  $g^n(z) = (g \circ \cdots \circ g)(z)$  where the function  $g$  is applied  $n$  times, e.g.,  $g^3(z) = g(g(g(z)))$ . Note that in this chapter  $g^3(z)$  does NOT denote the value  $g(z)$  raised to the third power, which would instead be denoted  $[g(z)]^3$ . We also define  $g^0$  to be the identity map, i.e.,  $g^0(z) = z$ . Furthermore, for any starting (seed) value  $z_0 \in \text{domain}(g)$ , the sequence of points  $z_n = g^n(z_0)$ , for  $n = 1, 2, 3, \dots$ , is called the **orbit** of  $z_0$  (under the map  $g$ ).

When trying to predict the behavior of the evolution of a seed value, we inquire about such things as: Does the orbit converge, fall into a repeating pattern, show no signs of following any pattern at all? What happens for different starting points  $z_0$ ? Do we get the same (or even similar) behavior if we choose starting points near  $z_0$ ? We keep these questions in mind as we consider the following examples.

EXAMPLE 1.9. Say  $f(x) = e^x$  for all  $x \in \mathbb{R}$ . Thus the iterates are  $f^0(x) = x$ ,  $f^1(x) = e^x$ ,  $f^2(x) = e^{e^x}$ ,  $f^3(x) = e^{e^{e^x}}$ , and so on. Experiment with this on the *Real Function Iterator Applet* to convince yourself that  $f^n(x) \rightarrow +\infty$  no matter what  $x \in \mathbb{R}$  we start with. Additional Exercise 1.155 asks for a formal proof.

EXAMPLE 1.10. Let  $f(x) = \sin x$  where  $x \in \mathbb{R}$  is given in radians. Experiment with this on the *Real Function Iterator Applet* to convince yourself that  $f^n(x) \rightarrow 0$  for *any* real number  $x$ . Additional Exercise 1.156 asks for a formal proof.

EXAMPLE 1.11. Let  $f(x) = \cos x$  where  $x \in \mathbb{R}$  is given in radians. Experiment with this on the *Real Function Iterator Applet* to convince yourself that  $f^n(x) \rightarrow 0.739085\dots$  for *any* real number  $x$ . Additional Exercise 1.157 asks for a formal proof.

EXAMPLE 1.12. Let  $f(x) = x^2 - 1$  and  $x_0 = 0.9$ . Use the *Real Function Iterator Applet* to convince yourself that the *tail end* of the orbit  $x_n = f^n(0.9)$  *appears* to oscillate back and forth between 0 and  $-1$ .

EXAMPLE 1.13. Let  $f(x) = 4x(1-x)$  and  $x_0 = 0.2$ . Use the *Real Function Iterator Applet* to see that the orbit  $x_n = f^n(0.2)$  *appears* to have no pattern to it at all, even after the first 25,000 orbit points are plotted. Zoom in on the orbit points to see how it *appears* that they are *dense* in the interval  $[0, 1]$ , that is, for every open interval  $(a, b)$  which meets  $[0, 1]$ , there is some orbit point  $x_n \in (a, b)$ .

<sup>3</sup>The **domain set** of a function  $g$  is the set of possible inputs and is denoted  $\text{domain}(g)$ .

<sup>4</sup>The Riemann sphere  $\overline{\mathbb{C}}$  is the natural setting for the functions in this chapter, and so the reader needs to be familiar with all the material in Appendix B starting on page 420.

Though many types of behavior can be exhibited in orbits, we wish to focus on one special type for the moment. In each of Examples 1.9, 1.10 and 1.11, we see that there is a point which “attracts” the orbits of many points in the domain of the function. This is a fundamental notion (and is at the heart of what we witnessed in the Newton’s method examples) and so we provide the following definition.

**DEFINITION 1.14 (Attracting Basin).** Let  $w \in \overline{\mathbb{C}}$ . For any complex valued function  $g$  mapping its domain set into itself, we define the *attracting basin* of  $w$  (also called *basin of attraction*) under the function  $g$ , to be the set  $A_g(w)$  of all seed values whose orbit limits to the point  $w$ , i.e.,  $A_g(w) = \{z \in \text{domain}(g) : g^n(z) \rightarrow w\}$ .

Note that the point  $w$  in the above definition does not necessarily have to lie  $\text{domain}(g)$  (as in Example 1.9). However, if  $w \in \text{domain}(g)$  and  $g$  is continuous (as in Examples 1.10 and 1.11), then the following result shows that  $w$  must necessarily be a **fixed point** of  $g$ , i.e.,  $g(w) = w$ , whenever  $A_g(w)$  is non-empty.

**THEOREM 1.15.** Let  $f : \text{domain}(f) \rightarrow \text{domain}(f)$  be a continuous map where  $\text{domain}(f) \subseteq \overline{\mathbb{C}}$ . Suppose  $a$  and  $x_0$  are both in  $\text{domain}(f)$  and  $f^n(x_0) \rightarrow a$ . Then  $f(a) = a$ .

**PROOF.** Since the sequence  $f^n(x_0) \rightarrow a$  and  $f$  is continuous at  $a$ , we must have  $f(a) = f(\lim_{n \rightarrow \infty} f^n(x_0)) = \lim_{n \rightarrow \infty} f(f^n(x_0)) = \lim_{n \rightarrow \infty} f^{n+1}(x_0) = a$ .  $\square$

Fixed points play a major role in dynamical systems and so we will be careful to pay special attention to them whenever they arise. In particular, we note from our previous examples that roots of  $f$  always *appear* to be fixed points of the corresponding Newton map  $F(z)$ , a fact we formally prove in Proposition 1.21. Additional Exercise 1.159 will shed some light on the extent to which the converse holds.

We call the fixed points in Examples 1.10 and 1.11 *attracting* fixed points because seed values near the the respective fixed points will iterate toward the respective fixed points. In order to be more precise we give a formal definition, but before we do, we remind the reader of a key relationship between the Euclidean metric on  $\mathbb{C}$  and spherical metric  $\sigma$  on  $\overline{\mathbb{C}}$ , which is stated in Proposition B.7 on page 425. Namely, for points  $z, w \in \mathbb{C}$ , we have  $|z| > |w|$  if and only if  $\sigma(z, \infty) < \sigma(w, \infty)$ .

**DEFINITION 1.16 (Attracting Fixed Point).** Let  $f$  be a map from its domain set  $\Omega \subseteq \overline{\mathbb{C}}$  into itself (note that  $\Omega$  could be a subset of  $\mathbb{R}$ ).

(a) We call a (finite) fixed point  $a \in \mathbb{C}$  an *attracting fixed point* of  $f$  if there exists a neighborhood  $U$  of  $a$  such that for any point  $z \in \Omega \cap U \setminus \{a\}$ , we have  $|f(z) - a| < |z - a|$ , i.e., the action of  $f$  is to move each point in  $\Omega \cap U \setminus \{a\}$  *closer to*  $a$ .

(b) Suppose  $f(\infty) = \infty$ . We call  $\infty$  an *attracting fixed point* of  $f$  if there exists a neighborhood  $U \subseteq \overline{\mathbb{C}}$  of  $\infty$  such that for any point  $z \in \Omega \cap U \setminus \{\infty\}$ , we have  $|f(z)| > |z|$ , i.e., the action of  $f$  is to move each point in  $\Omega \cap U \setminus \{\infty\}$  *closer to*  $\infty$  (as measured by the spherical metric).

In Definition 1.16(a) we used the Euclidean metric to describe when the action of  $f$  moves points closer to  $a$ , but we could have equivalently used the spherical metric for this purpose by writing  $\sigma(f(z), a) < \sigma(z, a)$ . The reader should become comfortable with understanding when the particular metric used in a definition or result could equivalently be changed to another standard metric. We will often make use of the simplest metric at our disposal, relying on the reader to know when another metric could also be used. A good way to try to become comfortable with this concept is to frequently consider how sets appear when visualized in the flat plane  $\mathbb{C}$  and in the sphere  $\bar{\mathbb{C}}$ . The reader will find an exposition of this material in Appendix B on page 420.

If  $a$  is an attracting fixed point of a continuous map  $f$ , then there necessarily exists some neighborhood  $U$  of  $a$  such that  $U \subseteq A_f(a)$ . The proof of this does not require that  $f$  be (real or complex) differentiable at  $a$ , but without such a differentiability condition the proof is more technical. Since we are only interested in specific differentiable functions in this chapter, we provide the proof only for the case that  $|f'(a)| < 1$  (see Theorem 1.18 below).

REMARK 1.17. It is worth noting the curious fact that it may be the case that  $f$  has a fixed point  $a'$  such that  $A_f(a')$  contains a whole neighborhood of  $a'$  without  $a'$  being attracting according to Definition 1.16 (see Example 1.50).

THEOREM 1.18. Suppose  $\Omega \subseteq \mathbb{R}$  or  $\Omega \subseteq \mathbb{C}$ . Let  $f : \Omega \rightarrow \Omega$  be such that  $f(a) = a$  and  $|f'(a)| < 1$ . Then  $a$  is an attracting fixed point of  $f$ . Furthermore, there exists some  $\epsilon > 0$  such that<sup>5</sup>  $\Delta(a, \epsilon) \cap \Omega \subseteq A_f(a)$ .

Note that the proof given below applies equally well to both cases  $\Omega \subseteq \mathbb{R}$  or  $\Omega \subseteq \mathbb{C}$ , where  $f'$  denotes, respectively, the real or complex derivative.

PROOF. Since  $|f'(a)| < 1$  we may select some  $\beta$  such that  $|f'(a)| < \beta < 1$ . Since, by definition,  $f'(a) = \lim_{z \rightarrow a} \frac{f(z) - f(a)}{z - a}$ , there exists  $\epsilon > 0$  such that for any  $z \in \Omega \setminus \{a\}$  for which  $|z - a| < \epsilon$ , we have

$$\left| \frac{f(z) - a}{z - a} \right| = \left| \frac{f(z) - f(a)}{z - a} \right| < \beta.$$

Hence for  $z \in \Omega$  with  $|z - a| < \epsilon$ , we know that  $|f(z) - a| \leq \beta|z - a| < \epsilon$ . This says that for points  $z$  near  $a$  (within a distance of  $\epsilon$ ), the function  $f$  moves  $z$  closer to  $a$  by a factor of at least  $\beta < 1$ . Hence  $a$  is an attracting fixed point by Definition 1.16. If we then iterate the map  $f$  at  $z$ , generating the orbit of  $z$ , we know that each application of  $f$  takes the corresponding orbit point a step closer to  $a$  (by a factor of  $\beta$ ). Hence we may use induction to show that  $|f^n(z) - a| \leq \beta^n|z - a| \leq \beta^n\epsilon \rightarrow 0$  whenever  $z \in \Omega$  with  $|z - a| < \epsilon$ . Thus  $\Delta(a, \epsilon) \cap \Omega \subseteq A_f(a)$ .  $\square$

<sup>5</sup>Here,  $\Delta(z_0, r) = \{z \in \mathbb{C} : |z - z_0| < r\}$  is the open Euclidean disk with center  $z_0$  and radius  $r$ .

REMARK 1.19. Note that the smaller the value of  $|f'(a)|$  (and hence the smaller the value of  $\beta$  may be chosen) in the above theorem, the faster the convergence is. In particular, if  $f(a) = a$  and  $f'(a) = 0$ , then the  $\beta$  in the above proof can be taken to be extremely small leading to very fast convergence. Hence, in such a case the fixed point  $a$  is called *super attracting*.

EXAMPLE 1.20. Use the *Real Function Iterator Applet* to compare the rates of convergence given by the following maps. For  $f(x) = \sin x$  consider the rate at which  $f^n(\frac{1}{2})$  converges to 0. For  $g(x) = x^2$  consider the rate at which  $g^n(\frac{1}{2})$  converges to 0. For  $h(x) = \frac{1}{2}x$  consider the rate at which  $h^n(\frac{1}{2})$  converges to 0. Now compare the absolute value of the derivative at each function's fixed point and note the correspondence with Remark 1.19. **Try it out!**

By Theorem 1.18, in order to check if a fixed point is attracting, one can simply check the absolute value (or modulus) of the derivative at the fixed point. Note that in Example 1.11 one has  $|f'(0.739085\dots)| < 1$  which proves that this fixed point is indeed attracting. When considering the Newton's method dynamics, it appears, in each of the cases we explored experimentally, that the roots of  $f$  are attracting fixed points for the Newton map  $F$ . In fact, this is exactly the case, and we will prove this in Proposition 1.21 by showing that  $|F'| < 1$  at each root of  $f$ . But before we do, we give a word of caution.

We must be a bit careful with the use of Theorem 1.18 since it is not, in general, an if and only if statement. Consider the fixed point  $a = 0$  for the map  $f(x) = \sin x$  in Example 1.10. Here  $f'(0) = 1$ , but this function *as a real map*, defined only for all real numbers  $x$ , does have a genuine attracting fixed point at  $a = 0$  (see Additional Exercise 1.156). However, if we consider the *complex map*  $g(z) = \sin z$ , defined for all complex numbers  $z$ , the fixed point  $a = 0$  is no longer attracting. Indeed,  $g^n(\pm i\epsilon) \rightarrow \infty$  for any  $\epsilon > 0$ . The reader is asked to prove this formally in Additional Exercise 1.158. However, the reader can see this illustrated by using the *Complex Function Iterator Applet*. **Try it out!**

**1.2.4. Complex Newton's Method.** We now return to our investigation of the dynamics of Newton's method when we allow our variables and output values to be complex valued. As we saw with many earlier examples, our experimentation with the applets suggest that the Newton map always has an attracting fixed point at each root of  $f$ . We can now carefully state and prove this fact in both the real and complex cases.

PROPOSITION 1.21 (Attracting Property of Newton's Method). Given any non-constant *real analytic*<sup>6</sup> or complex analytic function  $f$  with a root at  $\alpha \in \mathbb{C}$ , the point  $\alpha$  is an attracting fixed point of the Newton map  $F$  and thus there exists  $r > 0$  such

<sup>6</sup>A real valued function of a real variable is said to be *real analytic* if it possesses derivatives of all orders and agrees with its Taylor series in a neighborhood of every point in its domain set.

that all points within a distance  $r$  of  $\alpha$  are necessarily in the set  $A_F(\alpha)$ . Put another way, for all initial values  $z_0$  that are close enough to  $\alpha$  (specifically, within a distance  $r$ ) the successive approximations  $F^n(z_0)$  converge to  $\alpha$ , i.e., starting from such a  $z_0$  and defining  $z_{n+1} = z_n - \frac{f(z_n)}{f'(z_n)}$ , we must have  $z_n \rightarrow \alpha$ .

**PROOF.** We consider the case that  $f(z)$  is complex analytic, noting that the same proof applies when  $f$  is real analytic. In light of Theorem 1.18, it suffices to show that for  $F(z) = z - \frac{f(z)}{f'(z)}$ , we have  $|F'(\alpha)| < 1$ . We first note that  $F'(z) = \frac{f''(z)f(z)}{(f'(z))^2}$ .

If  $f'(\alpha) \neq 0$ , then clearly  $F'(\alpha) = 0$  (since  $f(\alpha) = 0$ ). However, if  $f'(\alpha) = 0$ , that is,  $\alpha$  is a multiple root of  $f$ , then more care must be taken. Suppose this is the case and express  $f(z) = (z - \alpha)^k h(z)$  where  $h(\alpha) \neq 0$ , and  $k \in \mathbb{N}$  is the multiplicity of the root of  $f$  at  $\alpha$  (see Lemma A.21 on page 416). Since  $f'(\alpha) = 0$ , the quotient  $\frac{f(z)}{f'(z)}$  appearing in the definition of  $F(z)$  is not formally defined at  $\alpha$ . However, we can overcome this difficulty by showing that  $\frac{f(z)}{f'(z)}$  has a removable singularity at  $\alpha$ . Indeed, note that

$$\frac{f(z)}{f'(z)} = \frac{(z - \alpha)^k h(z)}{k(z - \alpha)^{k-1} h(z) + (z - \alpha)^k h'(z)} = \frac{(z - \alpha)h(z)}{kh(z) + (z - \alpha)h'(z)}$$

which equals 0 for  $z = \alpha$ . This lets us define  $F(\alpha) = \alpha$  even in the case that  $f'(\alpha) = 0$ .

We leave it to the reader to use the ideas from above to show that  $F'(z)$  also has a removable singularity at  $\alpha$  which, in particular, allows us to define  $F'(\alpha) = \frac{k-1}{k}$ . Since  $|F'(\alpha)| < 1$  we have completed the proof.  $\square$

**EXERCISE 1.22.** Provide the details in the above proof that  $F'(\alpha) = \frac{k-1}{k}$  when  $f$  has a root of order  $k$ . Also, note that  $\alpha$  is a super attracting fixed point of the Newton map  $F$  if and only if  $k = 1$ , i.e.,  $\alpha$  is a simple root<sup>7</sup> of  $f$ . **Try it out!**

**EXPLORATION 1.23** (Convergence rates for Newton's method). Let  $f(z)$  and  $g(z)$  be analytic, and consider the corresponding Newton Maps  $F_f(z) = z - \frac{f(z)}{f'(z)}$  and  $F_g(z) = z - \frac{g(z)}{g'(z)}$ . Suppose  $f$  has a root at  $\alpha$  of order  $k$  and  $g$  has a root at  $\alpha$  of order  $m$ , where  $k < m$ . The rate of convergence of  $F_f^n$  near  $\alpha$  is faster than the rate of convergence of  $F_g^n$  near  $\beta$  since  $|F'_f(\alpha)| = \frac{k-1}{k} < \frac{m-1}{m} = |F'_g(\alpha)|$  (recall Remark 1.19 which relates the rate of convergence to the derivative at the attracting fixed point). Let's explore this in the real variable case with the functions  $f(x) = x^k$  and  $g(x) = x^m$ . Use the *Real Newton Method Applet* to visualize how the degree of the root of  $f$  (respectively,  $g$ ) influences the tangent lines used in Newton's method. In particular, note the effect the degree of the root has on the curvature of the graph near the root and how this provides a visual way to understand the relative rates of convergence of  $F_f^n$  and  $F_g^n$  near  $\alpha$ . **Try it out!**

<sup>7</sup>It is interesting to note that the Newton map of  $f(z)/f'(z)$  (as opposed to the Newton map of  $f(z)$ ) always has super attracting fixed points at the roots of  $f$  regardless of the order of the root of  $f$  (see Additional Exercise 1.160).

REMARK 1.24. We see that the value  $r$  in Proposition 1.21 gives us a lower bound on how close an initial guess  $z_0$  must be to an actual root  $\alpha$  for Newton's method to be *guaranteed* to find  $\alpha$ . Because of this, we call any such  $r$  a **radius of convergence** (for  $F$  and  $\alpha$ ) and the corresponding circle  $C(\alpha, r) = \{z : |z - \alpha| = r\}$  is called a **circle of convergence**. In practice, it is very useful to gauge  $r$  so that we can guarantee the success of Newton's method. There is no universal estimate for  $r$  that always works since it very much depends on the particular map  $f$  being used (see Exercise 1.161). However, for certain classes of maps  $f$  we can provide useable estimates for  $r$  (see Exercise 1.162 and Small Projects 1.163 and 1.164).

Let us now explore some specific examples using complex functions.

EXAMPLE 1.25. For constants  $\alpha, \beta \in \mathbb{C}$ , consider the map  $f(z) = (z - \alpha)(z - \beta)$  which has roots at  $\alpha$  and  $\beta$ . The Newton Map for  $f$  is then  $F(z) = \frac{z^2 - \alpha\beta}{2z - (\alpha + \beta)}$ .

EXPLORATION 1.26. Set  $\alpha = 0$  and  $\beta = 1 + i$  in Example 1.25 and consider the iterates of the Newton Map  $F$  with starting values  $z_0 = 2$ ,  $z_0 = -3 - 2i$ , and  $z_0 = i + 1$ , which you can compute using the *Complex Newton Method Applet*. As expected we see that different starting values for  $z_0$  find different roots of  $f(z)$ . Can you make a guess as to which seed values will find which root? Try to determine if there are there any seed values  $z_0$  for which Newton's method fails to find either root? Experiment with the *Complex Newton Method Applet* to test your predictions. **Try it out!**

EXPLORATION 1.27. Using the function  $f(z) = z^3 - 1$ , determine  $F(z)$  the Newton Map for  $f$  and then analyze Newton's method using different initial guesses for  $z_0$  in the *Complex Newton Method Applet*. Describe (as best as you can) which seed values  $z_0$  will find which of the roots  $1, e^{2\pi i/3}$ , and  $e^{-2\pi i/3}$ . Thus we are asking you to describe (as best as you can) the attracting basins  $A_F(1), A_F(e^{2\pi i/3})$ , and  $A_F(e^{-2\pi i/3})$ . **Try it out!**

**1.2.5. Global Picture of Complex Newton Method Dynamics.** As with the real valued maps, we wish to achieve an understanding of the global dynamics of Newton's method, i.e., an understanding of how the orbits behave for *all* seed values. Thus we employ the **Graph basins of attraction** feature of the *Complex Newton Method Applet*, which uses different colors to display which initial guesses will find which roots, and so gives us a one picture snapshot of the dynamics of Newton's method.

EXERCISE 1.28. Use the *Complex Newton Method Applet* to view the basins of attraction for the Newton maps in Explorations 1.26 and 1.27. **Try it out!**

Looking carefully at the picture of the two attracting basins corresponding to Exploration 1.26, it appears that the boundary between these regions is a straight line; points on one side look closer to the root of  $f$  on that side than to the other root. That is, this boundary appears to be the perpendicular bisector (denoted by  $L$  in Figure 1.3

below) of the line segment from  $\alpha$  to  $\beta$ . This notion suggested by the picture is actually true (pictures, however, can sometimes be misleading) and we can prove it using a very useful technique of *global conjugation*.

**1.2.6. Global Conjugation.** One learns in Linear Algebra that a change of basis can be used to, among other things, greatly facilitate certain calculations, procedures, and overall give you a better understanding of the field. In particular, the notion of similarity of matrices plays a key role (recall, matrices  $A$  and  $B$  are called *similar* when there is an invertible matrix  $P$  such that  $A = PBP^{-1}$ ). A direct analog of this idea often used in dynamics is a type of *change of coordinates* provided by what we call *conjugation*.

DEFINITION 1.29. Let  $\phi$  be a Möbius<sup>8</sup> map. We say that *rational*<sup>9</sup> maps  $f$  and  $g$  are *globally conjugate* (by the map  $\phi$ ) if  $g = \phi \circ f \circ \phi^{-1}$ .

Often the point of conjugating a map  $f$  to a map  $g$  is that  $g$  is easier to work with than  $f$ . And, as we will see, the information we usually want from  $f$  can be quickly obtained by studying the simpler map  $g$ . In particular, we note that the iterates are related as such  $g^n = (\phi \circ f \circ \phi^{-1}) \circ (\phi \circ f \circ \phi^{-1}) \circ \dots \circ (\phi \circ f \circ \phi^{-1}) \circ (\phi \circ f \circ \phi^{-1}) = \phi \circ f^n \circ \phi^{-1}$ . Hence  $\phi$  in this way transfers information between the iterates of  $f$  and the iterates of  $g$ . In particular, fixed points and their corresponding derivatives are transferred in the following way.

EXERCISE 1.30. Suppose maps  $f$  and  $g$  are *globally conjugate* by the Möbius map  $\phi$ , i.e.,  $g = \phi \circ f \circ \phi^{-1}$ . Prove that for any  $a \in \overline{\mathbb{C}}$ ,  $f(a) = a$  if and only if  $g(\phi(a)) = \phi(a)$ . Furthermore prove that if  $a, \phi(a) \in \mathbb{C}$  and  $f(a) = a$ , then we also have  $f'(a) = g'(\phi(a))$ . **Try it out!**

Also, see Additional Exercises 1.165–1.168.

REMARK 1.31. There is also a very useful technique called *local conjugation* which can greatly simplify calculations in many situations. In fact, an important question is when we can locally conjugate a map of the form  $f(z) = a_1z + a_2z^2 + \dots$  having a fixed point at 0 to another map which is simply  $z \mapsto a_1z$ . This is called *linearizing* the map  $f$  near 0. It can always be done when  $0 < |a_1| \neq 1$ , but only sometimes when  $|a_1| = 1$ . The interested reader can pursue such results and their proofs in the literature (e.g., [1, 2, 24]).

**1.2.7. Analysis of the Newton map of a quadratic polynomial.** We now use this powerful global conjugation technique to greatly simplify the analysis of the Newton map  $F(z) = \frac{z^2 - \alpha\beta}{2z - (\alpha + \beta)}$  in Example 1.25. We first choose a Möbius map which sends  $\alpha$  and  $\beta$  to 0 and  $\infty$ , respectively, and then analyze the much simpler map

<sup>8</sup>Recall that a Möbius map is a map of the form  $z \mapsto \frac{az+b}{cz+d}$  where  $ad - bc \neq 0$ , and as such is a bijection of  $\overline{\mathbb{C}}$  onto itself.

<sup>9</sup>Recall that a *rational* map is a quotient of two polynomials.

obtained by conjugation. In particular, the map  $\phi(z) = \frac{z-\alpha}{z-\beta}$  conjugates  $F$  to the map  $g(z) = \phi \circ F \circ \phi^{-1}(z) = z^2$ , a calculation we leave to the reader. We also leave it to the reader to show that  $g^n(z) = z^{2^n}$ .

Our goal is to show that if  $z \in \mathbb{C}$  is closer to  $\alpha$  than to  $\beta$ , then  $F^n(z)$  iterates to  $\alpha$ , i.e.,  $|z - \alpha| < |z - \beta|$  implies  $F^n(z) \rightarrow \alpha$ . Let  $|z - \alpha| < |z - \beta|$  and note that this implies  $|\phi(z)| < 1$ . Since  $|g^n(\phi(z))| = |\phi(z)^{2^n}| = |\phi(z)|^{2^n} \rightarrow 0$ , we have  $g^n(\phi(z)) \rightarrow 0$ . By the conjugation property above we have  $F^n(z) = \phi^{-1}(g^n(\phi(z))) \rightarrow \phi^{-1}(0) = \alpha$ . Thus we have shown that the points  $z \in \mathbb{C}$  which are closer to  $\alpha$  than to  $\beta$  are indeed in  $A_F(\alpha)$ .

**EXERCISE 1.32.** Show that the points  $z \in \mathbb{C}$  which are closer to  $\beta$  than to  $\alpha$  are in  $A_F(\beta)$ . *Try it out!*

We illustrate the conjugation used above by the following diagram, called a *commutative diagram* because each of the maps  $\phi \circ F$  and  $g \circ \phi$  from the upper left to the bottom right are equal.

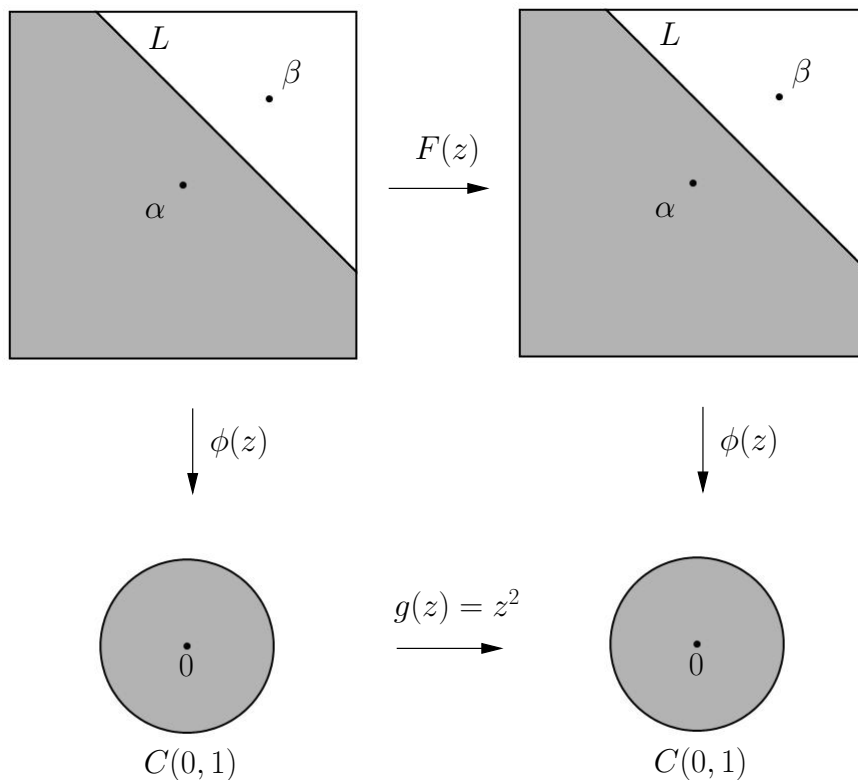


FIGURE 1.3. Commutative diagram for global conjugation of Newton map  $F(z) = \frac{z^2 - \alpha\beta}{2z - (\alpha + \beta)}$ .



Note how the points  $\alpha$  and  $\beta$  are moved by  $\phi$  to the points 0 and  $\infty$ , and that the line  $L \cup \{\infty\}$  in the top pictures is transformed to the unit circle  $C(0, 1)$  in the bottom pictures. By using this conjugation, we are able to analyze the relatively simple dynamics of  $g$  to get corresponding information about the dynamics of  $F$ , in particular,  $A_f(\alpha) = \phi^{-1}(A_g(0))$  and  $A_f(\beta) = \phi^{-1}(A_g(\infty))$ .

Let's return to the question of whether Newton's method can fail in this example. Are there initial values for which the Newton's method orbit never finds any root of  $f$ ? In Example 1.5, we saw that Newton's method fails (or more properly, the *formula* for Newton's method fails) when an initial value  $x_0$  is such that  $f'(x_0) = 0$ . This, what we term an *analytic* obstruction of having a zero in the denominator, however, is overcome when one allows  $\infty$  to take its equal place with all the values in the Riemann Sphere  $\overline{\mathbb{C}}$ . In particular, even though in Example 1.25, we have  $f'(\frac{\alpha+\beta}{2}) = 0$ , the Newton Map gives  $F(\frac{\alpha+\beta}{2}) = \infty$  (see Appendix Section B.4 on page 425 for a review of a discussion on functions defined at  $\infty$ ). Also, since  $F(\infty) = \infty$ , we see that an initial value  $z_0 = \frac{\alpha+\beta}{2}$  will never find either root  $\alpha$  or  $\beta$  because this seed generates the following sequence of Newton "approximations":  $\frac{\alpha+\beta}{2}, \infty, \infty, \infty, \dots$ . Note that the actual obstruction for the success of Newton's method starting with seed value  $z_0$  is not that the function  $F$  cannot be appropriately defined at  $z_0$ , but that such a definition forces the map  $F$  to never iterate  $z_0$  to a root of  $f(z)$  (since  $F^n(z_0) = \infty$  for all  $n \geq 1$ ). The seed  $\frac{\alpha+\beta}{2}$  is not the only complex number which fails to find a root of  $f(z)$  though. We can show, again with the help of the conjugation above, that the boundary line  $L$  which divides  $A_F(\alpha)$  from  $A_F(\beta)$  consists of exactly those points in  $\mathbb{C}$  for which Newton's method fails to find either root. As witnessed in the real variable examples, we can understand this *dynamically* since this line divides those points which are pulled or attracted to  $\alpha$  and those points which are attracted to  $\beta$ . And so by an informal use of symmetry, it would stand to reason that something must fail to work out for points exactly on this line. Of course, we have not proven this fact carefully yet. We have only looked at compelling computer generated evidence, which, as is a common theme in this chapter, is always to be viewed with a healthy bit of skepticism.

A formal argument can be made however. For a point  $z \in L$ , we have  $|\phi(z)| = \frac{|z-\alpha|}{|z-\beta|} = 1$  and thus by the conjugation property above we have  $|g^n(\phi(z))| = |\phi(z)^{2^n}| = |\phi(z)|^{2^n} = 1$  for all  $n \in \mathbb{N}$ . Hence for all  $n \in \mathbb{N}$ , we see that  $F^n(z) = \phi^{-1}(g^n(\phi(z))) \in \phi^{-1}(C(0, 1)) = L \cup \{\infty\}$ . In particular,  $F^n(z)$  neither converges to  $\alpha$  nor  $\beta$ .

**EXERCISE 1.33.** The above analysis applies to any *monic* quadratic polynomial  $p(z)$  with distinct roots, but what if the leading coefficient is not 1? Also, what if the quadratic polynomial  $p(z)$  has a double root instead of two distinct roots? Analyze what happens in these situations. ***Try it out!***

**1.2.8. Analysis of the Newton map of a cubic polynomial.** The behavior found in Exploration 1.27 with the cubic function  $f(z) = z^3 - 1$  is far more complicated

than the quadratic case. It is not simply the case that a starting point under Newton’s method will find the root to which it is nearest. If it were, then the picture of the global dynamics would look like the picture in Figure 1.4. However, the better picture to represent the actual dynamics is given in Figure 1.5, showing that the set of initial guesses in the complex plane is divided into very intricate regions of points that find the various roots.

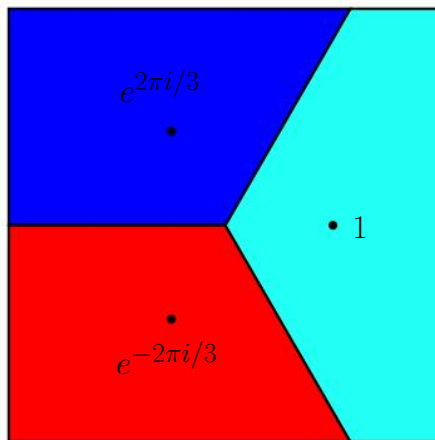


FIGURE 1.4. A reasonable (but false) guess for the picture description of the global dynamics of  $F(z)$ , the Newton Map for  $f(z) = z^3 - 1$ .

Let’s experiment with the zoom feature of the *Complex Newton Method Applet* to investigate this. In particular, notice that when you zoom in on any point that is on the boundary of one colored region (attracting basin), you always find tiny “bulbs” of the other two colors (attracting basins) nearby. In fact, this happens no matter how much you zoom in! This shocking feature is why we call such sets *fractals*.<sup>10</sup> In this case, at a large scale there are extremely tiny bulbs (smaller than a single pixel) that are not revealed in the picture unless one zooms in far enough to see them.

So again we see that Newton’s method became very complicated to understand globally when the original function  $f(z)$  changed from a quadratic to a cubic map. Earlier we posed the questions: Why? How? Is there a way to know when a system will necessarily be simple or complicated ahead of time? With the use of our deep knowledge and fancy tools in complex analysis we can give some good reasons why the pictures, and hence the dynamics they represent, must be so complicated. We first remind ourselves of some key concepts.

DEFINITION 1.34. The *boundary of a set*  $E$  in  $\overline{\mathbb{C}}$  is  $\partial E = \overline{E} \cap \overline{\overline{\mathbb{C}} \setminus E}$ , which is equal to the set of points  $z \in \overline{\mathbb{C}}$  which have the property that every open disk (in the

<sup>10</sup>A *fractal* is a set which when you zoom in reveals new features not seen from the coarse larger scale picture.

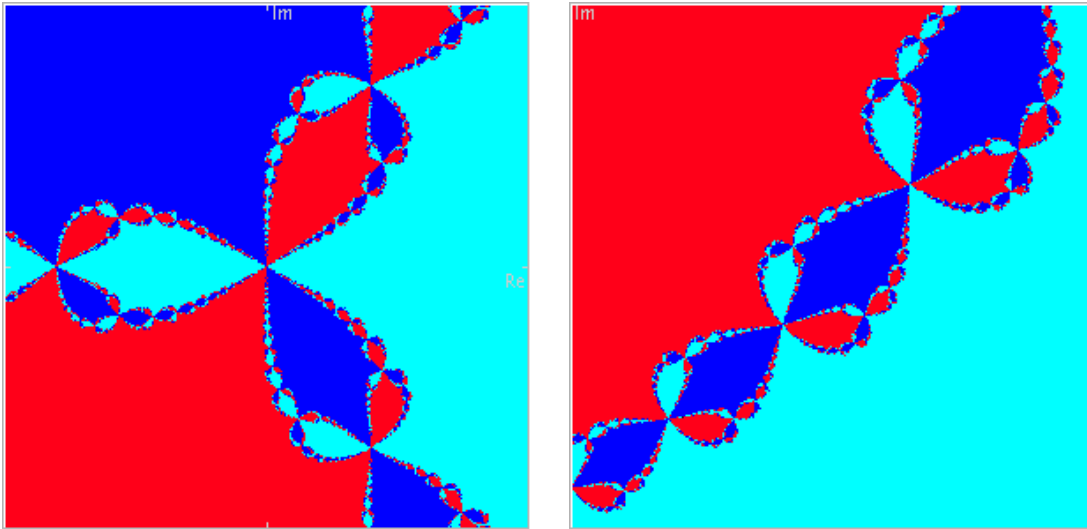


FIGURE 1.5. A more accurate picture of the global dynamics of  $F(z)$ , the Newton Map for  $f(z) = z^3 - 1$  (with magnification on the right). Here the turquoise represents  $A_F(1)$ , the blue represents  $A_F(e^{2\pi i/3})$  and the red represents  $A_F(e^{-2\pi i/3})$ .

spherical metric)  $\Delta_\sigma(z, r)$  intersects both  $E$  and the complement of  $E$  no matter how small  $r > 0$  is.

We can now describe the fractal features we already observed in Figure 1.5 by saying  $\partial A_F(1) = \partial A_F(e^{2\pi i/3}) = \partial A_F(e^{-2\pi i/3})$ . In fact, we see this same phenomenon in Example 1.4 and Explorations 1.6 and 1.26 as well when we consider the complex versions of all these maps. It turns out that, in general, all attracting basins of a Newton Map  $F$  must share the exact same set of boundary points. Specifically, we have the following Common Boundary Condition.

**THEOREM 1.35 (Common Boundary Condition).** Let  $f(z)$  be an analytic function such that its Newton Map  $F(z) = z - \frac{f(z)}{f'(z)}$  is a rational map. If  $w_1$  and  $w_2$  are roots of  $f(z)$ , then  $\partial A_F(w_1) = \partial A_F(w_2)$ .

**PROOF.** This result can be proven using Proposition 1.21 and the forthcoming Theorem 1.60.  $\square$

Let's examine how Theorem 1.35 forces the dynamics illustrated in Figure 1.5 to necessarily be complicated. According to Proposition 1.21 there exists some  $r > 0$  such that  $\Delta(1, r) \subseteq A_F(1)$ ,  $\Delta(e^{2\pi i/3}, r) \subseteq A_F(e^{2\pi i/3})$ , and  $\Delta(e^{-2\pi i/3}, r) \subseteq A_F(e^{-2\pi i/3})$ . And so starting from the picture shown in Figure 1.6 we need to consider how to color in the rest of the points in  $A_F(1)$ ,  $A_F(e^{2\pi i/3})$ , and  $A_F(e^{-2\pi i/3})$  with turquoise, blue, and red, respectively, *while also being certain to make sure that the boundary of each color exactly matches the boundary of the other two colors*. A moment's thought tells

us that this Common Boundary Condition forces the picture to necessarily be *very* complicated, and also rules out having the global dynamics behaving as suggested by Figure 1.4 (since, for example, a point on the negative real axis in that picture lies on the boundary of only two of the three color basins).

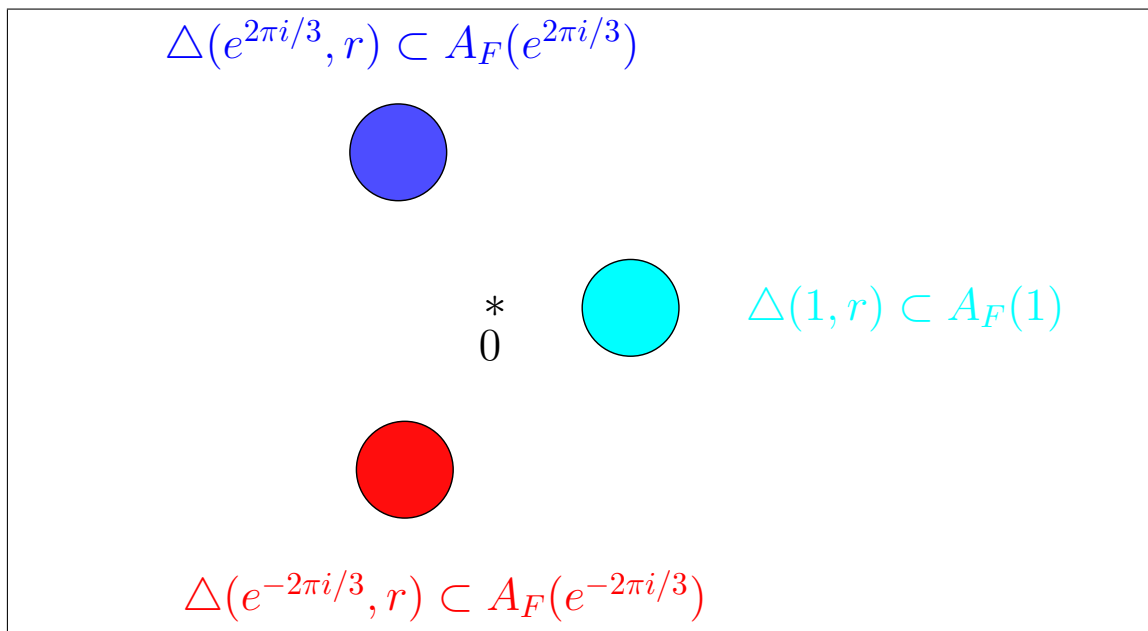


FIGURE 1.6. Consequence of the Attracting Property of Newton's Method (Proposition 1.21).

This Common Boundary Condition is also at the heart of what we will learn to call *chaos* in the dynamics of Newton's method. Consider any point  $z$  on the boundary of any basin and then draw a tiny disk  $B$  around it. According to the Common Boundary Condition, this tiny disk  $B$  must contain all three colors in it. So if we wish to determine the fate of the orbit of  $z$  with a computer, what we will find is that any tiny error (like roundoff error) from inputting the coordinates of  $z$  could lead to drastically different results. We see that by changing  $z$  even by the slightest amount, we can change the orbit of  $z$  tremendously as  $z$  could slip into any of the red, turquoise, or blue regions. So with such a point  $z$ , we see that the behavior of the orbit in the long run will be quite different even if we change  $z$  only a little. This is the essence of what we call chaos. Although a more formal and more thorough understanding of chaos will come later in the text, use this understanding of this notion to explain why each point on the line  $L$  that appeared in the analysis of the quadratic Newton method case has this behavior. Also, explain why each point in one of the attracting basins (which has a tiny disk of all the same color) is NOT such a point. ***Try it out!***

REMARK 1.36. We mention here a remarkable fact about sets which share a complicated boundary. The three sets  $A_F(1)$ ,  $A_F(e^{2\pi i/3})$ , and  $A_F(e^{-2\pi i/3})$  above share the same boundary because each set is broken up into an infinite number of pieces which are then arranged in the complicated fractal pattern you see in Figure 1.5. However, it is true that three open sets (or even  $n$  open sets for any fixed  $n \in \mathbb{N}$ ) can all share the same boundary set and also have the property that each set is connected.<sup>11</sup> Such sets are complicated indeed! The interested reader is encouraged to read about the Lakes of Wada in [16], p. 143.

Let us now consider the question of whether or not there are any starting (seed) values for which the Newton Map for  $f(z) = z^3 - 1$  fails to find a root of  $f(z)$ . In all the previous examples there always exist such points; however, these were, in some sense, relatively few. You might guess that each point in  $\partial A_F(1) = \partial A_F(e^{2\pi i/3}) = \partial A_F(e^{-2\pi i/3})$  is such a point...and you would be right. Heuristically, we can use our intuition to imagine that such points fail to find any root since any such point is, in some sense, being pulled or attracted by each of the three different roots with equal force. You are asked to prove this in Additional Exercise 1.169. Note however, that even assuming the result that each point in  $\partial A_F(1) = \partial A_F(e^{2\pi i/3}) = \partial A_F(e^{-2\pi i/3})$  fails to iterate under  $F(z)$  to any of the roots of  $f(z)$ , we still do not necessarily know the fate of ALL starting points. Specifically, we wonder if it is true that all points in  $\overline{\mathbb{C}}$  lie in either one of the attracting basins or on the common boundary of these sets. We pose this and a related question as follows.

1. Is there a point not in  $\partial A_F(1) = \partial A_F(e^{2\pi i/3}) = \partial A_F(e^{-2\pi i/3})$  which fails to find any root of  $f(z)$ ?
2. Can there be a whole open disk of such points?

When considering the particular map  $f(z) = z^3 - 1$  (or any of the maps  $f$  mentioned thus far in this chapter) and its related Newton Map  $F(z)$ , the answer to both of these questions is no (see Additional Exercise 1.180). However, in general, it is possible for the answer to the second question (and hence also the first) to be yes.

EXPLORATION 1.37. Consider the map  $f(z) = z * (z - 1) * (z - .909 - .416i)$  and its related Newton Map  $F(z)$ . Using the the *Complex Newton Method Applet* you can find regions of seed values colored black which fail to find any root of  $f(z)$  under Newton's method. For example you will find such a region of points by zooming in on the point  $0.64 + 0.14i$ . Use the applet to select such points and then iterate  $F(z)$  to explore the behavior. Experiment with many seed values chosen from the black regions to see what type of behavior you can find. Use the zoom feature to see whether or not it appears that the boundary of the black region matches the boundary of the attracting basins for the three roots of  $f(z)$ . **Try it out!**

<sup>11</sup>Recall, an open set  $A$  is called *connected* when given any two points  $z, w \in A$  there exists a *polygonal line* in  $A$  which connects  $z$  to  $w$ . See Appendix B.3 on page 423.

The reader can investigate Newton's method applied to other cubic polynomials in Additional Exercise 1.170.

**1.2.9. Newton's method applied to any cubic polynomial.** In this section we study Newton's method applied to an arbitrary cubic polynomial. We begin by introducing a (nearly) representative class for all cubic polynomials. Let  $\mathcal{F}$  denote the collection of all polynomials  $p_\rho(z) = z(z-1)(z-\rho)$  where  $\rho$  is in  $D = \{\rho : \text{Im } \rho \geq 0, |\rho| \leq 1, |\rho-1| \leq 1\}$ .

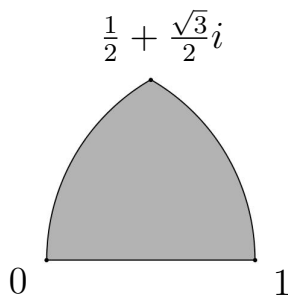


FIGURE 1.7. Region  $D$  of  $\rho$  values corresponding to the maps  $p_\rho$  in  $\mathcal{F}$ .

This class of polynomials  $\mathcal{F}$  is then representative of all polynomials with three distinct roots in the following sense.

**PROPOSITION 1.38.** For each cubic polynomial  $p(z)$  with three distinct roots, there exists  $\rho \in D$  such that the Newton map  $F_p$  is globally conjugate by a linear map  $T$  to the Newton map  $F_{p_\rho}$  of  $p_\rho(z)$ , i.e.,  $T \circ F_p \circ T^{-1} = F_{p_\rho}$ .

In order to prove the above proposition we require the following proposition, which we note applies to polynomials of any degree.

**PROPOSITION 1.39.** Let  $p(z)$  be a polynomial and let  $T(z) = az + b$  for  $a \neq 0$  where  $a, b \in \mathbb{C}$ . Then for the polynomial  $q(z) = p(T(z))$ , we have

$$T \circ F_q \circ T^{-1} = F_p$$

where  $F_q$  and  $F_p$  are the Newton maps of  $q$  and  $p$  respectively.

We leave the proof of Proposition 1.39 to the reader. However, we say a few words about its meaning and usefulness. Note that the polynomial  $q$  (which is sometimes called the “rescaling” of  $p$ ) will have the same degree as  $p$ . Furthermore, if  $p$  has roots at  $r_1, \dots, r_d$ , then  $q$  will have roots at  $T^{-1}(r_1), \dots, T^{-1}(r_d)$ . Hence the result of the proposition says that we can “move” the roots of  $p$  by choosing  $T^{-1}$  appropriately and generating a new polynomial  $q$ . Furthermore, studying the dynamics of  $F_q$  will be *essentially* the same as studying the dynamics of  $F_p$  since these are globally conjugate to each other.

EXAMPLE 1.40. Consider  $p(z) = (z + i/2)(z - 1)(z + 1)$ . We wish to illustrate Proposition 1.38 by finding  $\rho \in D$  so that  $F_{p_\rho}$  is conjugate to  $F_p$ . Consider the triangle formed by the roots of  $p(z)$  at  $-i/2, 1$ , and  $-1$ . We now construct a linear map  $T^{-1}$  to transform this triangle into a triangle with longest side being the interval  $[0, 1]$  and third vertex (which will be our choice of  $\rho$ ) in the upper half plane  $\{\text{Im } z \geq 0\}$ . These constrictions then force  $T^{-1}(1) = 0$  and  $T^{-1}(-1) = 1$ , which in turn determine that  $T^{-1}(z) = \frac{-1}{2}z + \frac{1}{2}$  and  $\rho = T^{-1}(-i/2) = 1/2 + i/4$  (which is in  $D$ ).

Let's verify that this choice of  $\rho$  works. Note that  $q(z) = p(T(z))$  must have roots at  $0, 1$ , and  $\rho$ . Since  $q$  and  $p_\rho$  share the exact same roots, they must agree up to a multiplicative constant, i.e., we must have  $q(z) = cp_\rho(z)$  for some constant  $c \neq 0$ . This, however, implies that  $F_q = F_{p_\rho}$  (why?). Hence, by Proposition 1.39 we have that  $T \circ F_{p_\rho} \circ T^{-1} = T \circ F_q \circ T^{-1} = F_p$  as desired.

The reader should use the *Complex Newton Method Applet* to compare the pictures of the attracting basins for  $F_p$  and  $F_{p_\rho}$  noting the similarities one would expect from the fact that these maps are globally conjugate. In particular, see if you can see the effects of the specific map  $T$  when you compare the two pictures. **Try it out!**

EXERCISE 1.41. Find  $\rho \in D$  so that for  $p(z) = (z - 4)(z + i)(z + 4)$  we have  $F_{p_\rho}$  is globally conjugate to  $F_p$ . **Try it out!**

In the same manner as Example 1.40, one can prove Proposition 1.38, and so we omit the details. However, we leave it to the reader to investigate what can be said about the dynamics of  $F_p$  when  $p(z)$  is a cubic polynomial with a double or triple root. In addition, we invite the reader to consider generalizations such as the following.

SMALL PROJECT 1.42. Consider how Proposition 1.39 is used to “move roots” by a linear transformation  $T^{-1}$  in the proof of Proposition 1.38. With this idea in mind, can you justify the statement that all cubic polynomials whose roots form an equilateral triangle have globally conjugate Newton maps (and hence essentially the same dynamics)? What about quartic polynomials whose roots form a square? Does this generalize to higher degree polynomials? Do the roots need to form regular  $n$ -gon? What can you say about generalizing the class  $\mathcal{F}$  (and the set  $D$ ) from above when considering polynomials of fixed higher degree?

Aside from the exceptional cases mentioned above, we can study the Newton's method dynamics of all cubic polynomials by studying just the maps  $p_\rho$  where  $\rho \in D$ . We have created the *Cubic Polynomial Complex Newton Method Applet* to help. This applet allows the user to generate the pictures of the attracting basins for Newton's method applied to any  $p_\rho$  (not just  $\rho \in D$ ). Also, it allows the user to investigate the *parameter plane* of  $\rho$  values since each such value will be colored according to the corresponding dynamics of  $F_{p_\rho}$ .

A note about the coloring of the parameter plane of  $\rho$  values. You will see in Section 1.4 that the orbit of all points where  $F'_{p_\rho}(z) = 0$  are critically important to understanding the dynamics of  $F_{p_\rho}$ . Since  $F'_{p_\rho}(z) = \frac{p_\rho(z)p''_\rho(z)}{(p'_\rho(z))^2}$ , we see that  $F'_{p_\rho}(z) = 0$

only at the roots of  $p_\rho(z)$  or when  $p_\rho''(z) = 0$ . Since the roots of  $p_\rho(z)$  are attracting fixed points for  $F_{p_\rho}$ , their orbits are understood. However, since  $p_\rho''(z) = 0$  for  $z = (1 + \rho)/3$  we see that this, so-called, *free critical point* is important. Hence in the *Cubic Polynomial Complex Newton Method Applet*, we track, for each  $\rho$ , the *critical orbit* of  $z_0 = (1 + \rho)/3$ . When this critical orbit is attracted to one of the roots of  $p_\rho$ , we color the point  $\rho$  in the parameter plane the corresponding color of the attracting basin. To illustrate, click on the **Show Critical Orbit** checkbox to see this critical orbit appear as white dots in the right picture (dynamical plane). Thus, if this critical orbit converges to, say, the red root of  $p_\rho$ , then the corresponding parameter  $\rho$  (marked by a +) is colored red in the left picture (parameter plane). If this orbit is not attracted to any of the roots of  $p_\rho$ , we color the point  $\rho$  in the parameter plane black. Try clicking in the parameter plane to select different colored  $\rho$  value, and then witness the convergence of the critical orbit to a different colored root of  $p_\rho$ .

EXPLORATION 1.43. Use the *Cubic Polynomial Complex Newton Method Applet* to investigate the dynamics of Newton's method applied to any  $p_\rho$ . Look for symmetries and experiment with the dynamical behavior you find. Make conjectures, and then see if you can prove them! **Try it out!**

### 1.3. Iteration of an Analytic Function

In this section we focus our study on the dynamics of analytic maps which do not necessarily arise as Newton Maps of polynomials. One goal is to understand which dynamical features of Newton's method extend to such a wider class of maps. We pay particular attention to the iteration of polynomial maps of the form  $z^2 + c$  where  $c$  is a complex parameter since these are the simplest maps which still produce a rich variety of dynamical behaviors.<sup>12</sup> We also note that with the help of the global conjugation technique (see Section 1.2.6), every quadratic map is globally conjugate, and in some sense dynamically equivalent, to exactly one map of the form  $z^2 + c$  (see Additional Exercise 1.167). Hence, in this way the dynamics of maps  $z^2 + c$  represent the dynamics of all quadratic maps.

One need not have worked through all of Section 1.2; however, it is critical that Sections 1.2.3 and 1.2.6 be read before proceeding with this section.

Though the quadratic maps of the form  $z^2 + c$  are genuinely very simple and well understood *as functions*, we will see that their *dynamics* can be extremely complicated. We will explore this carefully, not only the dynamics of each map  $z^2 + c$ , but we will also study how the dynamics of such maps change as the parameter  $c$  changes, leading us into the study of what is called *bifurcation theory*.

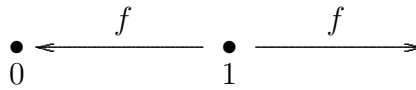
In Section 1.6, we consider the dynamics of more exotic transcendental entire complex analytic maps such as  $ce^z$ ,  $c \sin z$ , and  $c \cos z$ .

<sup>12</sup>The dynamics of the iteration of Möbius maps is simpler to study because such maps have such relatively simple dynamical behavior. See Section 1.B for a classification of the dynamics of Möbius maps.

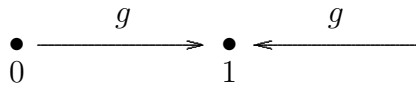


**1.3.1. Classification of Fixed Points for Analytic maps.** Having noted the importance of fixed points in Section 1.2.3, where we defined attracting fixed points, we extend our discussion here to understand the two remaining types of fixed points, *repelling* and *indifferent*. We begin with an example.

EXAMPLE 1.44. Let  $f(x) = x^2$  and  $g(x) = \sqrt{x}$  each restricted so that  $f, g : \mathbb{R}^+ \rightarrow \mathbb{R}^+$  where  $\mathbb{R}^+ = \{x \geq 0\}$ . We leave it to the reader to quickly check that 0 and 1 are each fixed points of both  $f$  and  $g$ . Further, we have  $f^n(x) \rightarrow 0$  if  $0 < x < 1$ , and  $f^n(x) \rightarrow \infty$  if  $x > 1$ . Also we have  $g^n(x) \rightarrow 1$  for all  $x \in \mathbb{R}^+ \setminus \{0\}$ . Note that 0 is an attracting fixed point for  $f$  (why?). However, we see that for  $x$  values close to, but not equal to 1, we have that the orbit  $f^n(x)$  moves away from 1. We then call 1 a *repelling* fixed point for  $f$  (which we formally define below). We also note that the function  $g(x)$  has an attracting fixed point at 1 and a repelling fixed point at 0. We illustrate the dynamics of these two maps graphically in Figure 1.8.



Dynamics of  $f(x) = x^2$  has attracting fixed point 0 and repelling fixed point 1.



Dynamics of  $g(x) = \sqrt{x}$  has repelling fixed point 0 and attracting fixed point 1.

FIGURE 1.8. Graphical description of the dynamics of  $f$  and  $g = f^{-1}$ .

Note that  $f = g^{-1}$  and  $g = f^{-1}$ . Giving some thought to this fact that  $f$  and  $g$  “undo” each other in this fashion, it stands to reason that an attracting fixed point for  $f$  must be a repelling fixed point for  $g$ , and vice versa.

Inspired by this example, we formally define a repelling fixed point as follows.

DEFINITION 1.45 (Repelling Fixed Point). Let  $f$  be a map with domain set  $\Omega \subseteq \overline{\mathbb{C}}$  (note that  $\Omega$  could be a subset of  $\mathbb{R}$ ).

(a) We call a (finite) fixed point  $a \in \mathbb{C}$  a *repelling fixed point* of  $f$  if there exists a neighborhood  $U$  of  $a$  such that for any point  $z \in \Omega \cap U \setminus \{a\}$ , we have  $|f(z) - a| > |z - a|$ , i.e., the action of  $f$  is to move each point in  $\Omega \cap U \setminus \{a\}$  farther from  $a$ .

(b) Suppose  $f(\infty) = \infty$ . We call  $\infty$  a *repelling fixed point* of  $f$  if there exists a neighborhood  $U \subseteq \overline{\mathbb{C}}$  of  $\infty$  such that for any point  $z \in \Omega \cap U \setminus \{\infty\}$ , we have  $|f(z)| < |z|$ , i.e., the action of  $f$  is to move each point in  $\Omega \cap U \setminus \{\infty\}$  farther from  $\infty$  (as measured by the spherical metric).

THEOREM 1.46. Suppose  $\Omega \subseteq \mathbb{R}$  or  $\Omega \subseteq \mathbb{C}$ . Let  $f : \Omega \rightarrow \Omega$  such that  $f(a) = a$  and  $|f'(a)| > 1$ . Then  $a$  is a repelling fixed point of  $f$ . In fact, there exists  $\epsilon > 0$  such that

for all  $z \in \Omega \cap \Delta(a, \epsilon) \setminus \{a\}$  the orbit  $f^n(z)$  eventually leaves  $\Delta(a, \epsilon)$ , i.e., there exists  $N$  such that  $f^N(z) \notin \Delta(a, \epsilon)$ .

REMARK 1.47. The proof is given by a quick modification of the proof of Theorem 1.18, and so we leave the details to the reader. Note, however, that the theorem does not preclude the case that the orbit of  $z$ , after leaving  $\Delta(a, \epsilon)$ , might reenter  $\Delta(a, \epsilon)$  (see Additional Exercise 1.171).

REMARK 1.48. Again we note that Theorem 1.46 is not, in general, an if and only if result. In particular, the reader is encouraged to find a **real valued function**  $f : \mathbb{R} \rightarrow \mathbb{R}$  such that 0 is a repelling fixed point which has  $|f'(0)| = 1$ . Hint: Consider maps of the form  $x \mapsto x \pm x^n$ .

Above we provided examples of *real valued* maps which show that the converses of Theorems 1.18 and 1.46 do not, in general, hold. However, the next theorem shows that such examples cannot be found for *complex analytic* maps.

THEOREM 1.49. Let  $f(z)$  be an analytic map on an open set  $\Omega \subseteq \mathbb{C}$  such that  $f(a) = a$ . Then we have the following,

- (i)  $a$  is an attracting fixed point if and only if  $|f'(a)| < 1$ , and
- (ii)  $a$  is a repelling fixed point if and only if  $|f'(a)| > 1$ .

Theorems 1.18 and 1.46 provide two of the four implications. The proofs of the remaining two, outlined in the Exercise 1.172, use special properties of complex analytic maps.

We note that Theorem 1.49 only applies to finite fixed points and so we ask if there is a corresponding result when  $\infty$  is fixed. Let us examine the following examples in preparation of handling this issue.

EXAMPLE 1.50. Consider the map  $h(z) = z + 1$  on  $\overline{\mathbb{C}}$ , which fixes  $\infty$  and shifts each point in the complex plane one unit to the right. Note that for  $z$  near  $\infty$  with very large and *positive* real part, for example  $z = 10^6 + 2i$ , we have  $|h(z)| > |z|$ , which makes it appear that  $\infty$  is attracting. However, for  $z$  near  $\infty$  with very large and *negative* real part, for example  $z = -10^6 + 5i$ , we see that  $|h(z)| < |z|$ , which makes it appear that  $\infty$  is repelling. We then are left to conclude that for  $h$ , the fixed point at  $\infty$  is neither attracting nor repelling. Also note that the  $n$ -th iterate  $h^n(z) = z + n$  and so for any point  $z$  in  $\overline{\mathbb{C}}$  we have  $h^n(z) \rightarrow \infty$  (always moving parallel to the  $x$ -axis). Thus  $A_h(\infty)$  is equal to the entire Riemann Sphere  $\overline{\mathbb{C}}$ . This is somewhat surprising given that  $\infty$  is not even an attracting fixed point. We graphically represent the dynamics both on  $\mathbb{C}$  and  $\overline{\mathbb{C}}$  in Figure 1.9.

EXAMPLE 1.51. Consider the map  $g(z) = z/2$  on  $\overline{\mathbb{C}}$ . Each point in  $\mathbb{C}$  is mapped to a point with one half the modulus, but with the same argument. Clearly then the origin is an attracting fixed point and  $A_g(0) = \mathbb{C}$ . We also note that  $g(\infty) = \infty$  and if  $z$  is near  $\infty$ , then  $g(z)$  moves away from  $\infty$ , i.e.,  $|g(z)| < |z|$ . Thus  $\infty$  is a repelling

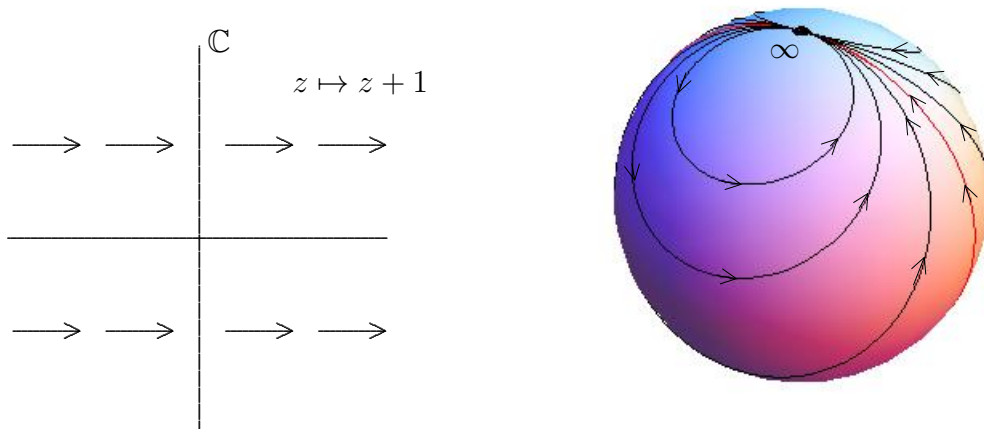


FIGURE 1.9. Graphical representations of the dynamics of  $h(z) = z + 1$  on the plane  $\mathbb{C}$  (left) and on the Riemann sphere  $\overline{\mathbb{C}}$  (right).

fixed point. Note also that  $g^n(z) = z/2^n$ . We graphically represent the dynamics both on  $\mathbb{C}$  and  $\overline{\mathbb{C}}$  in Figure 1.10.

**EXAMPLE 1.52.** Consider the map  $f(z) = z^2$  on  $\overline{\mathbb{C}}$ . Convince yourself that  $f^n(z) = z^{2^n}$  for all  $n = 1, 2, \dots$ . Thus, we see that  $|z| < 1$  implies both  $|f(z)| = |z|^2 < |z|$  and  $|f^n(z)| = |z^{2^n}| = |z|^{2^n} \rightarrow 0$ . Also,  $|z| > 1$  implies both  $|f(z)| = |z|^2 > |z|$  and  $|f^n(z)| = |z^{2^n}| = |z|^{2^n} \rightarrow +\infty$ . Thus we conclude that both  $0$  and  $\infty$  are attracting fixed points with attracting basins  $A_f(0) = \Delta(0, 1)$  and  $A_f(\infty) = \overline{\mathbb{C}} \setminus \overline{\Delta(0, 1)}$ . We represent the dynamics graphically in Figure 1.11, being careful to note that the angle doubling property of the  $z^2$  map is not represented in this picture. To be more precise, if  $z_0 = re^{i\theta}$  in polar form we have that  $f(z_0) = r^2e^{i2\theta}$ . Thus, for example, starting with seed  $z_0 = 0.999e^{i\pi/100}$ , the orbit  $z_n$  will converge towards  $0$ , doubling the angle at each step, which we encourage the reader to visually see this using the *Complex Function Iterator Applet* (using the **Polar seed form** and the **Polar computation mode** of the applet).

The last three examples were chosen to illustrate fixed points at  $\infty$ , but we should note that they can be misleading in another regard. Namely, in each example we were to be able to calculate a formula for  $f^n$ . We caution the reader that this is very rare. We also make the point that having an actual formula for the iterates  $f^n$  was really unnecessary. We can analyze the dynamics without appealing directly to these formulas.

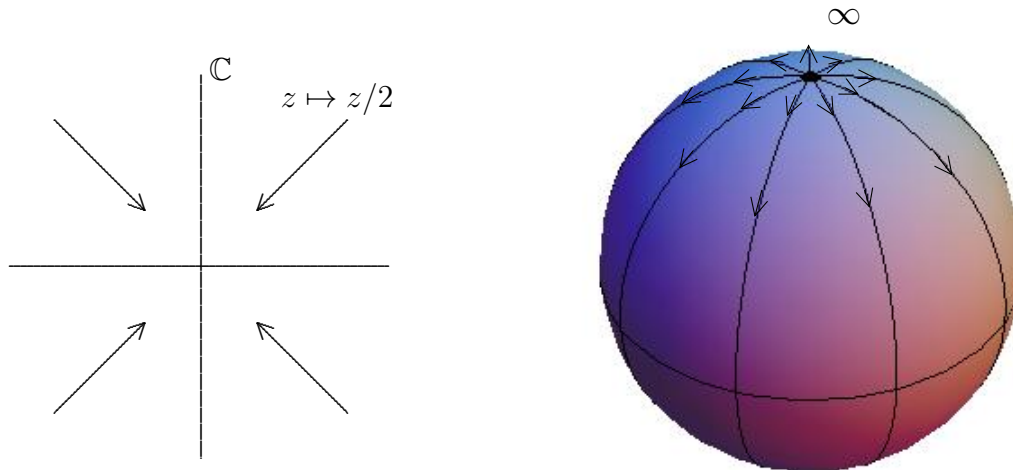


FIGURE 1.10. Graphical representations of the dynamics of  $g(z) = z/2$  on the plane  $\mathbb{C}$  (left) and on the Riemann sphere  $\overline{\mathbb{C}}$  (right).

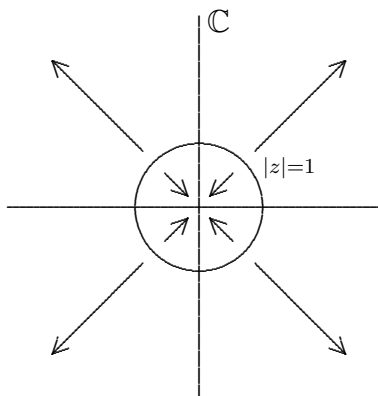


FIGURE 1.11. Graphical representation of the dynamics of  $f(z) = z^2$ .

In each of Examples 1.50, 1.51, and 1.52 we see that  $\infty$  is a fixed point that we were able to classify by carefully examining the dynamics near  $\infty$ . However, we wonder (in light of Theorem 1.49) if we can also make use of the derivative to classify fixed points at  $\infty$ . It turns out that we can; however, we must be careful. Above we saw that  $|h'(\infty)| = 1$  corresponded to a fixed point that was neither attracting nor repelling,

$|g'(\infty)| = 1/2$  corresponded to a repelling fixed point, and  $f'(\infty) = \infty$  corresponded to an attracting fixed point. Clearly, the derivative evaluated at  $\infty$  does not play the same role as it does in Theorem 1.18 for finite points. However, as we now see, it is not far off.

**DEFINITION 1.53** (Multiplier of a fixed point). Let  $f$  be analytic at  $\infty$  such that  $f(\infty) = \infty$  (see Definition B.13 on page 426 for the definition of what it means for a map to be analytic at  $\infty$ ). We define the *multiplier*  $\lambda$  at  $\infty$  to be  $1/f'(\infty) = \lim_{z \rightarrow \infty} 1/f'(z)$ . If  $a$  is a finite fixed point in  $\mathbb{C}$ , then we define the *multiplier*  $\lambda$  at  $a$  to be  $f'(a)$ .

**DEFINITION 1.54** (Classification of Fixed Points). With this definition and with Theorem 1.49 in mind, we now classify all fixed points of analytic maps, whether finite or not, based on their multiplier  $\lambda$ . Suppose  $f : \Omega \rightarrow \Omega$  is analytic where  $\Omega$  is an open subset of  $\mathbb{C}$  and  $a$  is a fixed point with multiplier  $\lambda$ . Then  $a$  is called

- a) *super attracting* if  $\lambda = 0$
- b) *attracting* if  $0 < |\lambda| < 1$
- c) *repelling* if  $|\lambda| > 1$
- d) *indifferent* if  $|\lambda| = 1$ .

We write that  $a$  is (super)attracting, when it is known that either case (a) or (b) holds.

The reader can check that these classifications match what we found in Examples 1.50, 1.51, and 1.52. Further, we note the motivation for the definition of the multiplier when  $f$  has a fixed point at  $\infty$ . In this case, by globally conjugating  $f$  by  $\phi(z) = 1/z$  we obtain the map  $k(z) = 1/f(1/z)$  which has a fixed point at 0. We chose to define the multiplier of  $f$  at  $\infty$  to be the multiplier of  $k$  at 0, which is shown in Lemma B.19 on page 427 to be  $k'(0) = 1/f'(\infty)$ . In Additional Exercise 1.173 you are asked to prove that this multiplier, thusly defined, does correctly correspond to the notions of attracting and repelling fixed points as given in Definitions 1.16 and 1.45.

**REMARK 1.55.** We note that indifferent fixed points can exhibit both a partial attracting nature and a partial repelling nature. For example, we saw in Section 1.2.3 that the indifferent fixed point at the origin for the *complex* map  $g(z) = \sin z$  is “attracting” for real valued seeds, but “repelling” for purely imaginary seeds. Likewise, the indifferent fixed point at  $\infty$  for the map  $h(z) = z + 1$  “attracts” points with large and positive real part, but “repels” (at least initially) points with large and negative real part. However, sometimes an indifferent fixed point, like the origin under the map  $f(z) = e^{\sqrt{2\pi}i}z$ , acts in neither an attracting nor repelling manner. Indifferent fixed points of analytic maps can exhibit many different types of dynamical behavior and their study can be quite complicated. In fact, it is complicated enough that we will not say more about them here, but will only refer the interested reader to [1, 2, 24].

**1.3.2. A Closer look at the Dynamics of  $f(z) = z^2$ .** Let us return to considering the dynamics of the map  $f(z) = z^2$ . First we note that if  $|z| = 1$ , then  $|f^n(z)| =$

$|z^{2^n}| = |z|^{2^n} = 1^{2^n} = 1$ , i.e., if a point is on the unit circle  $C(0, 1) = \{z : |z| = 1\}$ , then its entire orbit  $\{f^n(z)\}_{n=1}^\infty$  is also on the unit circle. It might appear from this and from our previous work in Example 1.52 that all the mysteries concerning the dynamics of this map have been solved. But as we will see this is not at all close to the truth!

Consider the question, if we know the orbit of one seed value, will all nearby seed values have similar orbits? If  $z$  lies within the unit disk, then it and all the nearby points within the unit disk have the same behavior – namely each orbit converges to 0. Likewise, if  $z$  lies outside of the closed unit disk, then it and all the nearby points outside of the closed unit disk have the same behavior, namely each orbit converges to  $\infty$ . However, the story is quite different for seed values on the unit circle. In particular, for any seed on  $C(0, 1)$  we can find other seed values *arbitrarily* close which have drastically different orbits (namely which limit to either  $\infty$  or 0).

Let's examine this behavior using the computer to iterate for us. For the map  $f(z) = z^2$  use the *Complex Iteration Applet* to iterate the seed value  $z_0 = 1 + i$  as well as various seed values very close to  $z_0$ . You can see that this seed value and all of the nearby seed values have the same behavior. Now repeat this by iterating  $z_0$  for the values  $-0.4 + 0.5i, 1, i$ , and  $0.6 + 0.8i$ , being sure to test various nearby seed values that you choose yourself.

**REMARK 1.56** (A word of caution about using the computer). We must always keep in mind that if we are trying to calculate the orbit under the map  $f(z) = z^2$  of a point on  $C(0, 1)$ , we may have some serious problems getting our computer to provide accurate results. Let's test this out now on the *Complex Iteration Applet*. For the map  $f(z) = z^2$  try iterating seed value  $z_0 = 0.6 + 0.8i$  (which lies on  $C(0, 1)$ ) by entering in the seed value in **Euclidean form** and using the **Euclidean computation mode**. Iterating 20 times, you will see what you would expect. However, after iterating about 55 times you will see the orbit move inside of the unit disk (where it will then iterate to 0). Why? Well, the problem is that if the computer truncates, rounds, or approximates any of the values in the orbit (as computers often do), these small errors will likely push the orbit outside or inside of the unit circle, causing the computer to mistakenly calculate the orbit as tending to either  $\infty$  or 0. Thus, when using a computer it is important to know (a) if the computer will approximate values it uses, and (b) whether these approximations will be significant or not in the end result.

As an illustration of the subtle issues that can wreak havoc on your computations, we show the problems that can arise from the fact that  $z * z$  and  $z^2$  are not always equivalent. Of course we know that the expressions  $z^2$  and  $z * z$  are *mathematically* equivalent, but these expressions are not *computationally* equivalent. The former is evaluated as  $e^{2\text{Log } z}$ , where  $\text{Log } z$  is the principal logarithm, and the latter is evaluated through usual complex multiplication. Thus each will incorporate different rounding errors at times. The end result of this very subtle difference is quite evident when iterating the seed  $0.6 + 0.8i$  in **Euclidean computation mode** under each of these maps. *Try it out!*

In line with the concerns one has when using the computer, specifically item (b) above, we see that it is important to clearly identify those seed values where approximations (or more precisely errors introduced by using approximations in place of exact values) would lead to significant errors in future calculations of orbit values. Such seed values are said to be in the *chaotic set*. The chaotic set in this context is usually called the *Julia set*, in honor of the mathematician Gaston Julia who in 1918, at the age of 25, published his 199 page masterpiece titled “Mémoire sur l’itération des fonctions rationnelles” describing the iteration of complex rational functions (see [17]).

REMARK 1.57. Note that our notion of Julia set is not tied only to errors or approximations that a computer might introduce. The issue is to know whether or not a tiny error in the seed value (no matter what or who created the error) *could* produce a significant error in some orbit value. For example, the seed  $z_0 = i$  would be in the Julia set of  $f(z) = z^2$  even though its orbit  $i, -1, 1, 1, 1, \dots$  is computed *exactly* by a computer. However, we still say it is a chaotic seed value since given *any* allowable error in the seed value (even an error as small as  $10^{-631}$ ), we can always find another seed  $z'_0$  *close to*  $z_0 = i$  (i.e., within the tiny allowable error) such that  $z'_0$  has a drastically different orbit from the orbit of  $z_0$ . Thus, even if a computer wouldn’t introduce an error of any kind in its orbit calculation for a specific seed  $z_0$ , the seed value might still be in the Julia set.

From the above discussion we see that the Julia set for  $f(z) = z^2$  is  $C(0, 1)$  because the dynamics there are *chaotic*, i.e., for any  $z_0 \in C(0, 1)$  there is a point  $z'_0$  arbitrarily close by that has a drastically different orbit. As we have seen, the computer often fails to be accurate here since we would need the computer to store such a value (and each point in its orbit) with an *infinite* degree of accuracy. To put it another way, approximation of the starting value (or some future iterate value) ruins our confidence in the calculations of the long term behavior. This is called *sensitive dependence on initial conditions*, and this is the defining feature in what is called *chaos*.

We call the complement  $\overline{\mathbb{C}} \setminus C(0, 1)$  the *stable set* for  $f(z) = z^2$  because orbits are stable there, i.e., for any  $z_0 \in \overline{\mathbb{C}} \setminus C(0, 1)$  its orbit  $z_n$  will behave like the orbit  $z'_n$  of any seed value  $z'_0$  chosen sufficiently close to  $z_0$ . In honor of Pierre Fatou the stable set is commonly called the *Fatou set* because of his role in developing the theory of complex function iteration in 1917 (see [12, 13, 14]). In honor of their pioneering work in the field, dynamics of complex analytic functions is often called the Fatou-Julia theory.

EXERCISE 1.58. Use your intuitive understanding of the meanings of the Fatou and Julia sets to determine each of these sets for the maps  $h(z) = z + 1, g(z) = z/2$  and  $k(z) = 3z$ . **Try it out!**

EXERCISE 1.59. Try on your own to write down a precise mathematical definition of the Fatou set and the Julia set that will work for any rational function  $g(z)$  defined on  $\overline{\mathbb{C}}$ . In particular, try to formulate what it means for orbits to be drastically or significantly different. **Try it out!**

**Notation:** For a rational function  $g(z)$ , we employ the notation  $F(g)$  for the *Fatou set* of  $g$  and  $J(g)$  for the *Julia set* of  $g$ . Formal definitions are given in chapter Appendix 1.A on page 96. These should be read, but note that it is not necessary to know these formal definitions well to continue on in the text; an intuitive understanding of these ideas will allow you to progress through this text just fine.

We showed that  $J(f) = C(0, 1)$  for the map  $f(z) = z^2$  by noting that for any seed  $z_0 \in C(0, 1)$  there is a point arbitrarily close to  $z_0$  whose orbit tends to  $\infty$  (and is thus drastically different from the orbit of  $z_0$  which must remain on  $C(0, 1)$ ). However, it is also true that  $f$  is even chaotic on  $C(0, 1)$  if we restrict ourselves to only using seed values from  $C(0, 1)$ . To see this, consider  $z_0 = e^{i\theta}$  written in polar form. For any nearby point  $z'_0 = e^{i\alpha}$  we must, due to the angle doubling nature of  $f$ , have that the distance  $|f(z_0) - f(z'_0)| > |z_0 - z'_0|$ . Indeed, denoting the (arclength) distance between  $z_0$  and  $z'_0$  along the unit circle by  $\beta = |\theta - \alpha|$ , we see that the distance between  $f(z_0)$  and  $f(z'_0)$  along the unit circle will then be  $2\beta$ . Inductively, we see that the distance between  $f^n(z_0)$  and  $f^n(z'_0)$  along the unit circle will be  $2^n\beta$ , as long as  $2^n\beta < \pi$ . Clearly then, no matter how close  $z_0$  and  $z'_0$  start out, i.e., no matter how small  $\beta$  is, corresponding orbit points will eventually be “far” apart. More precisely, as soon as  $2^n\beta > \pi/3$  we must have  $|f^n(z_0) - f^n(z'_0)| > 1$ . Thus arbitrarily close seed values on  $C(0, 1)$  do not have corresponding orbit values that *forever* stay arbitrarily close. Use the *Complex Function Iterator Applet* (using both **Polar computation** mode and **Polar seed form**) to witness this sensitive dependence. In particular, simultaneously iterate (one step at a time) **Seed 1**  $z_0 = e^{2.18i}$  and **Seed 2**  $z'_0 = e^{2.19i}$ .

We close this section by reflecting on some commonalities between the Newton Map dynamics we have seen in Section 1.2.4 and the dynamics of  $f(z) = z^2$ . As we saw in each Newton’s method example, so too for the  $f(z) = z^2$  dynamics, any two basins of attraction of attracting fixed points share a common boundary. In the case of  $f(z) = z^2$ , the basins  $A_f(0)$  and  $A_f(\infty)$  share the common boundary which turns out to be exactly the Julia set  $J(f) = C(0, 1)$  where, informally speaking, the attractive “pull” of each attracting fixed point is balanced by the other. The reader who read all of Section 1.2 should now go back and consider each complex Newton’s method example to convince himself or herself that in those cases too the Julia set of the Newton map is exactly the common boundary of any attracting basin. This is no coincidence and we state the precise result as follows.

**THEOREM 1.60.** Let  $f(z)$  be a rational map. If  $w$  is an attracting fixed point of  $f(z)$ , then  $\partial A_f(w) = J(f)$ .

**REMARK 1.61.** Theorem 1.60 together with Proposition 1.21 implies Theorem 1.35.

**REMARK 1.62.** In Theorem 1.60, if we do not demand that the fixed point be attracting, then the conclusion might not follow. We saw this in Example 1.50 where  $A_h(\infty) = \overline{\mathbb{C}}$  which has empty boundary, but  $J(h) = \{\infty\}$  which we leave the reader to show.



AN INCOMPLETE SKETCH OF THE PROOF OF THEOREM 1.60. Showing the full details of this proof requires both a precise definition of Julia set and a little advanced complex analysis beyond the level of this text. Instead we provide just a sketch of some of the arguments. By Additional Exercise 1.169,  $A_f(w)$  is an open set. Thus each point in  $A_f(w)$  has a whole neighborhood of points whose orbits all act the same way, showing (albeit informally)  $A_f(w) \subseteq F(f)$ . Likewise, any point in  $\partial A_f(w)$  contains points arbitrarily close which iterate to  $w$  and points arbitrarily close whose orbit points stay far away from  $w$ . Thus such a point must be in the Julia set, i.e.,  $\partial A_f(w) \subseteq J(f)$ . What remains is to show that  $\overline{\mathbb{C} \setminus A_f(w)}$  is in the Fatou set. By showing  $f(\overline{\mathbb{C} \setminus A_f(w)}) \subseteq \overline{\mathbb{C} \setminus A_f(w)}$ , one may use Montel's Theorem (Theorem 1.208) to conclude  $\overline{\mathbb{C} \setminus A_f(w)} \subseteq F(f)$ . We leave it to the interested reader to pursue the finer details of the proof in p. 58 of [2].  $\square$

**1.3.3. Dynamics of maps of the form  $f_c(z) = z^2 + c$ .** We have carefully investigated the dynamics of the map  $f(z) = z^2$  (though there is still more to say since a finer analysis of the dynamics on  $C(0, 1)$  reveals some very interesting behavior - see Remark 1.212 and Additional Exercises 1.171 and 1.206). Now we investigate what effect there will be when we change the map by adding a constant.

One justification for studying this (although the only justification a mathematician usually requires is that the resulting problem be interesting) is in line with our theme of wanting to know what happens when the system we are studying is tweaked a little bit, or has some error causing us to believe that we cannot be 100% certain that our mathematical model is *exactly* correct (as opposed to being just a very good approximation). In the dynamics of  $f(z) = z^2$  above, we identified which seed values  $z_0$  were stable (i.e., in the Fatou set) or chaotic (i.e., in the Julia set) by studying the effects of allowing arbitrarily small errors in the *seed value*. Now we will investigate what type of stability may or may not be present when we allow for an error or *perturbation* in the *map* we are iterating.

Hence, we will consider the dynamics of maps of the form  $f_c(z) = z^2 + c$  where  $c$  is a complex parameter. Thus, we will fix a  $c_0$  value and study the dynamics of  $f_{c_0}$ . Then we will vary the  $c$  parameter a little and study whether or not the dynamics of the resulting maps  $f_c$  have similar behavior. Just as we saw the seed values  $z$  for a fixed map get naturally split into the stable Fatou set and the chaotic Julia set, so too will we see the set of all parameter values  $c$  be naturally split into *stable* parameters and what we will call *bifurcation* parameters.

We begin by noting a common aspect of the dynamics of  $f_c$  for all values of  $c$ . Each map  $f_c$  has a super attracting fixed point at  $\infty$  (which the reader should formally verify by either checking the behavior of  $f_c$  near  $\infty$  or by checking the multiplier of the fixed point at  $\infty$ ). Thus, if any part of the orbit  $z_n = f_c^n(z_0)$  of some seed value  $z_0$  should be *large enough* (by this we mean that  $|z_n|$  is large enough), then the orbit will tend to  $\infty$ . A careful calculation in Additional Exercise 1.189 shows that for the maps  $f_c$ , we have  $|z_k| > \max\{2, |c|\}$  for some  $k \in \mathbb{N}$  if and only if  $z_n \rightarrow \infty$ .

We begin by considering a small perturbation of the map  $f_0(z) = z^2$ . If we let  $c$  be very small (by which we mean  $|c|$  is small), then we might expect the dynamics of  $f_c$  to be very similar to the dynamics of  $f_0(z) = z^2$ . This turns out to be true in many respects.

EXPLORATION 1.63. Fix  $c = 0.1$  and use the *Complex Function Iterator Applet* to study the dynamics of  $f_{0.1}(z) = z^2 + 0.1$ . Try many different seed values including  $z_0 = 0, 1 + i, -2 - 0.5i, \dots$  and record the different types of behavior you are able to find. **Try it out!**

As in the  $f_0$  case, it seems we have only two types of long term behavior. In particular, iterates of  $f_{0.1}$  seem to either approach  $\infty$  or they approach the attracting fixed point  $p \approx 0.1127$ . The intuition we've built up, however, tells us that this cannot be the whole story. If there are two attracting fixed points, then we expect there to be some "tension" between attracting basins, and that points on the boundaries of these basins will not be attracted to either fixed point. Recall, that the boundaries of the two attracting basins for the map  $f_0(z) = z^2$  were both equal to the chaotic set  $J(f_0) = C(0, 1)$ . Similarly, this same phenomenon occurs with the map  $f_{0.1}$ , except that the chaotic set  $J(f_{0.1})$  is not a circle (though some advanced mathematics can show that it is a simple closed curve, see [2], p. 126). Let's now use the *Global Complex Iteration Applet for Polynomials* to see a picture of  $J(f_{0.1})$ . This applet will color each seed in the basin of attraction of  $\infty$  for the map  $f_{0.1}$  based on how many iterates it takes for the orbit to become strictly larger than  $\max\{2, |0.1|\} = 2$ , and it will color the remaining points black. By Theorem 1.60, the basin  $A_{f_{0.1}}(\infty)$  has boundary set equal to  $J(f_{0.1})$ . Experiment with iterating seed values (two at a time) near  $J(f_{0.1})$  to see the sensitive dependence on initial conditions. **Try it out!**

The set of points colored in black in the applet has a special name which we present here in general terms for any polynomial.

DEFINITION 1.64. For a polynomial  $g(z)$ , we define the *filled-in Julia set*  $K(g)$  to be the set of points which do not iterate to  $\infty$ , i.e.,

$$K(g) = \{z \in \mathbb{C} : \{g^n(z)\}_{n=0}^{\infty} \text{ is bounded in } \mathbb{C}\} = \overline{\mathbb{C}} \setminus A_g(\infty).$$

REMARK 1.65. For a polynomial  $g(z)$  of degree greater than or equal to two (which must then have a super attracting fixed point at  $\infty$ ), it is true that  $\partial A_g(\infty) = \partial K(g)$ , and so by Theorem 1.60 we have  $J(g), \partial A_g(\infty)$  and  $\partial K(g)$  are all identical sets. The reader is asked to prove this in Additional Exercise 1.174.

Returning to the dynamics of the map  $f_{0.1}$ , we ask if we could have predicted ahead of time that there would be a finite attracting fixed point? The answer is yes, and here is how. We find the two finite fixed points of  $f_{0.1}$  by solving the equation  $f_{0.1}(z) = z$  (do you see why?). Doing this we then show that the two finite fixed points  $p = (1 - \sqrt{0.6})/2$  and  $q = (1 + \sqrt{0.6})/2$  are attracting and repelling, respectively, since  $|f'_{0.1}(p)| < 1$  and  $|f'_{0.1}(q)| > 1$ .

One way to relate the dynamics of  $f_0$  and  $f_{0.1}$  is to say that when the  $c$  parameter moves from  $c = 0$  to  $c = 0.1$ , (a) the super attracting fixed point at  $0$  with multiplier  $\lambda_0 = 0$  becomes an attracting fixed point at  $p \approx 0.1127$  with multiplier  $\lambda_p = f'_{0.1}(p)$ , (b) the circle  $J(f_0)$  becomes a slightly distorted circle  $J(f_{0.1})$ , and (c) the super attracting fixed point at  $\infty$  persists, i.e., remains a super attracting fixed point for  $f_{0.1}$ . Thus the small change in the  $c$  parameter led to only a small change in the dynamics.

Let us explore other  $c$  values to decide which  $c$  values have similar dynamics to  $f_0$  and which do not.

EXERCISE 1.66. Fix  $c = 0.2 + 0.2i$  and use the *Global Complex Iteration Applet for Polynomials* to study the dynamics of  $f_{0.2+0.2i}(z) = z^2 + 0.2 + 0.2i$  and to see the global picture of the attracting basins and the Julia set. Calculate by hand the *exact* value of the attracting fixed point of this map. You can test your calculation by using the applet to iterate a nearby seed. **Try it out!**

Now let us see what happens if we move the parameter  $c$  somewhat far from  $0$ .

EXERCISE 1.67. Fix  $c = -1$  and use the *Global Complex Iteration Applet for Polynomials* to study the dynamics of  $f_{-1}(z) = z^2 - 1$ . Are the dynamics similar to that of  $f_0$ ? **Try it out!**

EXERCISE 1.68. By generalizing the calculations done in the  $c = 0.1$  case, mathematically describe the set  $K_1$  of all  $c$  values such that  $f_c$  has a finite attracting fixed point in  $\mathbb{C}$ . Start by solving an equation to find the fixed points, and then consider what conditions need to be met to make one of these fixed points attracting. Note that for all  $c$  values,  $f_c$  always has fixed points. Our goal is to determine for what  $c$  values will there be a fixed point which is *attracting*. You can see the picture of  $K_1$ , which is called a *cardioid* (heart shaped region) in Figure 1.13. **Try it out!**

By examining the attracting basins and Julia sets for maps  $f_c$  where  $c \in K_1$  (using the *Global Complex Iteration Applet for Polynomials*) you will see that each such function has dynamics similar to the dynamics of  $f_0$ . Thus we have witnessed our first example of ***stability in the parameter***, i.e., for any  $c$  in this set of parameters, the dynamics does not fundamentally change when you move the parameter around a little bit. Another way of saying this is that  $K_1$  is an *open* set of parameter values.

We know that for each  $c \in K_1$  there is an attracting fixed point  $p_c$  of the map  $f_c$ . Let's call  $\lambda(c)$  the multiplier at  $p_c$  and thus, using Theorem 1.49 which says that the multiplier of a (super) attracting fixed point must have modulus strictly less than 1, we may regard  $\lambda$  as a map from  $K_1$  into  $\Delta(0, 1)$ . If we follow the calculations in the above Exercise 1.68 carefully, we see that this ***multiplier map***  $\lambda : K_1 \rightarrow \Delta(0, 1)$  is one-to-one, continuous, and onto (onto means that for every  $\lambda_0 \in \Delta(0, 1)$  there is a parameter  $c_0 \in K_1$  such that  $\lambda(c_0) = \lambda_0$ ). In fact, this map can be *extended*<sup>13</sup> to be

<sup>13</sup>We say a map  $g$  defined on its domain set  $D$  can be *extended* to a larger set  $\tilde{D} \supset D$ , if there exists an extension map  $\tilde{g}$  on  $\tilde{D}$  such that  $\tilde{g} = g$  on  $D$ . By a slight abuse of notation we use  $g$  to denote the extension, which simply means that we assume  $g$  itself is defined on the larger set  $\tilde{D}$ .

defined and continuous on all of  $\overline{K_1}$ . However, for  $c \in \partial K_1$  we only have  $\lambda(c) \in C(0, 1)$  and the corresponding fixed point  $p_c$  is indifferent.

Let us explicitly compute this multiplier map and consider the meaning and significance of its inverse map. By a direct calculation, we see that  $p_c = (1 - \sqrt{1 - 4c})/2$  and  $q_c = (1 + \sqrt{1 - 4c})/2$  are the fixed points of  $f_c$ . Note that  $p_c$  will be attracting for an appropriate choice of  $c$ , but  $q_c$  will always be repelling (why?). Hence, the multiplier map is given by  $\lambda = \lambda(c) = f'_c(p_c) = 2p_c = 1 - \sqrt{1 - 4c}$ , when  $c \in K_1$ . The inverse of the multiplier map, as you can readily compute, is then  $c = c(\lambda) = \frac{\lambda}{2} - \frac{\lambda^2}{4}$ , which gives the  $c$  value for a fixed point with prescribed multiplier  $\lambda$ . Since  $c$  values in  $K_1$  must correspond to (super)attracting fixed points, the set  $K_1$  must be the image of the set of all  $\lambda \in \Delta(0, 1)$  under the map  $c(\lambda)$ . This produces the set  $K_1$  illustrated in Figure 1.13 which you should take a moment to verify using the *ComplexTool Applet*.

**EXERCISE 1.69.** The Multiplier map and its Inverse.

- Find the  $c$  value such that  $f_c$  has an attracting fixed point  $p_c$  with multiplier  $\lambda = 0.7e^{\pi i/4}$ , and then use an applet to illustrate the attractiveness of  $p_c$  by iterating points near it.
- Find the  $c$  value such that  $f_c$  has an indifferent fixed point  $p_c$  with multiplier  $\lambda = e^{\pi i/3}$ , and then use an applet to illustrate the behavior of orbits of points near  $p_c$ .

Additional Exercise 1.175 will help the reader gain a better understanding of the role the multiplier plays in the dynamics near a fixed point. The reader may go on without doing this exercise now, but for a deeper understanding the reader should take the time to do it now.

**1.3.4. Cycles for the map  $f_c(z) = z^2 + c$ .** As we saw above, the orbit of 0 under the map  $f_{-1}(z) = z^2 - 1$  is  $-1, 0, -1, 0, -1, 0, \dots$ . We summarize this situation by saying that  $f_{-1}$  has a 2-cycle  $\{0, -1\}$ . Also, as we saw (for example, by iterating the seed  $z_0 = 0.2 - 0.3i$ ), this 2-cycle seems to be *attracting* (actually, we discuss later that this cycle can even be properly labeled *super attracting*).

**EXERCISE 1.70.** Modify Definition 1.16 of an attracting fixed point to come up with your own definition of an attracting 2-cycle. ***Try it out!***

**EXERCISE 1.71.** Modify Definition 1.14 of an attracting basin of a point to come up with your own definition of an attracting basin for a 2-cycle. ***Try it out!***

Using an applet to produce the orbit of several seed values, we again seem to have only two types of long term behavior for the map  $f_{-1}$ . In particular, iterates of  $f_{-1}$  seem to either approach  $\infty$  or they “approach” the 2-cycle  $\{0, -1\}$ . Our intuition, however, suggests that this cannot be the whole story. Tension between attracting “basins” probably leads to points which are neither attracted to  $\infty$  nor to the 2-cycle  $\{0, -1\}$ . Use the *Global Complex Iteration Applet for Polynomials* to see these basins, and the corresponding Julia set. ***Try it out!***

EXAMPLE 1.72. Let  $c = -0.9 - 0.1i$  and use one of the applets to study the dynamics of the map  $f_{-0.9-0.1i}(z) = z^2 + (-0.9 - 0.1i)$  to verify that this map also has an attracting 2-cycle. **Try it out!**

EXAMPLE 1.73. Let  $c = -0.13 + 0.73i$  and use one of the applets to study the dynamics of the map  $f_{-0.13+0.73i}(z) = z^2 + (-0.13 + 0.73i)$  to verify that this map has what we should naturally call an attracting 3-cycle. **Try it out!**

Ultimately we would like to calculate (by hand, or at least only use the computer when we know we will get trustworthy results) which  $c$  parameters will lead to the map  $f_c(z) = z^2 + c$  having an attracting 2-cycle, an attracting 3-cycle, an attracting 4-cycle, and so on. We will be able to make some progress on this question, but our methods, as you will see, will hit the familiar road block of trying to find the roots of a polynomial of high degree. We begin by first defining cycles of any length and then we see how to classify cycles as attracting/repelling/indifferent by using the derivative (or more precisely the multiplier).

### 1.3.5. $p$ -Cycles and their Classification.

DEFINITION 1.74 (Cycles). A point  $w \in \overline{\mathbb{C}}$  is called *periodic with period  $p$*  for the map  $f$  if  $f^p(w) = w$  and  $w, f(w), \dots, f^{p-1}(w)$  are distinct points. In this case we call the set  $\{w, f(w), \dots, f^{p-1}(w)\}$  a  *$p$ -cycle* for the map  $f$ .

Thus we see that periodic points correspond exactly to fixed points of higher iterates  $f^p$  of the map  $f$ . For example, the periodic point of period 2 at  $w = 0$  for the map  $f_{-1}$  is a fixed point of the second iterate  $f_{-1}^2$ . We can then use this fact to classify a *cycle* as attracting/repelling/indifferent based on the multiplier of the corresponding iterate.

DEFINITION 1.75 (Multiplier for Cycles). Suppose the set  $\{w_0, \dots, w_{p-1}\}$  forms a  $p$ -cycle for the map  $f$ . We define the *multiplier*  $\lambda$  of this cycle (also called the multiplier of each point  $w_0, \dots, w_{p-1}$  of period  $p$ ) to be the multiplier of the map  $f^p$  at its fixed point  $w_0$ . Then the  $p$ -cycle  $\{w_0, \dots, w_{p-1}\}$  of the map  $f$  is called

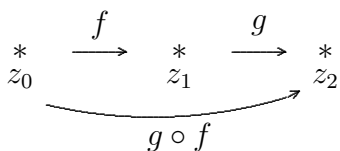
- a) *super attracting* if  $\lambda = 0$
- b) *attracting* if  $0 < |\lambda| < 1$
- c) *repelling* if  $|\lambda| > 1$
- d) *indifferent* if  $|\lambda| = 1$ .

As for fixed points, we say the cycle is (super)attracting when it is known that either case (a) or (b) holds.

EXAMPLE 1.76. The 2-cycle  $\{0, -1\}$  for the map  $f_{-1}$  is super-attracting since  $\lambda = (f_{-1}^2)'(0) = f_{-1}'(0) \cdot f_{-1}'(f_{-1}(0)) = f_{-1}'(0) \cdot f_{-1}'(-1) = 0$ . We note also that instead of using 0 we could have used the other point in the 2-cycle to calculate  $\lambda = (f_{-1}^2)'(-1) = f_{-1}'(-1) \cdot f_{-1}'(f_{-1}(-1)) = f_{-1}'(-1) \cdot f_{-1}'(0) = 0$ .

Since the multiplier  $\lambda$  of a  $p$ -cycle is defined via the derivative of  $f^p$ , the  $p$ -fold composition of  $f$  with itself, is very important to understand the use of the chain rule, as seen in Example 1.76, in the classification of  $p$ -cycles. And so we now examine it more closely.

**Chain Rule in  $\mathbb{C}$ :** If  $f$  and  $g$  are analytic functions at **finite points**  $z_0$  and  $z_1$ , respectively, and if  $z_0 \xrightarrow{f} z_1 \xrightarrow{g} z_2$ , then  $(g \circ f)'(z_0) = g'(f(z_0))f'(z_0) = g'(z_1)f'(z_0)$ . In other words, in order to compute the derivative of the composite function, we simply multiply the derivatives of each function (evaluated at the appropriate point) along the way.



Now suppose that set of **finite points**  $\{w_0, \dots, w_{p-1}\}$  forms a  $p$ -cycle for the analytic map  $f$  as pictured in Figure 1.12.

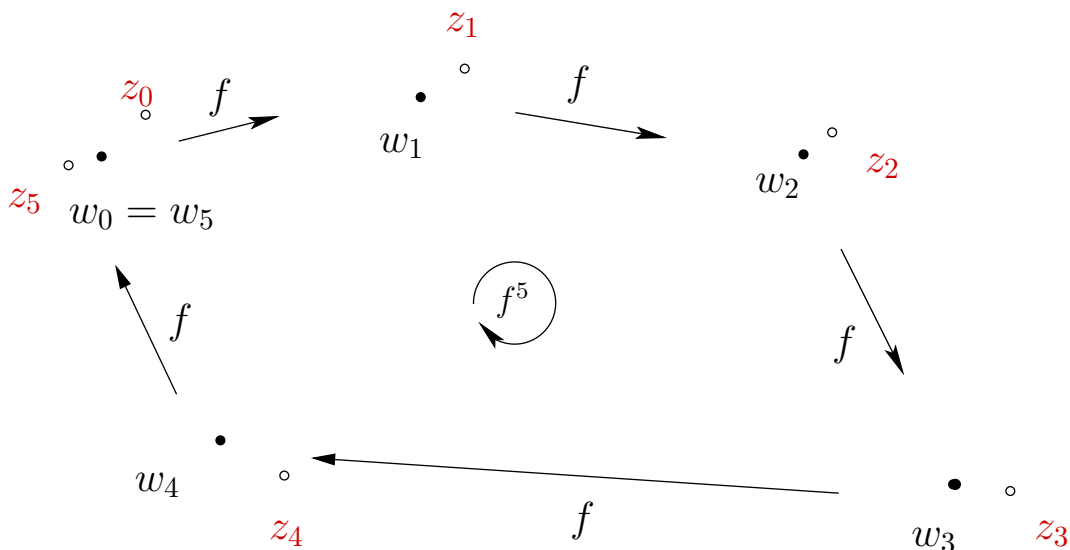


FIGURE 1.12. Illustration of a 5-cycle  $\{w_0, w_1, \dots, w_4\}$  along with the partial orbit of a point  $z_0$  chosen near  $w_0$ .

We have  $f^p(w_0) = w_0$ , and so by the chain rule we compute

$$(1) \quad \lambda = (f^p)'(w_0) = f'(w_0)f'(w_1) \dots f'(w_{p-1}) = (f^p)'(w_j), \text{ for } j = 0, \dots, p-1,$$

which shows, among other things, that the definition of the multiplier in Definition 1.75 is well defined since the derivative of  $f^p$  is the same at any point in the cycle.

We now wish to understand the relationship between the classification of the cycle as attracting/repelling/indifferent (determined by  $\lambda$ ) and the dynamics of the map  $f$  near the cycle. We first note that simply by *continuity* of the map  $f$ , for any seed  $z_0$  sufficiently close to  $w_0$ , the orbit points  $z_1, \dots, z_{p-1}, z_p$  will be close to the points  $w_1, \dots, w_{p-1}, w_0$ , respectively. Supposing that  $|\lambda| < 1$ , the map  $f^p$  has an attracting fixed point at  $w_0$ . Thus, if we choose a seed  $z_0$  sufficiently close to  $w_0$ , we must have that  $f^p(z_0)$  is closer to  $w_0$  than  $z_0$  is (i.e.,  $|f^p(z_0) - w_0| < |z_0 - w_0|$ ) by Definition 1.16 applied to the fixed point  $w_0$  of the map  $f^p$ . We also note that this argument works equally well for any of  $w_1, \dots, w_{p-1}$  as it does for  $w_0$ , and so one way to describe such an attracting cycle is to say that each time you apply the map  $f$  for a total of  $p$  times, points near any  $w_k$  will move around the cycle only to return closer to  $w_k$ . See Figure 1.12 where the orbit of  $z_0$  exhibits this behavior. In a similar way we justify the classification of repelling cycles.

Note that the above calculations require only minor modifications when one of the points  $w_k$  in the cycle is  $\infty$ . In the spherical metric, where  $\infty$  does not play a more special role than any other point in  $\mathbb{C}$ , one sees that the dynamic behavior (attraction/repulsion) of the cycle behaves in the same fashion as described above for cycles in the finite plane  $\mathbb{C}$ .

**1.3.6. Attracting cycles for the maps  $f_c(z) = z^2 + c$ .** Let us return to investigating the dynamics of the maps  $f_c$ . We have seen two examples of maps of the form  $f_c(z) = z^2 + c$  with attracting 2-cycles. Let us now determine the set  $K_2$  of all  $c$  values such that  $f_c$  has an attracting 2-cycle.<sup>14</sup> Any point in a 2-cycle must (a) be a fixed point of  $f_c^2$ , and (b) **not** be a fixed point of  $f_c$ . Thus we wish to solve the equation A:  $(z^2 + c)^2 + c = z$  and exclude the solutions of equation B:  $z^2 + c = z$ . Since each solution to B, rewritten as  $z^2 + c - z = 0$ , is a solution to A, rewritten as  $(z^2 + c)^2 + c - z = 0$ , we have that  $z^2 + c - z$  must divide  $(z^2 + c)^2 + c - z$ . After doing some long division, we can then rewrite A as  $(z^2 + z + 1 + c)(z^2 + c - z) = 0$ . Thus a 2-cycle  $\{u, v\}$  must be such that both  $u$  and  $v$  solve the equation  $(z^2 + z + 1 + c) = 0$ , i.e.,  $(z - u)(z - v) = z^2 + z + 1 + c$ , which after expanding and comparing coefficients implies  $uv = 1 + c$ . According to Equation (1) the multiplier of the 2-cycle  $\{u, v\}$  is  $\lambda = f'_c(u)f'_c(v) = 4uv = 4(1 + c)$ . Hence this 2-cycle will be attracting exactly when  $4|1 + c| = |\lambda| < 1$ , i.e., when  $|c - (-1)| < 1/4$ . Hence  $K_2 = \Delta(-1, 1/4)$ , which is the disk pictured in Figure 1.13.

EXPLORATION 1.77. Test various  $c$  values in  $K_2$  by using the *Global Complex Iteration Applet for Polynomials* to see that you do indeed get an attracting 2-cycle. Which seed values in the picture produced by the applet seem to “find” the attracting 2-cycle? **Try it out!**

In Additional Exercise 1.176 the reader is asked to investigate the relationship between the multiplier and the convergence towards the 2-cycle. And in Additional

<sup>14</sup>As 2-cycles generally exist, the issue here is to determine when such a cycle will be *attracting*.

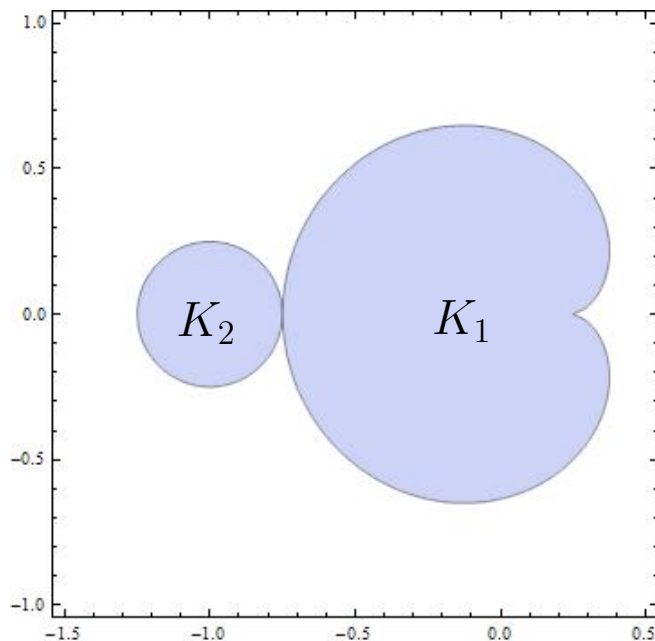


FIGURE 1.13. Parameter space of  $c$  values showing the cardioid  $K_1$  with cusp at  $c = 1/4$  and the disk  $K_2 = \Delta(-1, 1/4)$ . The boundaries of  $K_1$  and  $K_2$  meet at  $c = -3/4$ .

Exercise 1.177 the reader is asked to investigate another multiplier map (this time defined on  $K_2$ ) and its inverse.

Let us now try to determine the set  $K_3$  of all  $c$  parameters which lead to attracting 3-cycles for  $f_c(z) = z^2 + c$ . Any point in a 3-cycle must (a) be a fixed point of  $f_c^3$ , and (b) **not** be a fixed point of  $f_c$ , and so must solve (when substituted for  $z$ ) the eighth degree polynomial  $[(z^2 + c)^2 + c]^2 + c - z = 0$ , but not be a root of  $z^2 + c - z = 0$ . After long division, as above, we are still left with a degree six polynomial to solve if we are to find the points of the 3-cycle. Thus we see that since we cannot, in general, solve a polynomial of degree five or greater, we will have considerable more difficulty determining the attracting 3-cycles for maps of the form  $f_c(z) = z^2 + c$ . However, in the above calculation we were able to locate the  $c$  values that correspond to attracting 2-cycles without ever having to explicitly solve for the points of the cycle (although we could have since it is just a matter of applying the quadratic formula). We wonder then if it is possible to use similar techniques, or devise new ones, to describe as much as we can of this set  $K_3$ .

LARGE PROJECT 1.78. Is it possible to determine the set  $K_3$  precisely, as was done for  $K_1$  and  $K_2$ ? Even though we might not be able to explicitly solve the degree six polynomial mentioned above, perhaps one can use other root solving techniques (such as Newton's method) to approximate roots to a high enough degree to be useful. Such



roots could then be tested with the *Global Complex Iteration Applet for Polynomials* to see their role in the dynamics of  $f_c$ . Related questions of interest are: Can you show the fact (not proven in this chapter) that  $K_3$  is an open set? It turns out that  $K_3$  has more than one connected component (as opposed to  $K_1$  and  $K_2$  which were connected). Can you determine how many connected components  $K_3$  has and what relationship these components have to each other? Can you find the  $c$  parameters which lead to *super attracting* 3-cycles? The roots of the aforementioned degree six polynomial must include three points which make up the attracting 3-cycle, but what do the other three points represent? Will any of these techniques yield useful results for the problem of finding the  $c$  parameters which yield attracting 4, 5, 6, . . . cycles?

We present a definition and theorem (whose proof is beyond the scope of this text) which might be of some use in understanding the above project.

**DEFINITION 1.79** (Hyperbolic Components). For each  $n \in \mathbb{N}$ , we define the set  $K_n$  to be the set of parameters  $c$  such that  $f_c$  has an attracting  $n$ -cycle. We call any connected component<sup>15</sup>  $W$  of some  $K_n$  a *hyperbolic component* of  $K_n$ .

Although  $K_1$  and  $K_2$  are connected sets, it is true that some of the  $K_n$  are disconnected. Each piece, that is, connected component of  $K_n$ , however, has the following nice property corresponding to its multiplier map.

**THEOREM 1.80** (Multiplier Map Theorem ([2], p. 134)). Let  $W$  be a hyperbolic component of some  $K_n$ . Let  $\lambda : W \rightarrow \Delta(0, 1)$  be the multiplier map which takes each parameter  $c \in W$  to the multiplier  $\lambda(c)$  of the associated attracting  $n$ -cycle. Then the map  $\lambda$  is one-to-one, analytic, and onto, i.e., it maps  $W$  conformally onto  $\Delta(0, 1)$ . Furthermore, the map  $\lambda$  extends<sup>16</sup> to be a one-to-one continuous map of  $\overline{W}$  onto  $\overline{\Delta(0, 1)}$ .

**DEFINITION 1.81.** For a hyperbolic component  $W$  of  $K_n$ , we call the unique  $c \in W$  the *center* of  $W$  if  $\lambda(c) = 0$ , i.e., it is the unique  $c$  in  $W$  for which  $f_c$  has a *super attracting*  $n$ -cycle.

**EXAMPLE 1.82.** We have already observed that the center of  $K_1$  is  $c = 0$  and the center of  $K_2$  is  $c = -1$ .

One can **explicitly** show this theorem to be true for the parameter sets  $K_1$  and  $K_2$  by actually writing down and studying the multiplier map (see Additional Exercise 1.177). For the other sets  $K_n$ , however, it is not so easy. The proof of Theorem 1.80 uses key properties of the multiplier map without explicitly constructing it. One important application of this result is that it proves that each hyperbolic component  $W$  of  $K_n$  is open since it is the *conformal*<sup>17</sup> image of an open set, namely  $W = \lambda^{-1}(\Delta(0, 1))$ . Hence, each  $K_n$  is also open.

<sup>15</sup>See Appendix B.3 on page 423 for the definition of a *component*.

<sup>16</sup>See Footnote 13 on p. 35.

<sup>17</sup>Recall, that a map is called *conformal* when it is both one-to-one and analytic.

As we have seen, if we move the parameter  $c$  within the cardioid  $K_1$ , the dynamics of  $f_c(z) = z^2 + c$  do not change much. Similarly, if we move the parameter  $c$  within the disk  $K_2$ , the dynamics of  $f_c(z) = z^2 + c$  do not change much. For these reasons we call  $K_1$  and  $K_2$  *stable* regions of parameter space. It is also true that each  $K_n$  is a stable region of parameter space, which, given its definition, is really just another way of saying that  $K_n$  is an *open* set. This follows from above, but also seems reasonable without appealing to Theorem 1.80. Note that if you gently tweak a function with an attracting cycle (keeping in mind the strict inequality condition on the multiplier), then it seems reasonable the new function will still have an attracting cycle (i.e., will have a strict inequality condition on the multiplier) in roughly the same place (see Additional Exercise 1.178). This is exactly what we witness when we move the  $c$  parameter by small amounts within the cardioid  $K_1$  or within the disk  $K_2$ . We **cannot**, however, expect this to happen with an indifferent fixed point (or cycle) since by tweaking the multiplier of an indifferent fixed point, the modulus could easily be strictly less than one (attracting) or strictly greater than one (repelling), instead of remaining exactly equal to one.

As opposed to the stable parameters found in the sets  $K_n$ , we call a parameter  $c$  **unstable** if there are parameters arbitrarily close for which the maps  $f_c(z) = z^2 + c$  have fundamentally different dynamics. For example,  $c = -3/4$  is an unstable parameter.

EXPLORATION 1.83. The reader should now pause before reading further to write down several reasons why  $c = -3/4$  is an unstable parameter. Use the *Global Complex Iteration Applet for Polynomials* to explore the dynamics when  $c$  is close to  $c = -3/4$ , paying special attention to the dynamics for  $c_1 = -0.75 + .05i$ ,  $c_2 = -0.75 - .05i$  and  $c_3 = -0.75 + .05i$ . **Try it out!**

Now that the reader has provided their own reasons, we go on to illustrate the unstable nature of the parameter  $c = -3/4$  by describing three particular ways in which the dynamics changes at this  $c$  value. We note how the type of attracting cycle, the Julia set, and the orbit of the origin all undergo *fundamental* changes. We call  $c = -3/4$  a *bifurcation point*, since it is the parameter on the boundary of two regions in parameter space where the corresponding dynamics undergoes a fundamental change.

1. **Attracting Cycle:** We first note that we don't even have to know the dynamics exactly at the point  $c = -3/4$  to show it is unstable. It is enough to know that there are parameters arbitrarily close to and less than  $c = -3/4$  (in  $K_2$ ) which give rise to an attracting 2-cycle (but no attracting fixed point) and there are parameters arbitrarily close to and greater than  $c = -3/4$  (in  $K_1$ ) which give rise to an attracting fixed point (but no attracting 2-cycle). The reader can verify that as  $c$  decreases to and then past  $-3/4$  the attracting fixed point becomes indifferent and then "splits" into an attracting 2-cycle.<sup>18</sup>

---

<sup>18</sup> A different way to look at this is to instead say that as  $c$  decreases to  $-3/4$  the attracting fixed point merges with a repelling 2-cycle to form an indifferent fixed point exactly at  $c = -3/4$ . Then

2. **Julia Set:** We can also see the result of this fundamental change in dynamics by looking at the Julia sets  $J(f_c)$  as we vary  $c$ . For example, if we start at  $c = 0$  and then slowly decrease  $c$ , we see the Julia sets  $J(f_c)$  change from a circle to a distorted circle. Decreasing  $c$  further towards  $c = -3/4$ , we see the distorted circle  $J(f_c)$  begins to have infinitely many “bulbs” partially forming as the distorted circle  $J(f_c)$  starts “pinching in”. Exactly at  $c = -3/4$  pinching in for each of the infinitely many distinct bulbs *simultaneously* becomes complete. Thus we have gone from having one bounded component of  $F(f_c)$  for  $c \in (-3/4, 1/4)$  consisting of one attracting basin of an attracting fixed point to the situation for  $c \in (-5/4, -3/4)$  where there exist infinitely many bounded components of  $F(f_c)$  consisting of the attracting basin of an attracting 2-cycle.

3. **Orbit of the origin:** Lastly, we notice another change in the dynamics as the parameter  $c$  moves from  $K_1$  to  $K_2$ . The orbit of the origin changes from being attracted to an attracting fixed point to being attracted to an attracting 2-cycle. As this will be a key aspect to keep in mind, we point out that in each of the examples we have considered where the map  $f_c(z) = z^2 + c$  had an attracting cycle, the origin was “absorbed” into the cycle in the sense that the tail end of the orbit (formally  $\{f_c^n(0) : n > N\}$  for very large  $N$ ) is nearly identical to the attracting cycle. Another way to say this is simply that the origin was **attracted to the cycle**. It turns out that this is true in general (see Remark 1.94 below), and the key fact, as we shall see, is that  $z = 0$  is a critical point, i.e.,  $f'_c(0) = 0$ .

EXERCISE 1.84. The reader should verify that  $c = 1/4$ , the cusp of the cardioid  $K_1$ , is also an unstable parameter. Use the *Global Complex Iteration Applet for Polynomials* to investigate this with respect to items 1-3 above. **Try it out!**

EXPLORATION 1.85. What do you think happens to the attracting fixed point and repelling 2-cycle when the parameter  $c$  decreases to  $-3/4$ , but then “makes a right turn” and starts heading towards  $-0.75 + 0.05i$ ? Investigate this with respect to item 1 above and Footnote 18 using the *Global Complex Iteration Applet for Polynomials*.

## 1.4. Critical Points and Critical Orbits

In this section, we are able to address some of the following natural questions you may have been asking yourself as we looked at the dynamics of the maps  $f_c(z) = z^2 + c$ .

- (1) Does every such map have an attracting cycle (other than  $\infty$ )?
- (2) How many attracting cycles can  $f_c$  have?
- (3) In all the examples we looked at, it seems that the orbit of the origin is always attracted to the attracting cycle. Is this true in general?

---

as  $c$  decreases further, the 2-cycle re-emerges as an attracting 2-cycle and the fixed point becomes repelling (see Exercise 1.179). Thus, the fixed point and the 2-cycle sort of exchange “polarity” in this transition.

In this section we see that the key to answering many of these questions involves the notion of *critical points*, and investigating how the orbit of such points largely determines many key dynamical features. We begin with a definition.

Recall that when the power series of an analytic map  $f(z)$  at  $z_0 \in \mathbb{C}$  has the form  $f(z) = f(z_0) + a_k(z - z_0)^k + a_{k+1}(z - z_0)^{k+1} + \dots$ , where  $a_k \neq 0$ , we say that  $z_0$  maps to  $f(z_0)$  with **degree**  $v_f(z_0) = k$  (we also call  $v_f(z_0)$  the **multiplicity** or **valency**).

REMARK 1.86. The condition that  $z_0$  and  $f(z_0)$  are both in  $\mathbb{C}$  will always be met in the examples in which we are concerned, and so we leave it to the interested reader to make the customary modifications to this definition when  $z_0$  and/or  $f(z_0)$  is infinity. When the term critical point is applied below to a point  $z_0$ , however, it will be understood that we do include the possibilities that  $z_0$  and/or  $f(z_0)$  is infinity.

DEFINITION 1.87. We call  $z_0$  a *critical point* of  $f$  if  $v_f(z_0) > 1$ .

If  $z_0$  and  $f(z_0)$  are both in  $\mathbb{C}$ , then  $z_0$  is a critical point exactly when  $f'(z_0) = 0$  (just like we define in Calculus I). Also, as described in Appendix Section A.6.1 on page 415, since near  $z_0$  the map  $f$  is locally a  $v_f(z_0)$ -to-one mapping, we see that  $z_0$  is a critical point exactly when  $f$  is not locally one-to-one.

DEFINITION 1.88. Let  $f$  be a rational or entire map. If  $w$  is a (super) attracting fixed point of  $f$ , then we define the *immediate basin of attraction*  $A_f^*(w)$  to be the connected component of  $A_f(w)$  which contains  $w$ . We point out (but leave it to the interested reader to show) that  $A_f^*(w)$  is the component of the Fatou set  $F(f)$  which contains  $w$ .

THEOREM 1.89. Let  $w$  be a (super) attracting fixed point of a non Möbius rational map  $f$ . Then there exists a critical point  $z_0 \in A_f^*(w)$  and hence  $f^n(z_0) \rightarrow w$ .

The proof of Theorem 1.89 is beyond the scope of this text, but the interested reader can find it as Theorem 7.5.1 in [1]. We do note, however, that we have witnessed this result in action many times now.

EXAMPLE 1.90. For  $c$  in  $K_1$  (see Figure 1.13), we know that  $f_c(z) = z^2 + c$  has a finite (super) attracting fixed point  $p_c$ . Since the origin is the only critical point (other than  $\infty$ , which is fixed) we must then have by Theorem 1.89 that  $0 \in A_{f_c}^*(p_c)$  and  $f_c^n(0) \rightarrow p_c$ . This is exactly what we observed (without proof) using the applets in many examples above.

In order to present the corresponding result for attracting *cycles* we will need the following definition.

DEFINITION 1.91. Let  $f$  be a rational or entire map which is non Möbius. For a (super) attracting  $p$ -cycle  $w_0, \dots, w_{p-1}$  of  $f$  we define the immediate basin of this cycle to be the union of components  $\cup_{j=0}^{p-1} F_j$  where  $F_j$  is the component of the Fatou set  $F(f)$  containing  $w_j$ .

EXERCISE 1.92. The map  $f_{-1}(z) = z^2 - 1$  has a super attracting 2-cycle  $\{0, -1\}$  and so the immediate basin of this cycle consists of two components of  $F(f_{-1})$ , one of which contains the point 0 and the other contains the point -1. Use the *Global Complex Iteration Applet for Polynomials* to investigate the picture shown in Figure 1.14. What are the dynamic properties of the other black “bulbs”, i.e., components of  $F(f_{-1})$ ? Try to find a pattern to the bulbs so you can experimentally approximate points  $z_0$  such that  $f_{-1}^3(z_0) = 0$ . How many such points are there? Do the same, but with changing 3 to 5. Can you generalize this? *Try it out!*

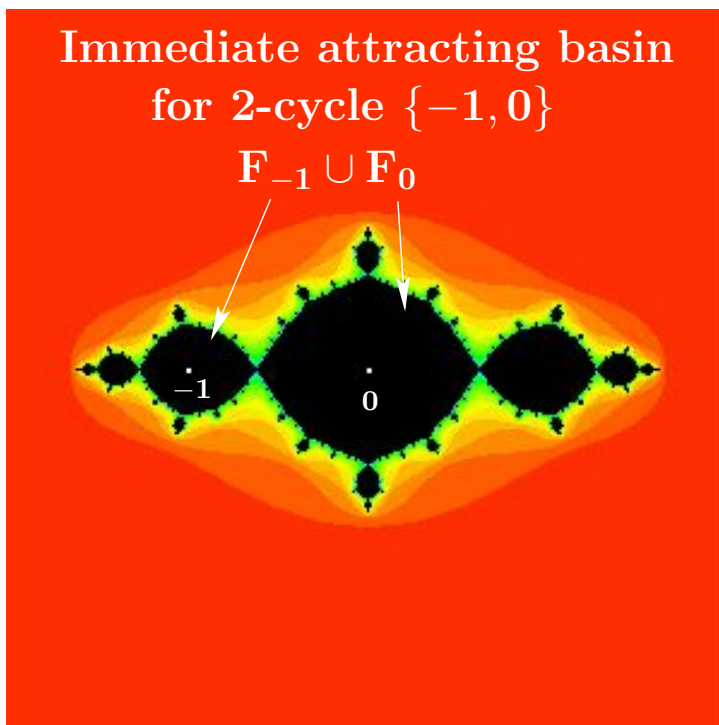


FIGURE 1.14. The immediate attracting basin of the 2-cycle  $\{-1, 0\}$  for  $f_{-1}(z) = z^2 - 1$  consists of the 2 components of the Fatou set containing the cycle points.

THEOREM 1.93. Let  $f$  be a rational map which is non Möbius. Then the immediate basin of each (super) attracting cycle contains a critical point of the map  $f$ .

The proof of this result takes advantage of the fixed point version of this theorem given in Theorem 1.89, the chain rule, and a couple other results which are slightly more than we want to take on at this point. The interested reader should consult [1] or [2]. However, it is pertinent to our discussion as it leads to the following remark.

REMARK 1.94. Since all maps of the form  $f_c(z) = z^2 + c$  have only one finite critical point (namely  $z = 0$ ), Theorem 1.93 implies that each such map can have at

most one **finite** (super) attracting cycle and any such cycle must “absorb” the orbit of the critical point at the origin. Thus we have answered Question 2 above and answered Question 3 in the case that  $f_c$  actually does have an attracting cycle.

DEFINITION 1.95. Both because 0 is a critical point of the map  $f_c$  and because its orbit is so important, we call  $\{f_c^n(0)\}_{n=1}^\infty$  the *critical orbit* of the map  $f_c$ .

We have seen that the critical orbit  $\{f_c^n(0)\}_{n=1}^\infty$  plays a special role in understanding the dynamics of the maps  $f_c(z) = z^2 + c$ . For some  $c$  values the critical orbit gets attracted to an attracting cycle (e.g.,  $c = 0, -1, 0.278 + 0.534i$ ) and for some other  $c$  values it gets attracted to the super attracting fixed point at  $\infty$  (e.g.,  $c = 0.3, 4+i, -2-0.3i$ ). One may wonder then, is it true that for *every*  $c$  value the critical orbit becomes attracted to some (super) attracting cycle? Here again we can use our intuition to say that this is probably not true. If we consider the **parameter plane**, also called the  $c$ -plane, of all  $c$  parameters for the maps  $f_c$ , we can think of a new type of tension created by those  $c$  values whose critical orbits are attracted to  $\infty$  and those  $c$  values whose critical orbits are not. It seems that maybe there are  $c$  values where the pull of the critical orbit towards  $\infty$  and the pull of the critical orbit to stay bounded is balanced. This informal reasoning can be the basis for a good guess, but since it is far from a formal proof, we take the easier route and settle the question by looking at the following example.

EXAMPLE 1.96. Show formally with paper and pencil (or informally with an applet) that for  $c = i, 1/4, -5/4, -2$ , and  $-3/4$ , the critical orbit under  $f_c(z) = z^2 + c$  is neither attracted to  $\infty$  nor attracted a finite *attracting* cycle. Thus we have answered Question 1 from above. **Try it out!**

In the case  $c = i$ , you noticed that the critical orbit  $i \mapsto i - 1 \mapsto -i \mapsto i - 1 \mapsto -i \mapsto \dots$  became cyclic, but the cycle did not include 0. These types of orbits have an important role in dynamics and so we give them a special name, as well as the  $c$  values which lead to these types of critical orbits.

DEFINITION 1.97. We call a point  $z_0$  *pre-periodic* (or *eventually periodic, but not periodic*) under the map  $f$  if it is not periodic, but some point on the orbit of  $z_0$  is periodic.

DEFINITION 1.98. We call a parameter  $c$  a *Misiurewicz* point if 0 is pre-periodic under  $f_c$ .

Thus we see that  $c = i$  and  $c = -2$  are Misiurewicz points. However,  $c = 0$  is not since  $f_0(z) = z^2$  has a critical orbit  $0 \mapsto 0 \mapsto \dots$  which is not pre-periodic. However,  $f_0(z) = z^2$  does have non-critical pre-periodic points, and in Additional Exercise 1.181 you are asked to find them.

It turns out that if  $c$  is a Misiurewicz point, then  $J(f_c) = K(f_c)$  (see [2], p. 133), in which case we call  $J(f_c)$  a *dendrite*. See Figure 1.15 for an example.

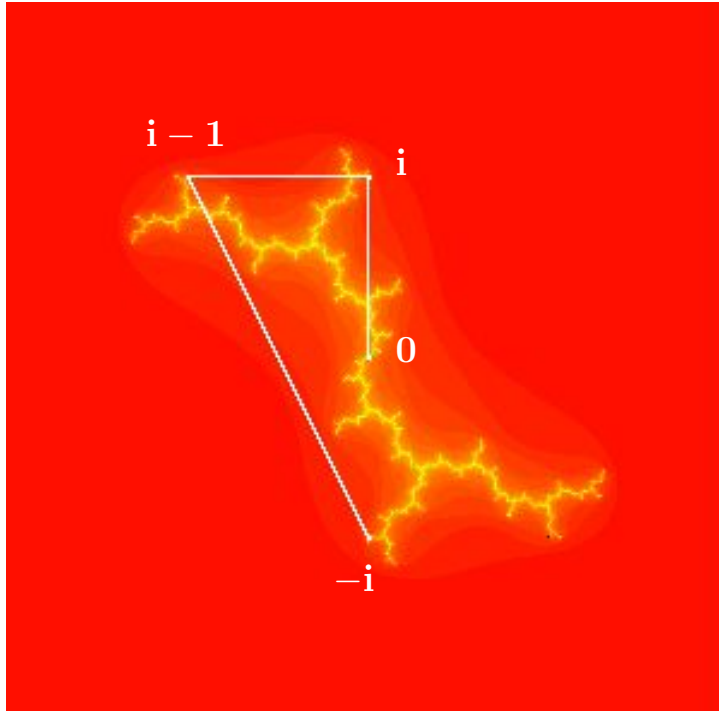


FIGURE 1.15. The dendrite  $J(f_i)$  along with the critical orbit  $i, i - 1, -i, i - 1, -i, \dots$

REMARK 1.99. In order to correctly understand the concepts of pre-periodic points and Misiurewicz points we note the important distinction between orbits that are *pre-periodic* (which we informally described above as those which *became* cyclic) and those orbits that are *attracted* to a cycle. The difference is the same as the difference between a sequence approaching a value and a sequence eventually *being* a value. For example, the sequence  $1, 1/2, 1/3, 1/4, \dots$  approaches 0, but never becomes 0. However, the sequence  $2, 1, 1/2, 0, 0, 0, \dots$  eventually becomes 0 (and stays at 0). When using technology, such as the provided applets, it can be very difficult, if not impossible, to distinguish between these two concepts. For example, set  $c = -0.9$  and look at the numerical values of the first 100 points of the orbit of  $z_0 = 0$  under  $f_c$ . Focusing on the 75th and higher orbit values, we see that the data bounces back and forth between what appears to be the same two values. This might falsely lead you to conclude that  $z_0 = 0$  is pre-periodic. The problem is that the *true* orbit in this case never actually *exactly* bounces back and forth between the *exact* same values. In fact, one can show (which we leave to the reader) that  $z_1 < z_3 < z_5 < \dots$  and  $z_0 > z_2 > z_4 > \dots$  with strict inequalities everywhere for all indices. However, the odd terms approach some value  $-0.8872983346207418 \dots$  and the even terms approach  $-0.1127016653792581 \dots$ . Since the applet truncates the data for each  $z_n$  it *appears* that the odd sequence and even sequence do eventually become constant. The moral

of the story here is that when trying to discern whether a point is pre-periodic or not, technology might very well mislead you. In such matters, careful analysis and proof needs to be used.

Let us return to the question we addressed above, namely, does the critical orbit for every map  $f_c(z) = z^2 + c$  get attracted to an attracting cycle? We saw that for  $c = i, 1/4, -5/4, -2$ , and  $-3/4$  this is not the case. However, in each case the critical orbit either became cyclic or was attracted to a cycle (though not necessarily an attracting cycle). As mathematicians we then must wonder, is this always the case? Is it possible for some  $c$  value to be such that the critical orbit neither becomes cyclic nor is attracted to any cycle? The answer happens to be yes. We cannot explain the deep mathematics behind this answer in these limited pages, but we do note that asking good questions like this, whether or not we can answer them, is an important part of contributing to mathematics.

So it is not true that every  $c$  parameter has a critical orbit that either becomes cyclic or is attracted to a cycle. What *is* true, however, is that every  $c$  parameter has a critical orbit that is either attracted to  $\infty$  or remains bounded. It is exactly this dichotomy which leads us to consider one of the most beautiful objects in all of mathematics, the Mandelbrot set.

DEFINITION 1.100. The *Mandelbrot set* is defined as  $M = \{c \in \mathbb{C} : f_c^n(0) \not\rightarrow \infty\}$ .

We have already encountered some important aspects of  $M$ , namely, it contains both  $K_1$  and  $K_2$  pictured in Figure 1.13. We also know that it must contain  $K_n$  for every  $n$  (since for  $f_c$  to have an attracting  $n$ -cycle, the critical orbit must be attracted to this cycle by Theorem 1.93, and thus not be attracted to  $\infty$ ). The calculation of the sets  $K_n$  is, however, a very arduous task and a complete description of all such sets has for years stumped mathematicians, and continues to stump us. Let us therefore use the computer to draw  $M$  for us and *experimentally* investigate the sets  $K_n$  and  $M$  (always keeping in mind that limitations of the sort discussed in Remarks 1.56 and 1.99 force us to moderate the confidence that we can place in such pictures). We begin by first using the following applet to construct a picture of  $M$ .

The *Mandelbrot Set Builder Applet* will color each selected point  $c$  in the parameter plane either red if  $c \notin M$  or black if  $c \in M$ . Thus, if the the critical orbit (under the map  $f_c$ ) limits to  $\infty$ , then the point  $c$  is colored red, otherwise it is colored black. Of course, we cannot compute the infinite number of points in the critical orbit, so the applet will compute only the number of iterates allowed in the **Maximum Iterations** input box. Setting this value to 100 will produce nice results (however, we encourage the reader to experiment with this value and investigate the effect it has on the picture). Also, the computer applet will color a selected  $c$  value red if and only if one of the calculated critical orbit points lands outside of  $\overline{\Delta(0, 2)}$ . This is justified by the following lemma, which you are asked to prove in Additional Exercise 1.189.



LEMMA 1.101. If the critical orbit  $f_c^n(0)$  ever *escapes* the closed disk of radius two centered at the origin, then the critical orbit must necessarily converge to  $\infty$ .

EXPLORATION 1.102. Take some time to experiment with the *Mandelbrot Set Builder Applet* to get a feel for the mathematics which defines the Mandelbrot set. **Try it out!**

One feature of the Mandelbrot set which stands out is that it is symmetric about the  $x$ -axis (see Additional Exercise 1.182). Another feature you may have observed is that  $M$  has no “holes” in it (see Additional Exercise 1.183). The *Mandelbrot Set Builder Applet* is a nice tool for visualizing  $M$  and can lead us as above to pursue some of its interesting features, but there are some important properties of  $M$  it cannot help with, such as whether  $M$  is a closed set or not. To do this we need more formal mathematics.

LEMMA 1.103. The Mandelbrot set  $M$  is a closed set.

PROOF. Suppose  $c_k \rightarrow c^*$  where each  $c_k \in M$ . We will show that  $c^* \in M$ , thus proving that  $M$  is closed. By observing that for  $f_c$  the terms of the critical orbit are  $0, c, c^2 + c, (c^2 + c)^2 + c, \dots$ , we see that the  $n$ th term can be written  $Q_n(c)$  for some polynomial  $Q_n$ . Fix some  $n \in \mathbb{N}$  and note that  $Q_n$  is continuous. Since  $|Q_n(c_k)| \leq 2$  for each  $k \in \mathbb{N}$  by Lemma 1.101, we must have  $|Q_n(c^*)| \leq 2$  since  $|Q_n(c_k)| \rightarrow |Q_n(c^*)|$  by the continuity of  $Q_n$ . Since this holds for every  $n$ , we have shown that the critical orbit of  $f_{c^*}$  is contained within  $\overline{\Delta(0, 2)}$ , and thus  $c^* \in M$ .  $\square$

We close this section by presenting (without proof) two interesting facts about  $M$ . First, the set of Misiurewicz points, each which is clearly in  $M$  (why?), is dense in the boundary  $\partial M$ . This means that given any open set  $U$  which contains a point in  $\partial M$ , the set  $U$  must also contain a Misiurewicz point (see [2], p. 133). Second,  $\partial M$  is contained in the closure of the centers of the hyperbolic components defined in Definition 1.81 (see [9], p. 100). Thus, any open set which contains a point in  $\partial M$ , must also contain the center of some (small) hyperbolic component. Taking into account the fact that each center of a hyperbolic component is in the interior of  $M$  and each such center is separated away from any other such center, we see that  $\partial M$  necessarily must be quite complicated. We encourage the reader to take a moment to reflect and fully digest the previous statement. Start by explaining how the set  $K_1 \cup K_2$  in Figure 1.13 fails to have this property, but that by attaching many tiny (what we will call) “bulbs” we can generate a set with this property.

REMARK 1.104. Although a lot is known about  $M$ , one very important question that has stumped mathematicians thus far, is whether or not  $M$  contains an open set which does not meet any  $K_n$ , that is, an open set of  $c$  values for which no  $f_c$  has an attracting cycle (other than  $\infty$ ). The conjecture that asserts that this cannot happen is known as the *density of hyperbolicity conjecture* and remains the focus of much intense research.

### 1.5. Exploring the Mandelbrot Set $M$

The Mandelbrot set has been called one of the most beautiful objects in mathematics, but our red and black picture created by the *Mandelbrot Set Builder Applet* does not do it justice. The set  $M$  has many tiny “hairs” and “bulbs” that are hard to see with this *bichromatic* picture, and the complexity of the picture cries out for a way to zoom in on these intricate tiny hairs and bulbs.

Initially it was conjectured that the Mandelbrot set is disconnected. This was motivated by the low resolution pictures that did not show the fine details and thin filaments that connect all the parts of  $M$ . However, it turns out that  $M$  is connected (see [1], p. 239). We cannot prove this here, but a much more sophisticated applet will give us pictures which certainly hint that this might be the case.

From now on we use the *Parameter Plane and Julia Set Applet*, which still colors points in  $M$  black, but colors the parameters  $c \notin M$  a different shade based on how many iterates it takes for the critical orbit to escape the disk  $\overline{\Delta}(0, 2)$ . This gives a much better feel for the immense detail of the Mandelbrot set  $M$  (see Figure 1.16). The applet also shows, for each selected  $c$  value, a picture of the corresponding Julia set.

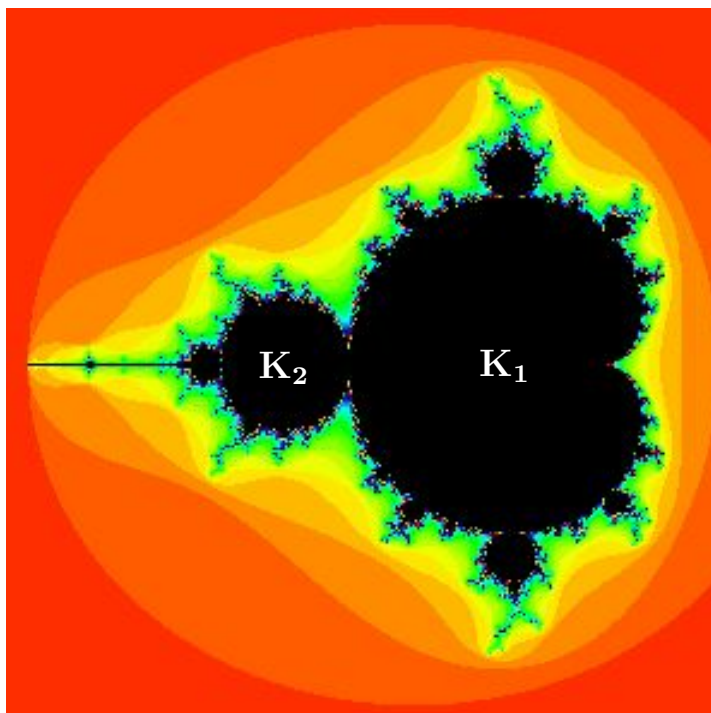


FIGURE 1.16. The Mandelbrot set.

EXPLORATION 1.105. The reader should now experiment and play with the *Parameter Plane and Julia Set Applet*, zooming in on various parts of  $M$  and the corresponding Julia sets. Look at not just the geometry of the pictures you see, but also at the dynamics you see. What do the bulbs and hairs mean dynamically? Is there a relationship between the geometry and the dynamics? Start looking for patterns and discovering new fine details in the hairs and bulbs. Describe what you find and make a list of observations, questions, and conjectures. You have the tools to explore an infinitely complex world. There are millions of new features of  $M$  and the related Julia sets to be found by using this applet. In fact, after exploring for a sufficient amount of time, zooming in on the fine details of the sets, you will likely find a picture that no other human has ever seen before! Take your time to explore this fascinating new world. *Try it out!*

We have quite a menagerie of pictures to see and investigate, including Rabbits, Dragons, and Elephants. We even have Star Clusters, Galaxies, and baby Mandelbrot sets (see Figure 1.17).

In the next section we investigate such star cluster sets more carefully so that we can better understand exactly what we are seeing (or not seeing) in such pictures.

**1.5.1. Cantor dust sets.** As mentioned before we must always be careful when using technology to represent mathematics. What we see is not always an accurate representation of what we are trying to see. For example, using  $c = 0.21 + 0.64i$  in the *Parameter Plane and Julia Set Applet*, it might appear that  $J(f_c)$  is empty and that all points iterate to  $\infty$  under  $f_c$ . In fact, if one displays the picture in Black and White via the **Dynamic plane black/white plot** checkbox on the **Settings tab**, you will see an all white screen, which taken at face value would mean  $J(f_c)$  is empty. That, however, is very far from the truth. There are infinitely many (in fact, uncountably many) points which do not iterate to  $\infty$  (see Additional Exercise 1.184). However  $J(f_c)$ , especially for having so many points, is rather small in the sense that it does not show up on the computer screen very well. To see such points better we view the color picture and then zoom in very far on the non-red parts (e.g., center each zoom in the middle of the largest “star cluster”) to eventually see regions of black, which represent points which do not iterate to  $\infty$ . However, even these regions of black are not what they seem to be. Because we are only using a finite number of **Dynamic plane max iterations** some of these black points would ultimately iterate to  $\infty$  if we would increase the number of iterations used. However, other of these black points will not iterate to  $\infty$  and so should truly be colored black.

EXERCISE 1.106. Adjust the **Dynamic plane max iterations** value to make  $J(f_c)$  (using  $c = 0.21 + 0.64i$ ) harder to see and more accurate or easier to see and less accurate. Also, use the Black and White picture feature to see how it can sometimes be used to give you a much better picture of  $J(f_c)$ . Of course, we must always keep

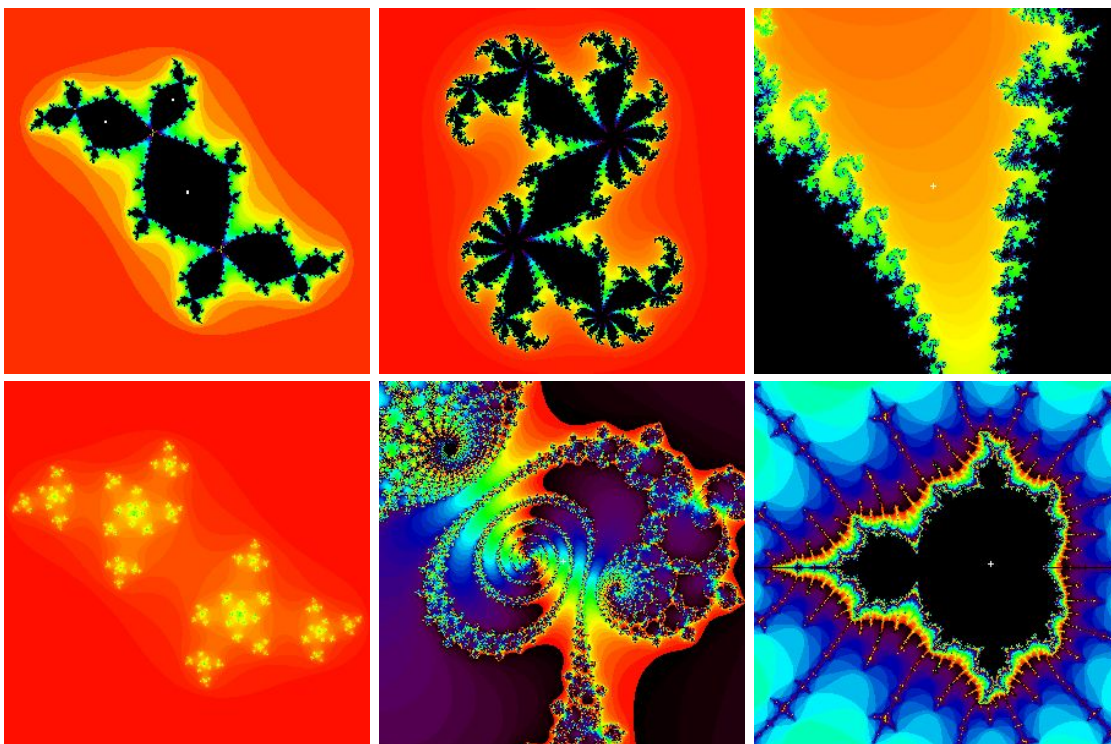


FIGURE 1.17. From top left to bottom right we see a Rabbit (Julia set when  $c = -0.12 + 0.75i$ ), a Dragon (Julia set when  $c = 0.36 + 0.1i$ ), Elephants (zoom in on the Mandelbrot set centered at  $c = -0.77 + .173i$ ), a Star cluster (Julia set when  $c = -0.4387 + 0.784i$ ), a Galaxy (zoom in on the Mandelbrot set centered at  $c = -0.75623053 + 0.06418323i$ ), and a baby Mandelbrot set (zoom in on the Mandelbrot set centered at  $c = -1.625$  and adjust the **Parameter plane max iterations** to 150 for a better resolution).

in mind that what we see on the computer screen is only an approximation to the real thing. *Try it out!*

The star cluster set  $J(f_{0.21+0.64i})$  and other such hard to see though infinite sets of points are what we call *Cantor dust* sets. It is hard to see such sets depicted with an applet because each point in the set is *disconnected* from any other point, that is, for any two points  $z_0$  and  $w_0$  in the set, there is a simple closed curve which never meets the Cantor dust set, but such that the curve winds around  $z_0$  without winding around  $w_0$ . Such a set is called *totally disconnected* because the only connected subsets are single points. We explore one method to prove that certain Julia sets have this property in Section 1.5.2. However we first use our applet to illustrate many examples of this phenomenon.

EXPLORATION 1.107. Experiment with the *Parameter Plane and Julia Set Applet* to find many (apparent) examples of Cantor dust Julia sets  $J(f_c)$ . Can you make a conjecture about which  $c$  values correspond to such Julia sets? **Try it out!**

**1.5.2. Connectedness Locus.** One of the many properties of  $M$  that you may have observed in your experimentation is that for each  $c \in M$ , the Julia set  $J(f_c)$  is connected, and for each  $c \notin M$ , the Julia set  $J(f_c)$  is disconnected.<sup>19</sup> Move the  $c$  value around the parameter plane in the *Parameter Plane and Julia Set Applet* to observe this. This is not a coincidence, and it is because of this that we call  $M$  the **connectedness locus** for the family of maps  $\{f_c : c \in \mathbb{C}\}$ , i.e.,  $M = \{c \in \mathbb{C} : J(f_c) \text{ is connected}\}$ . This fact is proven by using the following theorem and noting that  $f_c$  has its sole finite critical point at the origin.

THEOREM 1.108 (See [1], p. 202). Let  $f$  be a polynomial of degree greater than or equal to two. Then every *finite* critical point of  $f$  has a bounded orbit if and only if both  $J(f)$  and  $K(f)$  are connected.

The proof of this result is beyond this text, but for the maps  $f_c$  we will be able to illustrate the reasoning behind the following related dichotomy.

THEOREM 1.109 (See [2], p. 67). For the map  $f_c$ , either

- (i)  $\{f_c^n(0)\}_{n=1}^{\infty}$  is bounded in  $\mathbb{C}$  and  $J(f_c)$  is connected, or
- (ii)  $f_c^n(0) \rightarrow \infty$  and  $J(f_c)$  is totally disconnected.

We illustrate the method of proof, though a few technical details requiring advanced methods must be left for the interested reader to find in the literature. We first make an important definition.

DEFINITION 1.110. A *compact topological disk (ctd)* is a compact set<sup>20</sup> in  $\mathbb{C}$  whose boundary is a simple closed smooth path.

The importance of this definition comes from the following lemma and from noting that any ctd is connected.

LEMMA 1.111. If  $E$  is a ctd and  $c \notin \partial E$ , then  $f_c^{-1}(E)$  consists of

- (1) one ctd containing 0, if  $c \in \text{Int}(E)$ ,
- (2) two ctd's, neither containing 0, if  $c \notin E$ .

We do not prove this lemma, but with the help of our applet we will illustrate it as it is used in the following.

<sup>19</sup>Your informal understanding of connectedness will suffice in this text; however, the following is a formal definition. A compact set  $E$  in  $\mathbb{C}$  is **disconnected** if there exists a simple closed curve in  $\mathbb{C} \setminus E$  which winds around some points of  $E$ , but not all points of  $E$ .

<sup>20</sup>Recall that a compact set in  $\mathbb{C}$  is a closed and bounded set.

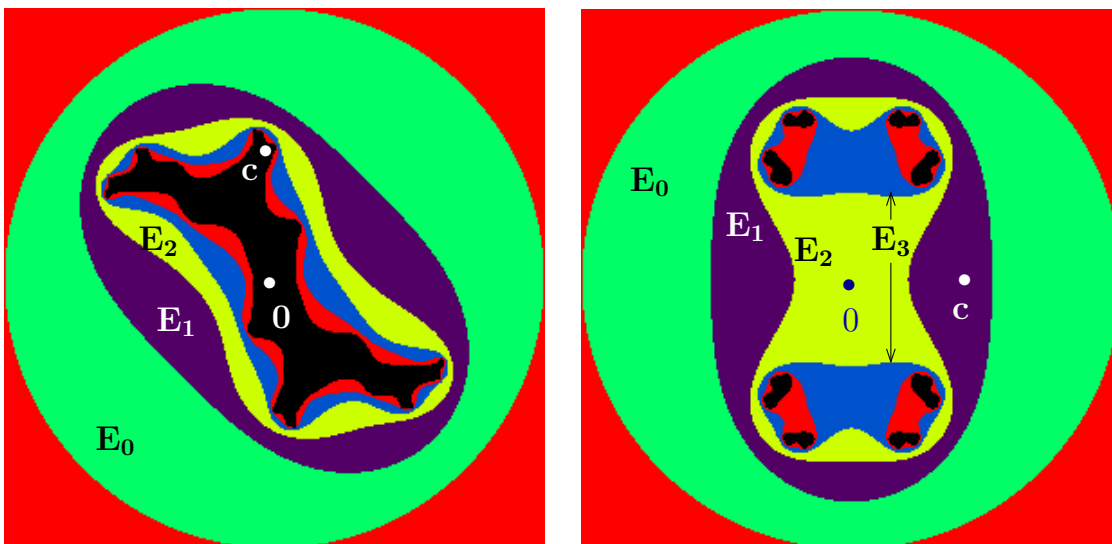


FIGURE 1.18. The sets  $E_0, \dots, E_5$  drawn using the *Parameter Plane and Julia Set Applet* with Dynamic plane escape radius  $r = 2.1$ , Dynamic plane max iterations = 5, Color sample rate = 7. In both pictures  $E_0 = \overline{\Delta}(0, r)$ . Left picture shows  $c = i$  with each  $E_n$  connected. Right picture shows  $c = 0.9$  with each  $E_0, E_1$  and  $E_2$  connected, but subsequent  $E_n$  disconnected.

SKETCH OF PROOF OF THEOREM 1.109. Choose some  $r > \max\{2, |c|\}$  with the property that  $|f_c^n(0)| \neq r$  for all  $n = 1, 2, \dots$ . Now define  $E_0 = \overline{\Delta}(0, r)$  and define  $E_n = \{z \in \mathbb{C} : f_c^n(z) \in E_0\}$  for each  $n = 1, 2, \dots$ . Thus  $E_n = f_c^{-1}(E_{n-1})$  for each  $n = 1, 2, \dots$  and  $c \notin \partial E_n$  for each  $n = 0, 1, 2, \dots$ . From Additional Exercise 1.189, we know that  $|z| > r$  implies both  $|f_c(z)| > |z| > r$  and  $f_c^n(z) \rightarrow \infty$ . Armed with this information the reader can now provide the details to show  $E_0 \supset E_1 \supset E_2 \supset \dots$  and  $K(f_c) = \bigcap_{n=0}^{\infty} E_n$ . We now investigate cases (i) and (ii) of the theorem by analyzing the sets  $E_n$ .

Suppose  $\{f_c^n(0)\}_{n=1}^{\infty}$  is bounded in  $\mathbb{C}$ , i.e.,  $0 \in K(f_c)$ . Since  $c = f_c(0)$ , we must also have  $c \in K(f_c)$ , and so  $c \in E_n$  for all  $n = 0, 1, 2, \dots$ . Since  $c \notin \partial E_n$ , we may then also conclude  $0 \in \text{Int}(E_n)$  for all  $n = 0, 1, 2, \dots$ . Applying Lemma 1.111 inductively we may then show that each  $E_n$  is connected as it consists of a single ctd (see Figure 1.18 (left)). Though we omit the details, it follows from a more advanced topological argument that  $K(f_c) = \bigcap_{n=0}^{\infty} E_n$  must also be connected, which by another advanced topological argument implies  $J(f_c) = \partial K(f_c)$  is connected.

Now suppose  $f_c^n(0) \rightarrow \infty$ , i.e.,  $0 \notin K(f_c)$ . By the choice of  $r$  we know  $c \in \text{Int}(E_0)$ . However, since  $0$  does not lie in every  $E_n$  (else  $0$  would lie in  $K(f_c)$ ), there is a positive integer  $m$  such that  $c \in \text{Int}(E_{m-1})$ , but  $c \notin E_m$ . Thus by Lemma 1.111 we see that  $E_m$  consists of one ctd, but  $E_{m+1} = f_c^{-1}(E_m)$  consists of two ctd's (see Figure 1.18 (right))

where  $m = 2$ ). Applying Lemma 1.111 to each ctd in  $E_{m+1}$ , we then see that  $E_{m+2}$  consists of four ctd's. Proceeding inductively we see that  $E_{m+k}$  must then consist of  $2^k$  ctd's. Although we do not have the tools here to prove it, the size of the ctd's which make up  $E_{m+k}$  shrinks to zero as  $k \rightarrow \infty$ , and so we can conclude that any two distinct points  $z$  and  $w$  in  $K(f_c)$  must lie in distinct ctd's of  $E_{m+k}$  when  $k$  is sufficiently large. Hence the boundary of such a ctd containing  $z$ , which lies in  $A_{f_c}(\infty)$  (why?), must then be a curve which encloses  $z$  but not  $w$ . Hence we conclude that  $K(f_c)$  is totally disconnected, and thus so is  $J(f_c)$  since by utilizing Remark 1.65 one can show in this case that  $J(f_c) = \partial K(f_c) = K(f_c)$ .  $\square$

So, modulo a few details, we were able to understand how Cantor dust sets naturally arise when considering  $J(f_c)$ . The following is another topological property which you may have observed in your explorations; however, in this case we have all the tools to completely prove this property holds. This result says that  $K(f)$  has no *holes*, where we define a **hole** as a bounded domain  $U$  in  $\mathbb{C} \setminus K(f)$  such that  $\partial U \subseteq K(f)$ .<sup>21</sup> We prove this as follows by appealing directly to the definition of  $K(f)$  and applying the Maximum Modulus Theorem.

**LEMMA 1.112.** Let  $f$  be a polynomial of degree greater than or equal to two. Then  $K(f)$  has no holes.

**PROOF.** Suppose the set  $U$  is a hole in  $K(f)$ . Let  $R > 0$  be such that  $|z| > R$  implies  $|f(z)| > |z| > R$  (such an  $R$  must exist given that the map  $f$  is a polynomial of degree greater than or equal to two). From this, one can show  $f^n(z) \rightarrow \infty$  whenever  $|z| > R$ . Thus we see that we must have  $|f^n(z)| \leq R$  for all  $n \in \mathbb{N}$  for any point  $z$  with a bounded orbit. This means, by definition of  $K(f)$ , we have  $K(f) = \{z \in \mathbb{C} : |f^n(z)| \leq R \text{ for all } n \in \mathbb{N}\}$ . Since  $\partial U \subseteq K(f)$ , we see that for any  $n \in \mathbb{N}$ , the polynomial  $f^n$  is bounded by  $R$  on  $\partial U$ . By a version of the Maximum Modulus Theorem given as Corollary A.18 on page 415, we then conclude that  $f^n$  is bounded by  $R$  on  $U$  as well. Since this works for all  $n \in \mathbb{N}$ , we see that  $U \subseteq K(f)$  contrary to our assumption that  $U$  is a hole in  $K(f)$  (which does not meet  $K(f)$ ). This contradiction proves the result.  $\square$

**1.5.3. Self-similarity and symmetry.** One of the properties you may have noticed in each dynamical plane picture for the maps  $f_c$  is that each picture is symmetric about the origin. Specifically, each set  $A_{f_c}(\infty)$ ,  $J(f_c)$ , and  $K(f_c)$  has the property that it contains  $z$  if and only if it also contains  $-z$  (see Additional Exercise 1.185).

Another property you may have noticed in each set  $J(f_c)$  is that small parts of  $J(f_c)$  look very much like other larger parts of  $J(f_c)$ . We call this property *self-similarity* and note that it actually is a property of all Julia sets.

<sup>21</sup>The advanced reader will recognize the absence of holes in  $K(f)$  to be equivalent to the set  $\mathbb{C} \setminus K(f)$  being connected. However, to formally prove this equivalency we would need to delve more deeply into some more advanced topological results, and so we do not undertake such a proof here.

EXPLORATION 1.113. In the *Parameter Plane and Julia Set Applet*, set  $c = 0.112 + 0.74667i$  and in the dynamic plane ( $z$ -plane) window set the  $x$  range to be 0.22026 to 0.28746 and set the  $y$  range to be 0.4648 to 0.532 (and then hit the **Update** button). Notice how similar the picture looks when we zoom in further by setting the  $x$  range to be 0.2277184 to 0.2475200 and setting the  $y$  range to be 0.50166592 to 0.52146752. Continue zooming in on any point of  $J(f_c)$  to see how at all scales (i.e., depth of zoom) the picture, after rotating, looks very much like the first picture. (Keep in mind that you can click on the thumbnails at the bottom to see any previously created pictures.) Now repeat this with a few other  $c$  values to get a sense that this is a general property of Julia sets. ***Try it out!***

How about the Mandelbrot set  $M$ ? Is it self-similar too? The answer is a definite...sort of. There are places in  $M$  which have small pieces that look like larger pieces, but it is not the case, as in the Star Cluster sets above, that the whole set  $M$  looks like a bunch of small copies of just one piece of itself. The Mandelbrot set is sometimes called *quasi*-self-similar for this reason.

EXPLORATION 1.114. In the *Parameter Plane and Julia Set Applet* set  $c = 0.41491386 + 0.60134804i$  and begin zooming in on the Mandelbrot set, centering the zoom at this  $c$  value. What you will see are pictures that appear to look the same as you zoom in. In fact, if you zoom in on the tips of any of the “antennae” of the Mandelbrot set you will see a type of self-similarity. Now see what you find when you repeatedly zoom in on a point in the middle of such an antenna. ***Try it out!***

Now zoom in on the point  $c = -1.2418406 - 0.32366967i$  to find what we call a *baby Mandelbrot set*. Set the **Parameter plane max iterations** to a higher value (such as 200 or 300) to see this picture better. You can also adjust the **Color sample rate** to adjust the color scheme to help create a nicer picture. What you have found is not an exact copy of the full Mandelbrot set, as you can tell by the long antennae coming out of it, but it certainly does have the unmistakable look of  $M$ . It turns out, due to a deep result, that these baby Mandelbrot sets are actually ***dense*** in the boundary of  $M$ , that is, given any neighborhood of a point in  $\partial M$ , no matter how small, there exists a baby Mandelbrot set in that neighborhood. Of course, to see it, we usually have to zoom in pretty far, but it’s there. This phenomenon, and more, is further discussed in Section 1.7.

EXPLORATION 1.115. Try zooming in on an arbitrary point in the  $\partial M$ , and then see if you can find a baby Mandelbrot set hiding in there. Keep in mind, however, that you might need to adjust the **Parameter plane max iterations** to give you a better view. Also, keep in mind that using a computer means there are limitations to how far we can zoom in and still get reasonable results. ***Try it out!***

**1.5.4. Bulbs in  $M$ .** Let’s now try to systematically classify some of what we see in  $M$ , in terms of both geometry and dynamics. Recall that each point  $c$  in the parameter plane (also called the  $c$ -plane) corresponds to a function  $f_c$  whose Julia set



$J(f_c)$ , Fatou set  $F(f_c)$ , and dynamics are viewed in the dynamic plane (also called the  $z$ -plane). With this in mind we will see that  $M$ , and all the parts which make it up, provide us with a sort of “dictionary” or index of the types of dynamics we may find for maps of the form  $f_c(z) = z^2 + c$ .

First we point out that we have already seen that the cardioid  $K_1$  (see Figure 1.16) consists of  $c$  values corresponding to maps with attracting fixed points. Off this main cardioid  $K_1$  there are infinitely many “bulbs” attached which we would like to understand both by their geometrical properties as sets in the  $c$ -plane and by the corresponding dynamic properties in the  $z$ -plane.

The most prominent bulb off  $K_1$  is the disk  $K_2 = \Delta(-1, 1/4)$  representing the parameters corresponding to maps with attracting 2-cycles. The next largest bulb off  $K_1$  is near the top. Select  $c = -0.12 + 0.77i$  from this bulb and consider the critical orbit in the dynamic plane to see that there exists an attracting 3-cycle. Use the *Parameter Plane and Julia Set Applet* to observe this by iterating the critical orbit one iterate at a time (by checking the **Show critical orbit** box, then checking the **Iterate orbits** box, and then hitting the  $+$  button that appears next to the **Iterate orbits** box). Also, note that for this  $c$ , the Julia set  $J(f_c)$  in the dynamic plane is pinched in such a way that 3 bulbs meet at every pinch point. Let’s call the pinch point which corresponds to the immediate basin of this attracting 3-cycle the **main pinch point** (which in this case is near  $-0.282 + 0.492i$ ). Then by iterating the origin one step at a time you can see that each iterate makes roughly a  $1/3$  rotation around this main pinch point.<sup>22</sup> Remember that you can use the **Connect orbit points** checkbox to help you track the path of the orbit. Trying other  $c$  values from this same bulb in the  $c$ -plane we find that we always get this same type of behavior. For this reason we call this bulb in  $M$  the  $1/3$  bulb.

**EXERCISE 1.116.** Now use the *Parameter Plane and Julia Set Applet* to investigate the dynamics for  $c = -0.513 + 0.5693i$ . Pause for a moment to decide what fraction  $p/q$  would best describe the bulb containing this point. **Try it out!**

In the dynamic plane we see an attracting 5-cycle, which cycles around a main pinch point at which 5 bulbs meet. Further, we see by iterating the origin one step at a time, the iterates make a  $2/5$  rotation about the main pinch point in each step. For this reason we call the bulb of  $M$  (in the  $c$ -plane) which contains  $c = -0.513 + 0.5693i$  the  $2/5$  bulb. Again, you should experiment to see this same type of behavior for other  $c$  values within this  $2/5$  bulb. **Try it out!**

**DEFINITION 1.117.** Let  $B$  be a hyperbolic component of  $K_q$ , whose boundary meets the boundary of the main cardioid  $K_1$ . We call  $B$  the  $p/q$  bulb, and denote it  $B_{p/q}$ , if for each  $c \in B$  the corresponding map  $f_c$  has an attracting  $q$  cycle and each step in

---

<sup>22</sup>When referencing rotations, we use the standard convention that a positive rotation is counterclockwise. Hence, a  $1/3$  rotation means a 120 degree rotation (one-third of a full rotation) in the counterclockwise direction.

the critical orbit in the dynamic plane makes roughly a  $p/q$  rotation about the main pinch point.

From what follows it will become clear that for each rational number  $0 \leq p/q \leq 1$ , there is *only* one  $p/q$  bulb and so we are justified in calling  $B_{p/q}$  **the**  $p/q$  bulb, as opposed to **a**  $p/q$  bulb.

EXERCISE 1.118. Experiment and prove a relationship between the  $p/q$  bulb and its conjugate bulb, that is, the bulb reflected over the  $x$ -axis (see Additional Exercise 1.182). In particular, find  $p'$  and  $q'$  if the conjugate of the  $p/q$  bulb is the  $p'/q'$  bulb. **Try it out!**

REMARK 1.119. Theorem 1.80 shows that the multiplier map  $\lambda_{p/q}$  maps  $B_{p/q}$  conformally onto  $\Delta(0, 1)$ . Furthermore, the map  $\lambda_{p/q}$  extends to be a one-to-one continuous map of  $\overline{B_{p/q}}$  onto  $\overline{\Delta(0, 1)}$ .

It turns out that  $\overline{B_{p/q}}$  meets the boundary of the main cardioid  $\partial K_1$  in just a single point, which we denote  $c_{p/q}$ , and call the **root of the  $p/q$  bulb**. For example,  $c_{1/2} = -3/4$  is the root of the  $1/2$  bulb  $B_{1/2} = K_2$ . In Additional Exercise 1.186 you are asked to investigate the multiplier maps evaluated at the root (note that since the root  $c_{p/q}$  of the  $p/q$  bulb lies on the boundary of two hyperbolic components, namely  $K_1$  and  $B_{p/q}$ , we see that there are two multiplier maps (namely,  $\lambda : \overline{K_1} \rightarrow \overline{\Delta(0, 1)}$  and  $\lambda_{p/q} : \overline{B_{p/q}} \rightarrow \overline{\Delta(0, 1)}$ ) that are defined at each  $c_{p/q}$ ). These root points happen play a special role and so further understanding of them is now warranted. In particular, it is important to understand the following dynamic property.

EXERCISE 1.120. The root  $c_{p/q}$  of the  $p/q$  bulb is the  $c$  parameter for which  $f_c$  has an indifferent fixed point with multiplier exactly equal to  $e^{2\pi ip/q}$ , i.e.,  $c_{p/q} = c(e^{2\pi ip/q})$  where  $c(\lambda)$  is the inverse of the multiplier map  $\lambda : \overline{K_1} \rightarrow \overline{\Delta(0, 1)}$ . Since  $c_{p/q}$  is a bifurcation parameter, you should describe three dynamical changes (as done in Exercise 1.84) which occur as the parameter  $c$  moves from the main cardioid  $K_1$  into  $B_{p/q}$  passing through the root  $c_{p/q}$ . **Try it out!**

EXPLORATION 1.121. Explore and label other bulbs in the same way as done in Exercise 1.116. We recommend that you print a large image of  $M$  and label each bulb as you go. **Try it out!**

While doing Exploration 1.121 you may have stumbled upon an interesting pattern that shows how one can quickly compute  $p/q$  for the largest bulb (measured by area) between two bulbs. We explain here the pattern we see, but for the detailed proofs we direct the interested reader to [6]. Looking at  $M$  we see  $B_{1/2}$  and  $B_{1/3}$  each attached to the main cardioid, with infinitely many  $p/q$  bulbs in between decorating the boundary of the main cardioid. The largest such bulb, as we have seen, is  $B_{2/5}$ . We can correctly “do the math” quickly in this situation by what is known as Farey addition to compute

$$\frac{1}{2} \oplus \frac{1}{3} = \frac{2}{5}.$$

In Farey addition, one “adds” fractions in the *unusual* way of simply adding the numerators and adding the denominators (much easier than that arduous task which involves finding a common denominator!). We call the two addends the **Farey parents** (e.g.,  $\frac{1}{2}$  and  $\frac{1}{3}$ ) and the resulting fraction the **Farey child** (e.g.,  $\frac{2}{5}$ ). Correspondingly, we will call the bulbs  $B_{1/2}$  and  $B_{1/3}$  the Farey parents of the Farey child bulb  $B_{2/5}$ .

EXAMPLE 1.122. The Farey child of  $B_{2/5}$  and  $B_{1/3}$ , that is, the largest bulb between these two, is  $B_{3/8}$  since

$$\frac{2}{5} \oplus \frac{1}{3} = \frac{3}{8}.$$

A quick check with the *Parameter Plane and Julia Set Applet* will confirm this result. Remember to use the **Connect orbit points** checkbox to help you track the path of the orbit. **Try it out!**

REMARK 1.123. We must be careful with our use of Farey addition of bulbs. The main rule we must be sure to adhere to is: **Two bulbs can only be Farey parents if all the bulbs between them are smaller than they are.** For example, one can check that the largest bulb between the  $4/11$  bulb (the one containing  $c = -0.292 + 0.633i$ ) and the  $2/5$  bulb is the  $3/8$  bulb. Here the Farey addition clearly does not work. However, since the supposed child  $3/8$  bulb is clearly larger than the supposed parent  $4/11$  bulb (which the reader should check on the applet), we know that Farey addition is not applicable in this instance.

There is another issue to be dealt with if this Farey addition is to truly help us compute the bulb fraction for all the  $p/q$  bulbs. Between the  $B_{1/3}$  and the cusp of the cardioid  $K_1$  there is a largest bulb, but how can one use Farey addition to determine it? The key is to treat the cusp itself like a Farey parent which is larger than all other bulbs. We leave it to the reader in Additional Exercise 1.188 to experimentally determine what Farey fraction should be used to represent the cusp.

**1.5.5. Sub-bulbs of M.** Just as the Main Cardioid  $K_1$  of  $M$  has many  $p/q$  bulbs attached to it, so does each  $p/q$  bulb have many “sub-bulbs” attached. Let’s investigate these small sub-bulbs. Use the *Parameter Plane and Julia Set Applet* to view the change in dynamics as we let  $c$  vary from  $c_1 = -0.16097811 + 0.80545706i$  within the  $1/3$  bulb to  $c_2 = -0.17462417 + 0.8296561i$  in an attached smaller sub-bulb. We see that the attracting 3-cycle became an attracting 15-cycle. Note also how the picture of the Julia set with the attracting 15-cycle has features common to both Julia sets with an attracting 3-cycles and Julia sets with an attracting 5-cycle. We see that 3 bulbs of  $K(f_{c_1})$  meet at each pinch point. In changing  $c$  to  $c_2$ , we see that these pinch points from  $K(f_{c_1})$  persisted, but also, within each bulb of  $K(f_{c_1})$ , new pinching occurs, such that at each of these newly formed pinch points 5 different bulbs of  $K(f_{c_2})$  meet. See Figure 1.19 and also take some time to use the zooming features in the *Parameter Plane and Julia Set Applet* to see this pattern repeat at all scales (remembering to adjust the **Dynamic plane max iterations** value as needed).

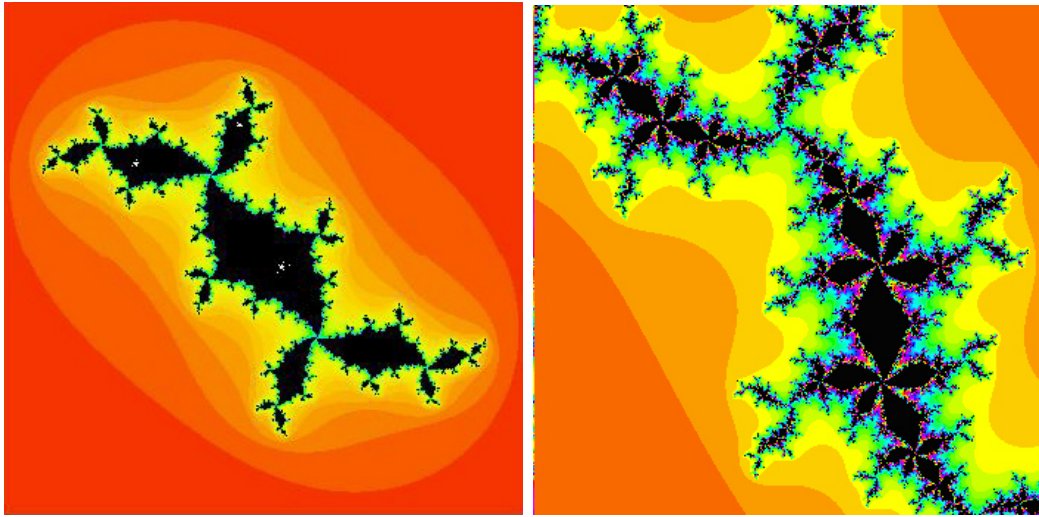


FIGURE 1.19. Left shows  $J(f_{c_1})$  and right shows  $J(f_{c_2})$ , slightly magnified to make it easier to see.

SMALL PROJECT 1.124. Investigate the behavior witnessed above by entering into a variety of sub-bulbs attached to a variety of  $p/q$  bulbs. Can you discern a pattern? If shown an example of a Julia set such as the one in Figure 1.20 below, can you identify which sub-bulb the  $c$  value came from?

**1.5.6. Limbs and Antennae in  $M$ .** It turns out that the Mandelbrot set  $M$  is a connected set. Your intuitive notion of what connected means will suffice in this chapter. However, we can also more formally describe the notion in this case by saying that any simple closed curve in the complement of  $M$  must either wind around no point of  $M$  or must wind around all of  $M$ . The fact that  $M$  is connected is not easy to prove and so we shall not attempt to do so here, but we will avail ourselves of this fact in order to describe some other important aspects of  $M$ . In particular, we make use of the fact that we can naturally “disconnect”  $M$  into two connected pieces by removing any root  $c_{p/q}$  of a  $p/q$  bulb (a fact we also will not prove here).

DEFINITION 1.125. The set  $M \setminus \{c_{p/q}\}$  consists of two connected sets, one which contains the cardioid  $K_1$  and the other containing  $B_{p/q}$ , which we call the  $p/q$  limb.

On each  $p/q$  limb there is the main  $p/q$  bulb with infinitely many sub-bulbs attached. Each of these sub-bulbs in turn has an infinite number of tinier sub-sub-bulbs, and so on. However, the  $p/q$  limb contains more than just these bulbs. It also contains what we informally call *antennae* made out of thin filaments that, sort of, reach out from the  $p/q$  bulb. Looking straight above the  $1/3$  bulb there is a junction where 3 equally spaced filaments, which we informally call *spokes*, meet (see Figure 1.21). The *main* or *principal spoke* is the one which attaches to the  $1/3$  bulb, and the

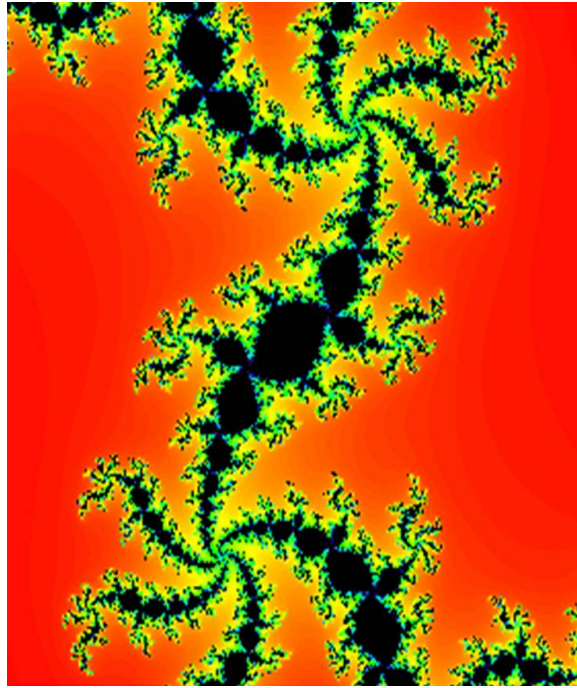


FIGURE 1.20. How can you tell where to find the corresponding  $c$  parameter for this picture of  $J(f_c)$ ?

shortest spoke is a  $1/3$  rotation about the junction point from the main spoke (and if you were wondering, yes, the  $1/3$  rotation here is, in fact, related to the  $1/3$  designation of the bulb). It turns out that this relationship between the short spoke and the  $p/q$  value occurs quite frequently, but not necessarily always (e.g., examine  $B_{1/5}$  which contains the point  $c = 0.39 + 0.33i$  using the *Parameter Plane and Julia Set Applet*). This generalization has been made into a formal theorem, but to do so, the notion of “shortest” had to be changed slightly (see [6]). We also note that if you zoom in on other junctions found on the antennae on the  $1/3$  limb, you will very often (but not always) see 3 spokes meeting at the junction. This type of (more than) coincidence cries out for further exploration indeed. First we make a definition.

DEFINITION 1.126. When  $q$  spokes meet at a junction point, we will call this a junction point of *order*  $q$ .

EXPLORATION 1.127. Investigate other  $p/q$  limbs and their principal spokes to get an idea of how often the spoke that is a  $p/q$  rotation from the main spoke is the shortest. Is there a similar pattern for the longest spoke? ***Try it out!***

EXPLORATION 1.128. Investigate other  $p/q$  limbs and the junction points within them to get an idea of how often the junctions there are of order  $q$ . What is the order

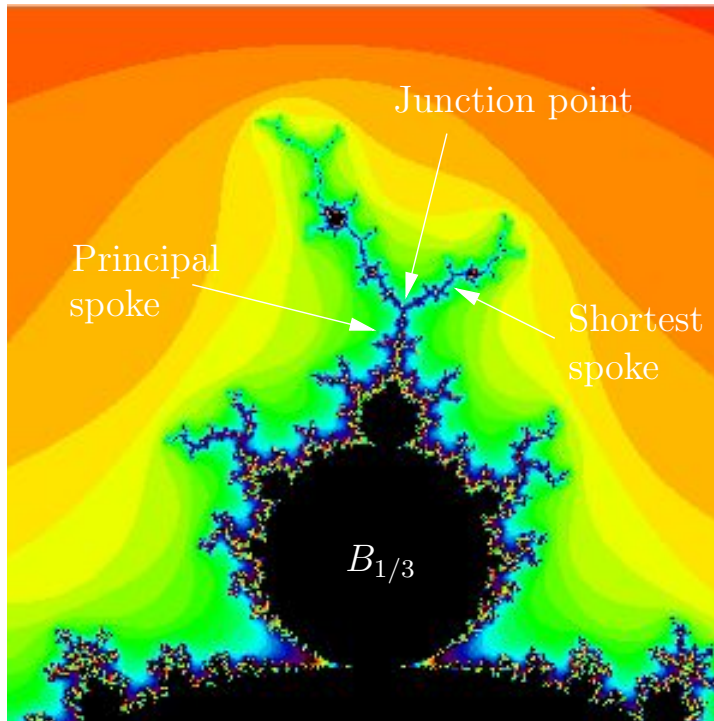


FIGURE 1.21. Illustration of main junction point of  $1/3$  limb of  $M$ .

of the other junctions? Is there a pattern to the types of junction orders one can find on a given  $p/q$  limb? ***Try it out!***

In the course of exploring the  $p/q$  limbs you may have stumbled upon many baby Mandelbrot sets like the one in Figure 1.22. In order to see these baby Mandelbrot sets clearly you will usually want to adjust the **Parameter plane max iterations** value to 300, 400, 500, or even 1,000 or more depending on the size of baby Mandelbrot set you want to see. Also, adjusting the **Color sample rate** can help. We mentioned before that these baby Mandelbrot sets are everywhere (to be more precise, they are dense in  $\partial M$ ); however, even though they are all unmistakable “copies” of the original  $M$  set, they are not all the same. They each have different decorations (antennae sprouting from them). If we pay close attention to these antennae and how many meet at the various junction points, can we get an idea how the given baby Mandelbrot set is related to the  $p/q$  limb it lives in? For example, in Figure 1.22 we see that the junction points near the “tips” of the antennae are all of order 3. Furthermore, we see that along these filaments, closer to the baby Mandelbrot set, we have junction points of order 5. Can this information be a clue to help you find where this baby Mandelbrot set lives? Imagine playing a game where your friend shows you a picture of a baby Mandelbrot set. Can you win the game by telling your friend where it lives? Note: These are very hard questions, but maybe by investigating these you will be able



to come up with some partial answers, connections, or maybe pose some interesting questions of your own.

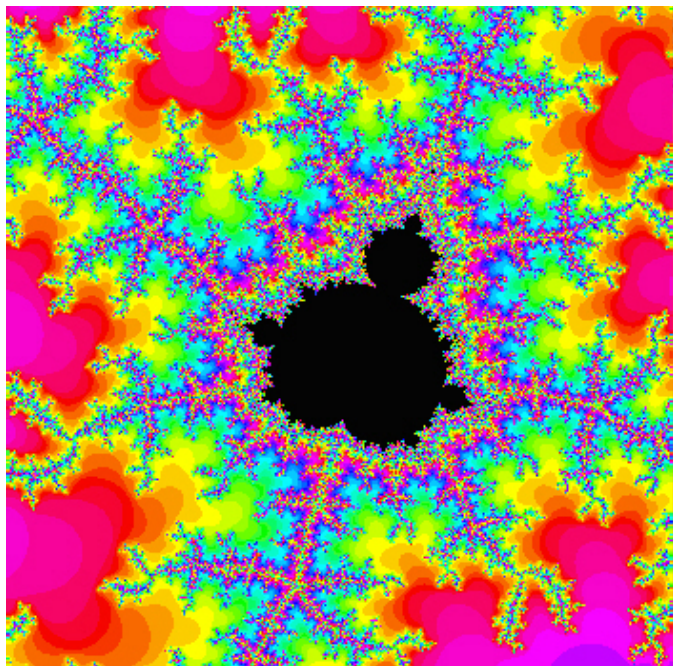


FIGURE 1.22. Which  $p/q$  limb contains this baby Mandelbrot set? Off of which sub-bulb of  $B_{p/q}$  does it live?

In your investigation of the antennae, bulbs, and limbs of  $M$  you may have also noticed that some of the parameter plane pictures (specifically enlarged areas of the tips of the antennae of  $M$ ) look very much like some of the dynamic plane pictures (specifically enlarged areas of the tips of certain Julia sets). In fact, these pictures can look so much alike that it can be confusing which is which (see Figure 1.23). This general phenomenon was proven in [20] where it was shown that zooming in the parameter plane near a Misiurewicz point  $c$  (see Definition 1.98) will show a portion of the Mandelbrot set which is a rotation of an enlargement of the Julia set of  $f_c$  in the dynamic plane near  $c$ . This fact is quite curious given that the parameter plane and the dynamic plane are, on the face of things, really different animals.<sup>23</sup> Why do parts of the Mandelbrot set seem identical to parts of certain Julia sets? The proof is too complicated for these pages, but we will be sure to witness and admire examples of it. Use the *Parameter Plane and Julia Set Applet* to zoom in very far on the point  $c = 0.4711819 + 0.3541484i$  in **both the parameter plane and the dynamic plane**

<sup>23</sup>This reminds the author of a comic strip which said, in paraphrased form, “Most mathematical discoveries are not accompanied by a shout of ‘Eureka!’, but rather a quietly spoken ‘Huh, now that’s curious.’”

(note that in the dynamic plane,  $c$  is the the first point in the critical orbit). Then compare the portion of  $M$  near  $c$  to the portion of  $J(f_c)$  near  $c$ . Up to a rotation it seems that these images are indeed identical.

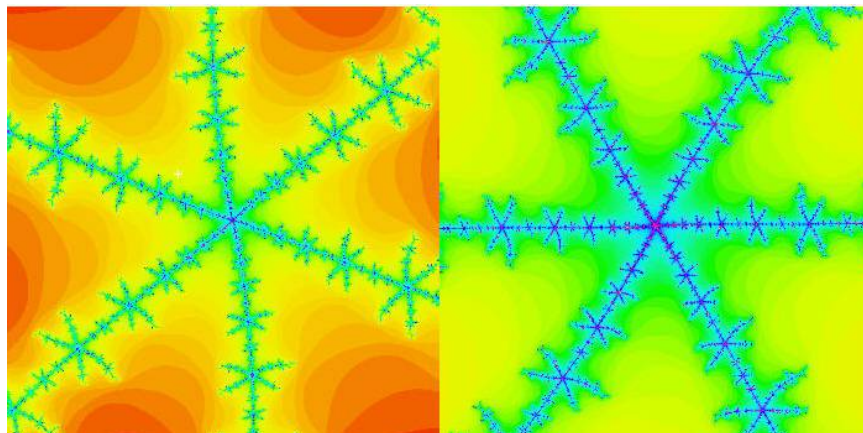


FIGURE 1.23. Which is part of the Mandelbrot set and which is part of a Julia set?

**1.5.7. Fixed points for  $f_c(z) = z^2 + c$ .** In this section we make a few remarks regarding the dynamics near the fixed points of  $f_c(z) = z^2 + c$ .

**EXAMPLE 1.129.** Using the *Parameter Plane and Julia Set Applet* set  $c = -0.513 + 0.5693i$  in the parameter plane and then choose seed  $z_0 = -0.4034 + 0.2896i$  (very near the main pinch point) in the dynamical plane. Zoom in close to the fixed point (with the **Plot fixed points** box, you can color these purple to more easily identify them) and then iterate this seed value one step at a time and observe the behavior. Try iterating several other seeds near the pinch point to see the same behavior. From this behavior we see that the main pinch point is a repelling fixed point whose multiplier  $\lambda$  has argument very close to  $(2/5) * 2\pi$ .

**EXERCISE 1.130.** Using paper and pencil (along with your calculator/computer) solve for the fixed points of  $f_c$  where  $c = -0.513 + 0.5693i$  as in Example 1.129. Compute their multipliers and verify that the “pinch point” multiplier  $\lambda$  does indeed have argument very close to  $(2/5) * 2\pi$ . Also, use the *Complex Function Iterator Applet* or *Global Complex Iteration Applet for Polynomials* to iterate the map  $z \mapsto \lambda z$  for various seed values near the repelling fixed point at the origin. Compare the dynamics of  $z \mapsto \lambda z$  near the origin and  $z \mapsto f_c(z)$  near the “pinch point”. **Try it out!**

**EXPLORATION 1.131.** Try investigating other  $c$  values in the  $2/5$  limb to see if it is always the case that the repelling fixed point has a multiplier with argument very close to  $(2/5) * 2\pi$ . You can do this experimentally by checking the behavior of orbits which start near the repelling fixed point (use the **Plot fixed points** feature in the



*Parameter Plane and Julia Set Applet* to locate the fixed points). Relate the argument of the multiplier to the dynamics near the repelling fixed point, specifically, note how this argument corresponds to the spiralling we see in  $K(f_c)$  near the repelling fixed point. How would this behavior change in other  $p/q$  limbs? **Try it out!**

Above we witnessed the role of the fixed point of  $f_c$  which also serves as a main “pinch point” in the set  $K(f_c)$ . What can you observe about the other fixed point? In what way does it appear to be different from the main “pinch point”? Does it have a special dynamic role? Can you prove anything or make a conjecture about this fixed point?

**1.5.8. Concluding remarks about the family of maps  $f_c(z) = z^2 + c$ .** Though we have witnessed and discussed many aspects of the Mandelbrot set there are many more things to know. We encourage the reader to delve deeper into the topics we discussed here and certainly pursue your own line of questions. There are many fascinating things left to discover in this infinite playground of mathematics. **Go enjoy it!**

We end this section with a remark about one of the goals we stated in the introduction to this chapter. This goal is to introduce, investigate, and understand what we can about chaotic dynamical systems. Systems involving the weather, the stock market, or the motion of all the heavenly bodies in the Milky Way galaxy are easy to believe to be chaotic. There are so many uncontrollable variables in these systems, and changing one, even just a little, will impact all the other variables. However, what we see with this family of maps  $f_c(z) = z^2 + c$  is also chaos. But with the family  $f_c(z) = z^2 + c$ , chaos ensued without a hundred unknown variables or any random processes. This simple system of one complex variable and one complex parameter turns out to produce chaotic behavior of an unimaginably wide and rich sort. This gives us small taste of what is truly a global phenomenon – chaos is all around us, even in what seems like the simplest of systems. For a wonderful and non-technical layperson’s look at some history of chaos, chaos theory, and the chaoticians who investigate it, we recommend the book *CHAOS: MAKING A NEW SCIENCE* by James Gleick [15].

**1.5.9. Other Uni-critical families of polynomials.** In this section we investigate the dynamics of polynomials of the form  $P_c(z) = z^d + c$  where  $d = 2, 3, 4, \dots$  (noting that we have already extensively studied the  $d = 2$  case). Since these maps also have only one finite critical point (at the origin), we can analyze the parameter space of these maps in much the same way as we did for the maps  $f_c(z) = z^2 + c$ . In particular, we define the  $d$ -th degree Mandelbrot set to be  $M_d = \{c \in \mathbb{C} : P_c^n(0) \not\rightarrow \infty\}$ , where it is understood that polynomial  $P$  is of fixed degree  $d$ . As we were told for the Mandelbrot set, the condition that the critical orbit  $\{P_c^n(0)\}$  tends to  $\infty$  is equivalent to the condition that some point in this orbit escape  $\Delta(0, 2)$ . Steps to prove this, and more, are given in Additional Exercise 1.189.

The reader is encouraged to explore the dynamics of each such family of maps using the *Parameter Plane and Julia Set Applet*. Where the function  $z^2 + c$  appears, use the drop down menu to select  $z^d + c$ , and then enter in any integer  $d > 2$ . Immediately, you will notice that the parameter plane and the dynamic plane exhibit certain symmetries (see Additional Exercise 1.190). Furthermore, you will recognize  $M_d$  as the connectedness locus for this new family as well (see Additional Exercise 1.191).

**LARGE PROJECT 1.132.** Investigate these families of maps using the *Parameter Plane and Julia Set Applet* in the same way as we did for the family  $f_c(z) = z^2 + c$ . Try to find patterns and relationships in the bulbs and antennae. Develop your own questions, make conjectures, and describe  $M_d$ .

## 1.6. Transcendental Dynamics

In this section we investigate the dynamics of three different families of maps  $E_c(z) = ce^z$ ,  $S_c(z) = c \sin z$ , and  $C_c(z) = c \cos z$ , where again  $c \in \mathbb{C} \setminus \{0\}$  is a parameter. We first consider the dynamic properties of these maps for fixed  $c$ , then we study the parameter plane, that is, we investigate what changes occur in the dynamics when the parameter  $c$  is varied. These functions all have one very striking difference from the maps  $P_c(z) = z^d + c$  studied above. They are *transcendental entire maps*,<sup>24</sup> and as such they not only fail to have an attracting fixed point at  $\infty$ , they fail to even be defined at  $\infty$ . In fact, these maps have an *essential singularity* at  $\infty$  which, among other things, means that they cannot be defined at  $\infty$  in any continuous way (see Example B.12 on page 426). However, it turns out that  $\infty$ , or more specifically the basin of  $\infty$ , still plays a central role. In fact, it turns out that instead of the basin of  $\infty$  being in the Fatou set like we have for polynomials, we have quite the opposite.

**PROPOSITION 1.133.** For each of the maps  $E_c(z) = ce^z$ ,  $S_c(z) = c \sin z$ , and  $C_c(z) = c \cos z$ , where  $c \in \mathbb{C} \setminus \{0\}$ , the Julia set is equal to the closure of the attracting basin of  $\infty$ , e.g.,  $J(E_c) = \overline{A_{E_c}(\infty)}$ .

The reader should pause for a moment to take in the striking difference asserted by this proposition between polynomial dynamics and the dynamics of the given transcendental maps. Though the proof of this is beyond the scope of this text, we will make use of this result (see [5, 8] as a general references on the dynamics of  $E_c$ ). In particular, we use this fact to program the computer to attempt to illustrate the Julia sets of these maps. However, in order to do so, we must first understand how, or rather in what direction, a point  $z_0$  can iterate to  $\infty$  under each of these maps. We first investigate the map  $E_c(z) = ce^z$ .

**REMARK 1.134.** For those readers who are familiar with *Picard's Theorem* (see [1], p. 242), we give some idea why the Julia set of certain transcendental entire functions

<sup>24</sup>A *transcendental entire* map is defined to be a map which is analytic on all of  $\mathbb{C}$  (entire), but which is not a polynomial.

is related to the closure of the points which iterate to  $\infty$ . Picard's Theorem says that given any entire map  $g$  with an essential singularity at  $\infty$  and given *any* neighborhood  $U$  of  $\infty$  (no matter how small),  $g$  will map  $U \setminus \{\infty\}$  *infinitely often* onto the entire complex plane  $\mathbb{C}$  minus at most one point. This means that with the exception of at most one point  $w \in \mathbb{C}$ , there are infinitely many points  $z \in \mathbb{C}$  such that  $g(z) = w$ .<sup>25</sup> Hence, there must be a very high degree of sensitive dependence as some points very near  $\infty$  must have very different orbits even in the first application of the map (let alone after repeated iteration of the map).

**1.6.1. Exponential dynamics.** In this section we investigate the dynamics of the complex exponential maps  $E_c(z) = ce^z$ . Recall that  $E_c(z) = ce^z = ce^x e^{iy}$  where  $x = \operatorname{Re} z$  and  $y = \operatorname{Im} z$ , and so  $|E_c(z)| = |c|e^x$ . Hence we see that  $E_c(z)$  is very large, and thus close to  $\infty$ , when  $x = \operatorname{Re} z$  is large. In particular, if  $\operatorname{Re} z > 50$ , then  $|E_c(z)| > |c|e^{50}$  is *extremely* large indeed (for any  $c$  that is not so small that a computer would recognize it as 0). We use this to justify the algorithm implemented in the *Parameter Plane and Julia Set Applet*, for drawing  $J(E_c)$ , which you can access by selecting  $ce^z$  from the function drop down menu. In particular, a point in the dynamic plane is colored based on how many iterates it takes to “escape”, by which we mean have its real part become greater than 50. Thus the colored points represent  $A_{E_c}(\infty)$ , which by Proposition 1.133, must visually look the same as the Julia set.<sup>26</sup> Points colored black do not escape, at least not after iterating the number of times set in the **Dynamic plane max iterations** box, and so these points represent the Fatou set. Since  $E_c^n(z_0) \rightarrow \infty$  if and only if  $\operatorname{Re} E_c^n(z_0) \rightarrow +\infty$  (see Additional Exercise 1.192), we say that points that iterate to  $\infty$ , do so *in the direction of the positive real axis*.

EXAMPLE 1.135. We show that for  $c = 0.2$  the Julia set  $J(E_{0.2})$  is what we will call a *Cantor Bouquet*. We note here that our proof will not make use of the applet, nor of its algorithm, but will employ only the notion of sensitive dependence on initial conditions. However, we will find it useful to get a visual by first viewing the Julia set as drawn by the *Parameter Plane and Julia Set Applet* (see Figure 1.24).

Recalling that points in black do not escape and other points iterate to  $\infty$  (in the direction of the positive real axis), we see that the colored set depicts  $J(E_{0.2})$ . It appears from the picture that  $J(E_{0.2})$  contains large open sets, but it turns out that this is simply an artifact of our algorithm's inability to iterate infinitely many times. Were we able to set the **Dynamic plane max iterations** equal to infinity we would not find any open sets in  $J(E_{0.2})$ . We explain why in a moment, but first use the

<sup>25</sup>As an example, consider the map  $e^z$  which has such an exceptional value at  $w = 0$ , but also is easily seen to have infinitely many preimages of any point in  $\mathbb{C} \setminus \{0\}$ .

<sup>26</sup>According to the algorithm just described a point  $z$  may be identified to be in the Julia set when in truth it is not. However, one can show that if such were to occur, there would have to be a point *very* close, depending on the parameter settings of the applet, to  $z$  which does truly lie in the Julia set (see Additional Exercise 1.193). Hence for the purpose of creating a visual representation of the Julia set, this technical issue does not pose a serious concern.

zooming feature to see that what appears to be tiny “fingers” in  $J(E_{0.2})$  are actually made of tinier fingers, which are themselves made of even tinier fingers and so on. **Try it out!** So we see self similarity again. We now explain why the picture of  $J(E_{0.2})$  shows these fingers inside of fingers.

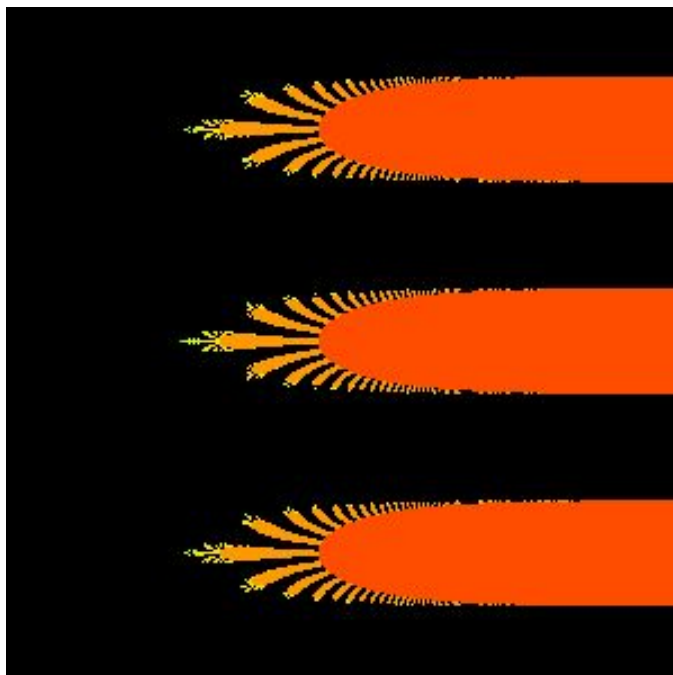


FIGURE 1.24. A portion of the Julia set of  $E_{0.2}$  shown for  $0 \leq x \leq 10$  and  $-10 \leq y \leq 10$ .

We begin by showing that  $E_{0.2}$  has a real attracting fixed point. Using the Intermediate Value Theorem we note that  $E_{0.2}$  has a fixed point  $p$  for some real value  $0 < p < 1$  since the  $E_{0.2}(x) - x$  is positive for  $x = 0$  and negative for  $x = 1$ . Also, we see that  $p$  is attracting since  $|E'_{0.2}(p)| < 1$ .

We now proceed to show that the half plane  $H = \{\operatorname{Re} z < 1\}$  is contained in the attracting basin  $A_{E_{0.2}}(p)$ . Set  $\eta = |E'_{0.2}(1)| = 0.2e$  and note that  $|E'_{0.2}(z)| < \eta < 1$  for all  $z \in H$ . Thus, for all  $z \in H$ , we have  $|E_{0.2}(z) - p| = |E_{0.2}(z) - E_{0.2}(p)| = |\int_p^z E'_{0.2}(s) ds| \leq \eta|z - p|$ , where the straight line path is used in the integral. Hence the action of  $E_{0.2}$  is to move points in  $H$  closer to  $p$  by a factor of at least  $\eta$ .<sup>27</sup> Formally using induction, along with the fact that  $E_{0.2}(H) \subseteq H$  (verify), the reader can show that for all  $z \in H$  we have  $E_{0.2}^n(z) \rightarrow p$ , i.e.,  $H \subseteq A_{E_{0.2}}(p)$ .

<sup>27</sup>Using the *Parameter Plane and Julia Set Applet* with  $E_{0.2}(z) = 0.2e^z$ , the reader can see this contraction in action. In the Dynamic Plane window with  $-2 \leq \operatorname{Re} z \leq 2$  and  $-2 \leq \operatorname{Im} z \leq 2$  (which will be all black), pick any two points and iterate the map one step at a time. You can clearly see that after each step the new points are much closer together.

The technique just employed which shows how a bound on the derivative can be used to show “contraction” of a map is a general, and very useful, one. We interrupt our proof of the Cantor bouquet result in order to state this as a lemma for future use (whose proof is left to the reader in Additional Exercise 1.194).

LEMMA 1.136 (Contraction Lemma). Let  $f$  be analytic and map *convex*<sup>28</sup> domain  $D$  into itself. Suppose that  $|f'(z)| < \eta < 1$  for all  $z \in D$ . Then  $f$  contracts distances by a factor of at least  $\eta$  on  $D$ , i.e.,  $|f(z) - f(w)| < \eta|z - w|$  for all  $z, w \in D$ . Furthermore,  $|f^n(z) - f^n(w)| < \eta^n|z - w|$  for all  $z, w \in D$ . Hence, if  $a \in D$  is a fixed point of  $f$ , then  $D \subseteq A_f(a)$ .

Returning to the proof that  $J(E_{0.2})$  is a Cantor bouquet we now consider  $E_{0.2}^{-1}(H) = \{z \in \mathbb{C} : E_{0.2}(z) \in H\}$ . The reader should use the transformation properties of the exponential map to justify the picture in Figure 1.25 showing that  $\mathbb{C} \setminus E_{0.2}^{-1}(H)$  consists of infinitely many components, which we call **fingers**. In particular, we label these fingers by  $C_k$  for each  $k \in \mathbb{Z}$ , noting that each  $C_k$  is just a translate by  $2\pi ik$  of  $C_0$ . We also note that  $H \subseteq E_{0.2}^{-1}(H)$ .

We note that each  $C_k$  is mapped *conformally*<sup>29</sup> onto the half plane  $\{\operatorname{Re} z \geq 1\}$ , and thus each  $C_k$  must contain a preimage under  $E_{0.2}$  of each  $C_j$  for all  $j \in \mathbb{Z}$ . These preimages, shown in red in Figure 1.26, are each sub-fingers of  $C_k$  with what we informally call **gaps** (in black) in between. We note that these gaps, just as in Figure 1.25, extend all the way to  $\infty$  (in the direction of the positive  $x$ -axis).

We continue to take inverse images of  $H$  to see that, for any  $n \in \mathbb{N}$ , the set  $E_{0.2}^{-n}(H)$  has a complement  $\mathbb{C} \setminus E_{0.2}^{-n}(H)$  consisting of fingers inside of fingers inside of fingers, and so on. More precisely, we make the following definition.

DEFINITION 1.137. We call each component of  $\mathbb{C} \setminus E_{0.2}^{-n}(H)$  a *stage  $n$  finger*.

For example, Figure 1.25 depicts stage 1 fingers in red and the bottom picture in Figure 1.26 depicts stage 2 fingers in red. The gaps (in black) are then portions of  $E_{0.2}^{-2}(H)$  which separate the fingers from each other. We encourage the reader to investigate these stage  $n$  fingers more closely using the *Parameter Plane and Julia Set Applet* by setting both the **Dynamic plane max iterations** and the **Dynamic plane min iterations** to  $n$ , while setting the **Escape criterion** to  $\operatorname{Re} z > 1$ . Note that each stage  $n$  finger is contained in a stage  $n - 1$  finger (for  $n \geq 2$ ). Also note that the boundary of each stage  $n$  finger (for  $n \geq 2$ ) is mapped by  $E_{0.2}$  onto the boundary of some stage  $n - 1$  finger and thus is mapped by  $E_{0.2}^n$  onto the vertical line  $\{\operatorname{Re} z = 1\}$ .

It will be important to understand how “thick” these fingers can be and so we make the following definition.

<sup>28</sup>A set  $D$  is called **convex** if for any points  $z, w \in D$ , the line segment connecting  $z$  and  $w$  is a subset of  $D$ .

<sup>29</sup>Recall, that a conformal map is one-to-one and analytic.

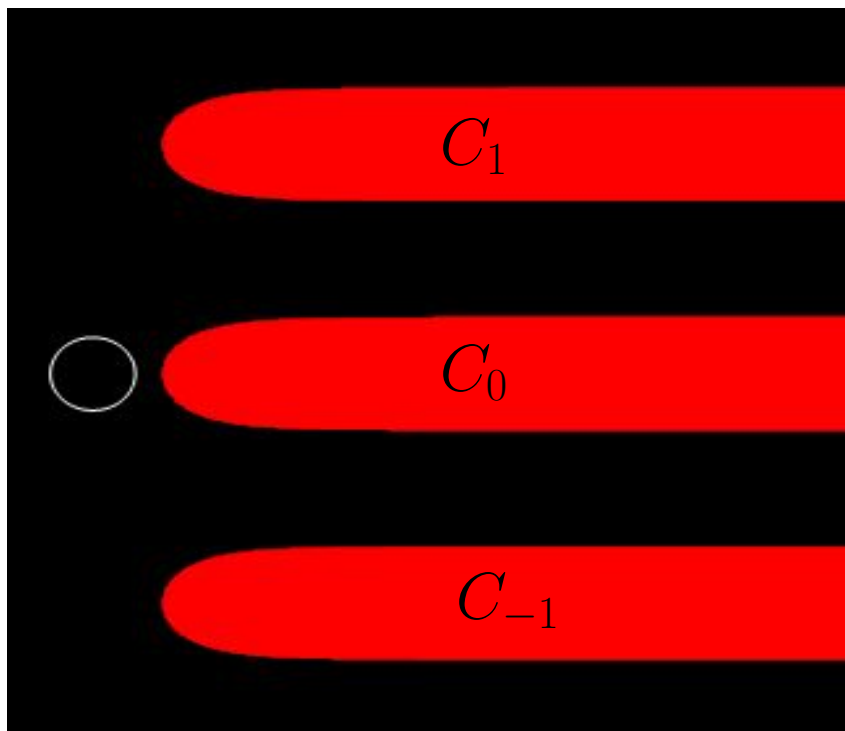


FIGURE 1.25. In this window of the complex plane, the set  $E_{0.2}^{-1}(H)$  is colored in black with components of its complement in red for  $-2 \leq x \leq 18$  and  $-10 \leq y \leq 10$ . For reference, the unit circle is also shown in white.

DEFINITION 1.138. Let  $F$  be a stage  $n$  finger. We define the *thickness* of  $F$  to be the special value of  $t$  such that  $F$  cannot contain an open Euclidean disk with diameter strictly larger than  $t$ , but for any value  $s < t$ , the set  $F$  does contain an open Euclidean disk with diameter  $s$ .<sup>30</sup>

EXERCISE 1.139. Use the mapping properties of the exponential map and the definition of stage 1 finger to prove that the thickness of each stage 1 finger  $C_k$  is  $\pi$ . **Try it out!**

Note that the set  $F_n = \mathbb{C} \setminus E_{0.2}^{-n}(H)$  is the union of all stage  $n$  fingers and because each stage  $n$  finger is contained in a stage  $n - 1$  finger we see that  $F_1 \supset F_2 \supset \dots$ , and in particular,  $F_1 \cap F_2 \cap \dots \cap F_n = F_n$ . Thus in some loose sense we can regard  $\bigcap_{n=1}^{\infty} F_n$  as the union of all of the stage “infinity” fingers. It is these stage “infinity” fingers together with the point at  $\infty$  that comprise the Julia set, a proposition we state as follows.

<sup>30</sup>Those familiar with the concept of supremum may recognize that  $t = \sup\{2r > 0 : \Delta(z, r) \subseteq F \text{ for some } z \in F\}$ , the *supremum* of the diameters all open disks contained in  $F$ .

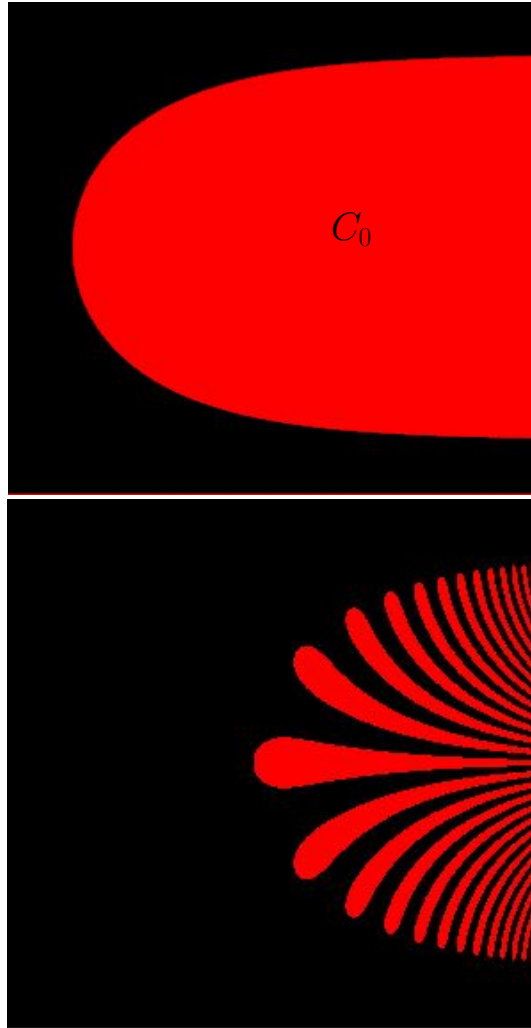


FIGURE 1.26. On top you can see the tip of the finger  $C_0$  and on bottom you can see a portion of  $E_{0.2}^{-2}(H) = E_{0.2}^{-1}(E_{0.2}^{-1}(H))$  for  $1 \leq x \leq 6$  and  $-2 \leq y \leq 2$ . The red sub-fingers each sit well inside of  $C_0$ .

PROPOSITION 1.140. The Julia set  $J(E_{0.2}) = \bigcap_{n=1}^{\infty} F_n \cup \{\infty\} = \overline{\mathbb{C}} \setminus A_{E_{0.2}}(p)$ .

PROOF. We set  $J = \bigcap_{n=1}^{\infty} F_n \cup \{\infty\}$  and outline the proof as follows. First, note the following facts, whose proof we leave to the exercises: (a) any two fingers are always separated by an infinitely long gap (of black) points in  $A_{E_{0.2}}(p)$  (see Additional Exercise 1.195), and (b) the thickness of the stage  $n$  fingers shrinks to zero as  $n$  goes to infinity (see Additional Exercise 1.196). Facts (a) and (b) can then show that the set  $J$  cannot contain any open set (see Additional Exercise 1.197). Hence for any point  $z \in J$  we see that there are points arbitrarily close which lie in  $\bigcup_{n=1}^{\infty} E_{0.2}^{-n}(H)$ , and thus iterate to  $p$ . Since the orbit of every  $z \in J$  lies forever in  $\{\operatorname{Re} z \geq 1\}$  by the

definition of  $J$  (and thus is quite different from an orbit which converges to  $p$ ), we get that  $z$  is sensitive to initial conditions and so  $z \in J(E_{0.2})$ . Likewise, for a point not in  $J$ , it and all the nearby points which also lie in the open set  $A_{E_{0.2}}(p)$  have the same dynamic behavior (in that they all iterate towards  $p$ ), placing such a point in the Fatou set  $F(E_{0.2})$ . Hence we have shown  $J = J(E_{0.2})$  as desired.  $\square$

EXPLORATION 1.141. Use the *Parameter Plane and Julia Set Applet* to track the orbit of nearby points in  $J(E_{0.2})$  to witness this sensitivity to initial conditions. It is a bit difficult to pick points that stay in the viewing window after more than a few steps, but by looking at the data in the **Orbits 1 and 2** tab at the bottom, you can see the orbits separate from each other. You can also zoom in on the picture so that you can choose your initial seed values very close to each other, and then zoom out to see their orbits. *Try it out!*

**1.6.2. Hairs and endpoints.** Thinking again about this construction of  $J(E_{0.2})$  we now describe this “Cantor Bouquet” by describing the “hairs” (previously called the stage “infinity” fingers) which make up this set. This section is not crucial to moving forward with the rest of the text, and we will not provide all of the details here to prove everything claimed, but we won’t let that get in the way of discussing some very fascinating aspects of what we have stumbled upon in the above example. This section is more about “points of interest” that may inspire the motivated reader to pursue such ideas further.

Pick a stage 1 finger  $C_{k_1}$ , and then from the infinite number of sub-fingers within  $C_{k_1}$  pick one sub-finger  $C_{k_1 k_2}$ . Then from the infinite number of sub-sub-fingers within that, pick one sub-sub-finger  $C_{k_1 k_2 k_3}$ . Continuing on in this fashion so that each  $C_{k_1 k_2 \dots k_n}$  is a stage  $n$  finger which lives in  $C_{k_1 k_2 \dots k_{n-1}}$ . We see that  $\gamma = \bigcap_{n=1}^{\infty} C_{k_1 k_2 \dots k_n}$  must, by (b) above, be infinitely thin (i.e., contain no open disk of any positive radius), but which also stretches to  $\infty$  in the positive  $x$ -direction. We call this intersection  $\gamma$  a **hair**, and note that there are infinitely many (actually uncountably many) of these hairs in  $J(E_{0.2})$  corresponding to all the different ways one can choose  $k_1 k_2 \dots$ . It turns out that each hair  $\gamma$  is actually a curve, that is, an image of a continuous map  $h_\gamma : [0, \infty) \rightarrow \mathbb{C}$  such that  $h_\gamma(t) \rightarrow \infty$  as  $t \rightarrow \infty$ . We call the point  $h_\gamma(0)$  the **endpoint** of the hair  $\gamma$ . There are a few important details to be shown to prove all this. In particular, an important detail we have yet to address at all is: how do we know that there is anything left in the set  $\gamma = \bigcap_{n=1}^{\infty} C_{k_1 k_2 \dots k_n}$ , or even in the larger set in  $\bigcap_{n=1}^{\infty} F_n$ ? Perhaps, the left “tips” of the stage  $n$  fingers move farther and farther to the right in a way that the set  $\bigcap_{n=1}^{\infty} F_n$  is actually empty. We leave it to the interested reader to pursue these matters in [5]. However, we do have another way to see that we have infinitely many hairs (clearly shown to have finite endpoints) in  $J(E_{0.2})$  and the interested reader can pursue this in Additional Exercise 1.198.

As one can see in the construction above, each hair is separated from any other hair by an infinite (though possibly very thin) gap which stretches out to  $\infty$  in the direction of the positive  $x$ -axis. Thus in the plane  $\mathbb{C}$  we would say these hairs are all



separated from each other. However, by including  $\infty$ , where all these hairs “meet”, we produce a set  $J(E_{0,2}) \cup \{\infty\}$  which is a connected subset of the sphere  $\overline{\mathbb{C}}$ .

We conclude this section with remarks about two truly fascinating properties of the Cantor Bouquet  $J(E_{0,2})$ . In order to discuss this properly we will need the following more general definition of what it means for a (not necessarily open or closed) subset of  $\overline{\mathbb{C}}$  to be connected.

**DEFINITION 1.142.** A set  $C$  is *connected* in  $\overline{\mathbb{C}}$  if one cannot find open subsets  $U$  and  $V$  of  $\overline{\mathbb{C}}$  such that (i)  $U \cap C \neq \emptyset$ , (ii)  $V \cap C \neq \emptyset$ , (iii)  $C \subseteq U \cup V$  and (iv)  $U \cap V \cap C = \emptyset$ . Another, perhaps more intuitive definition is as follows: A set  $C \subseteq \overline{\mathbb{C}}$  is connected in  $\overline{\mathbb{C}}$  if we cannot break up (*disconnect*)  $C$  into a disjoint union of non-empty sets  $A$  and  $B$  (thus  $C = A \cup B$ ) such that no sequence from  $A$  converges to a point in  $B$ , and vice versa.

We can now present (without proof) two startling properties of the Cantor Bouquet  $J(E_{0,2})$ .

**Property 1.** Let  $\mathcal{E}$  denote the set of all endpoints of all the hairs in  $J(E_{0,2})$ . Then the set  $\mathcal{E}^* = \mathcal{E} \cup \{\infty\}$  is *connected* in  $\overline{\mathbb{C}}$ . Informally, this says that these endpoints *together with*  $\infty$  are somehow bunched up together so tightly in such a way that it is impossible to disconnect this set in the manner described in Definition 1.142. However, and here comes the strange part, it turns out that removing  $\infty$  from  $\mathcal{E}^*$  creates a *totally disconnected* set  $\mathcal{E}$  (i.e., the only connected subsets of  $\mathcal{E}$  are sets which contain just a single point). In fact, we can show this second part quite easily by noting that between any two hairs there is a *gap* in  $F(E_{0,2})$  between them, thus showing that the endpoints of these hairs cannot both lie in the same connected subset of  $\mathcal{E}$ . This gap, however, extends to  $\infty$  and so cannot be used to create a disconnection of  $\mathcal{E}^*$ . However, it still remains to be shown that no other method of disconnecting  $\mathcal{E}^*$  can work either. Since this is too complicated for the present text we leave the interested reader to view the details in [21].

**Property 2.** The Hausdorff dimension is a concept that allows one to assign a number to each set in  $\overline{\mathbb{C}}$  which relates to the “size” of the set. The number is defined (see [11] for further details) in such a way that it shares many of the properties of our usual notion of dimension and so we refer to it as a “dimension” even though it need not be an integer. In particular, the Hausdorff dimension of a set measures, in some sense, “how much space the set fills up”. With this, the Hausdorff dimension of any *smooth* curve, in particular, any hair in  $J(E_{0,2})$  (which are shown to be smooth in [4]), has dimension 1, whether the endpoint is included or not. Let  $\mathcal{H}$  denote the union of all *open* hairs, that is, each hair with its endpoint removed. Thus  $\mathcal{H} = J(E_{0,2}) \setminus \mathcal{E}^*$ . These hairs, as you will recall, are each separated by gaps that prevent them from accumulating too much and “filling up” a lot of space. So, at least heuristically, it seems plausible that  $\mathcal{H}$  has Hausdorff dimension equal to 1, which it turns out it does.

What is astounding is that the set of endpoints  $\mathcal{E}$  has dimension equal to 2. Thus the endpoints seem to bunch up in a strange fashion so that the set of all of them “fills up” two dimensions worth of space. Since for each infinitely long hair there is only one endpoint, it seems impossible that the set of endpoints could be larger than the set of open hairs (as measured by Hausdorff dimension). But this is exactly what happens. The interested reader should see [18, 19] for the details.

**1.6.3. Critical orbits, Exploding Julia sets, Parameter space for  $E_c$ .** As we have seen, the role of critical points dictates much about the overall dynamics of a rational map, especially for the family of polynomials  $f_c(z) = z^2 + c$ . The exponential maps  $E_c(z) = ce^z$ , however, have no critical points (verify), but each such map does have 0 as what we call an *asymptotic value* and this will play a critical role very much like a critical point for a rational map does.

**DEFINITION 1.143.** An *asymptotic value* for an entire function  $f$  is a value  $a \in \overline{\mathbb{C}}$  such that there exists a curve  $\gamma : [0, +\infty) \rightarrow \mathbb{C}$  tending to  $\infty$  (i.e.,  $\gamma(t) \rightarrow \infty$  as  $t \rightarrow +\infty$ ) such that  $f(\gamma(t)) \rightarrow a$  as  $t \rightarrow +\infty$ .

We note that for the case of  $E_c$  we may choose the curve to be the negative real axis, along which the values  $E_c(z) \rightarrow 0$  since  $\operatorname{Re} z \rightarrow -\infty$ . The following theorem, whose proof can be found in [5], is a result which parallels Theorems 1.89 and 1.93 given for rational maps.

**THEOREM 1.144.** Let  $f$  be a transcendental entire map. Then the immediate basin of each (super) attracting cycle of  $f$  contains a critical point of  $f$  or an asymptotic value of  $f$ .

From this result we see that the orbit  $\{E_c^n(0)\}_{n=1}^\infty$  plays a very special role and so we call it the *critical orbit*.

**Fact 1.** Any attracting cycle of  $E_c$  must attract the *critical orbit*  $\{E_c^n(0)\}_{n=1}^\infty$ .

Fact 1 follows from Theorem 1.144. This next fact, however, has a proof beyond the scope of this text, but we shall nonetheless make frequent use of it.

**Fact 2.** If the *critical orbit*  $E_c^n(0) \rightarrow \infty$ , then  $J(E_c) = \overline{\mathbb{C}}$ .

Note that Fact 2 is strikingly different from anything we have yet seen. In fact, due to the super attracting fixed point at  $\infty$  for any polynomial we know that we could never have such a Fatou set be empty.

Fact 2 also leads us to discover the fascinating *exploding* Julia sets we can see when we vary the parameter  $c$  in the map  $E_c$ . As we saw in Example 1.135,  $J(E_{0.2})$  is a Cantor Bouquet of hairs and  $F(E_{0.2})$  consists of exactly the attracting basin of a finite attracting fixed point  $p \approx 0.26$ . However, if we increase  $c$  from  $c = 0.2$  to  $c = 0.5$  we see that  $E_{0.5}^n(0) \rightarrow +\infty$  and so, by Fact 2, we must have  $J(E_{0.5}) = \overline{\mathbb{C}}$ . Hence some real value  $c^*$  between  $c = 0.2$  and  $c = 0.5$  must be a bifurcation point where the dynamics

drastically change. What we see is that as  $c$  grows from being smaller than  $c^*$  to larger than  $c^*$  the Julia set goes from being confined to  $\{\operatorname{Re} z \geq 1\}$  to *exploding* to be all of  $\overline{\mathbb{C}}$  (see Additional Exercise 1.199).

So we see that we get very different dynamic behavior for  $E_c$  depending on whether or not the critical orbit escapes to  $\infty$ . We use this dichotomy to color the *parameter plane* based on how many iterates it takes for the critical orbit to escape (that is, have real part become greater than 50), leaving the  $c$  parameter black if the critical orbit does not escape. You can view and investigate this parameter space using the *Parameter Plane and Julia Set Applet*. Using this applet, set the window in the Parameter plane to show  $[-3.2, 3.2] \times [-3, 3]$  to find a cardioid shape region, with many bulbs attached. You will likely want to set the **Parameter plane max iterations** value to 40, 60, 80, or 100 to see this cardioid in more detail. However, due to the computing power needed to compute the complex exponential iterates, each picture may take a little while for the applet to complete.

EXPLORATION 1.145. Take some time to experiment with this applet to see if you can guess the dynamical significance of this cardioid and some of the attached bulbs. **Try it out!**

Let's investigate this exponential parameter plane much like we did for the family  $f_c(z) = z^2 + c$  by calculating the set  $L_1$  of  $c$  values for which  $E_c$  has an attracting fixed point  $p$ . In order for  $p$  to be an attracting fixed point we require  $E_c(p) = p$  and  $|E'_c(p)| < 1$ . The first condition yields  $ce^p = p$  which used with the second gives  $|p| = |ce^p| < 1$ . Notice in this case  $p$  is both the fixed point and the multiplier. Thus we are looking for  $c$  such that  $c = pe^{-p}$  for  $|p| < 1$ . By letting  $p$  move around the unit circle, the corresponding  $c$  values trace out the cardioid-like set in the parameter plane pictured in Figure 1.27. Use the *ComplexTool* applet to draw this.

This cardioid-like  $L_1$  has many similarities with the cardioid  $K_1$  found in the Mandelbrot set. For example, one can find  $p/q$  bulbs attached to its boundary. (Note that the letter  $p$  when used to refer to an attracting fixed point of  $E_c$  is a complex number, whereas the  $p$  used in the numerator of  $p/q$  to denote a particular bulb is always a positive integer (as is  $q$ ). Context will always make it clear which is which and so no confusion should arise.) These  $p/q$  bulbs might not be located where you first expect. For example, the  $1/3$  bulb in the Mandelbrot set  $M$  was found at the top of the cardioid  $K_1$  whereas the top of  $L_1$  has the  $2/5$  bulb attached.

EXPLORATION 1.146. Use the *Parameter Plane and Julia Set Applet*<sup>31</sup> to investigate the “new” locations of the  $p/q$  bulbs. One way to determine the location of these  $p/q$  bulbs is to experiment long enough to find a pattern (can you use Farey addition

---

<sup>31</sup>Be sure the settings for the applet are returned to values which will produce good pictures. In particular, you may want to check the values for the Escape criterion and max/min iterations which you adjusted earlier (or simply reload the applet).

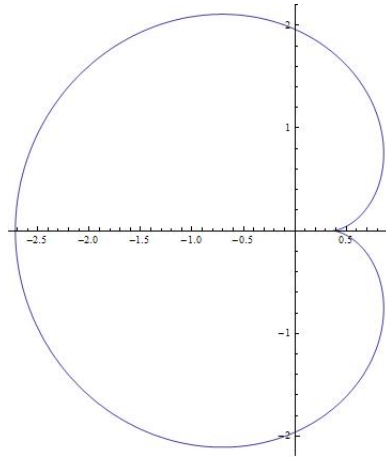


FIGURE 1.27. This cardioid-like shape is the boundary of  $L_1$ , the set of  $c$  parameters which give rise to an attracting fixed point for the map  $E_c(z) = ce^z$ .

here too?). Another way is to use the multiplier map, or more precisely, the inverse of the multiplier map (see Additional Exercise 1.200). **Try it out!**

EXPLORATION 1.147. Where is the  $1/2$  bulb located? Does it have a sub-bulb which corresponds to attracting 4-cycles? **Try it out!**

EXERCISE 1.148. Whether or not you think you can solve it, try to come up with an interesting mathematical question about what you see in the dynamics of exponentials. Try to draw parallels, or show where parallels do not hold, with the family  $f_c(z) = z^2 + c$ . **Try it out!**

**1.6.4. The Trigonometric maps.** Recall that  $\sin z = \frac{-i}{2}(e^{iz} - e^{-iz})$  and  $\cos z = \frac{1}{2}(e^{iz} + e^{-iz})$ , and set  $S_c(z) = c \sin z$  and  $C_c(z) = c \cos z$ . We leave it to the reader to use these facts to show that orbits under the maps  $S_c(z)$  and  $C_c(z)$  “escape” to  $\infty$  in the direction of the positive or negative imaginary axis (see Additional Exercise 1.201). Thus, using Proposition 1.133 to note  $J(S_c) = \overline{A_{S_c}(\infty)}$  and  $J(C_c) = \overline{A_{C_c}(\infty)}$ , the algorithm in the *Parameter Plane and Julia Set Applet* for creating the Julia sets for the exponential maps  $E_c(z) = ce^z$  can easily be modified. In particular, an orbit under either  $S_c$  or  $C_c$  is deemed to limit to  $\infty$  if any point in the orbit has imaginary part larger than 50 in absolute value. It is known that neither  $S_c$  nor  $C_c$  has a finite asymptotic value (see Additional Exercise 1.202), however, both have infinitely many critical points. At first glance this may appear to provide us with considerable difficulty, since a map having more than one critical orbit would pose a real challenge to coloring and analyzing the parameter space as easily as we have done for the maps  $z^d + c$  and  $ce^z$ . However, as we ask you to verify in Additional Exercise 1.203, each map  $S_c$  and

$C_c$  has just one critical orbit. In particular,  $\{S_c^n(c)\}_{n=1}^\infty$  is the critical orbit for  $S_c$  and  $\{C_c^n(c)\}_{n=1}^\infty$  is the critical orbit for  $C_c$ .

As in the exponential case we have key facts that will greatly aid in our understanding of the dynamics of these Trigonometric functions.

**Fact 1.** Any attracting cycle of  $S_c$  must attract its *critical orbit*  $\{S_c^n(c)\}_{n=1}^\infty$ .

**Fact 2.** Any attracting cycle of  $C_c$  must attract its *critical orbit*  $\{C_c^n(c)\}_{n=1}^\infty$ .

**Fact 3.** If the *critical orbit*  $S_c^n(c) \rightarrow \infty$ , then  $J(S_c) = \overline{\mathbb{C}}$ .

**Fact 4.** If the *critical orbit*  $C_c^n(c) \rightarrow \infty$ , then  $J(C_c) = \overline{\mathbb{C}}$ .

Because the orbit  $\{S_c^n(c)\}_{n=1}^\infty$  is critical to the dynamics of the map  $S_c$ , we can then draw the parameter plane much like we did for the family of maps  $E_c$ . In particular, the *Parameter Plane and Julia Set Applet* will color each  $c$  parameter based on how many iterates it takes for the critical orbit to escape, in this case in the direction of the positive or negative imaginary axis. As before, the  $c$  parameter is left black if the critical orbit does not escape. As always, we must heed the usual warnings that the computer is illustrating only an approximation (hopefully a good one) to the actual dynamics we are trying to study. The applet for  $C_c$  works similarly. Use this applet now to experiment and investigate the dynamics you find with the functions  $S_c$  and  $C_c$ . If you look closely in the parameter planes, you will find a familiar friend. ***Try it out!***

### 1.7. The Mandelbrot Set is Universal

You have probably noticed that the parameter planes for the maps  $f_c(z) = z^2 + c$ ,  $C_c(z) = c \cos z$ , and  $S_c(z) = c \sin z$  drawn by the *Parameter Plane and Julia Set Applet* all show black regions that contain sets which resemble the Mandelbrot set  $M$ . See Figure 1.28.

The appearance of copies of the Mandelbrot set in all of these diverse settings is quite unexpected. Why should the Mandelbrot set, a picture of the fundamental dichotomy in the study of the parameter space of quadratic maps  $f_c(z) = z^2 + c$ , have anything to do with the parameter space of the transcendental maps  $C_c(z) = c \cos z$  and  $S_c(z) = c \sin z$ ? It turns out that the Mandelbrot set, or at least various “copies” of it appear in so many parameter planes that it is truly a fundamental mathematical object (much like the numbers  $\pi$  and  $e$ ) which arises in many unexpected places. Just like we saw that baby Mandelbrot sets are dense in the full Mandelbrot set  $M$ , so too are they dense in many parameter spaces. The main reason behind all of this, which we can only state loosely in this text, is that very often iterates of maps have dynamic behavior very much like the dynamic behavior of iterates of a quadratic polynomial, when these maps are considered on relatively small domains. Thus, as a parameter is changed, we see the same type of changing behavior in the parameter plane of this family of maps as we do in the original family  $f_c(z) = z^2 + c$  corresponding the

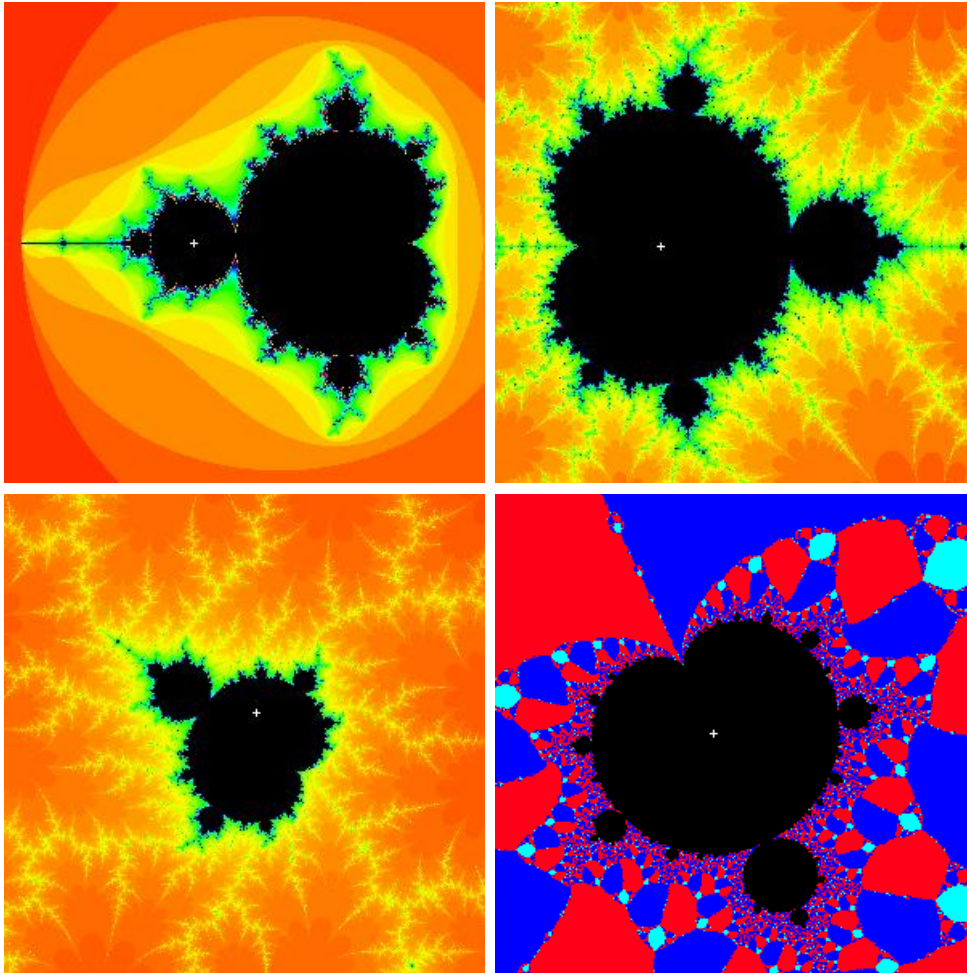


FIGURE 1.28. The original Mandelbrot set  $M$  (upper left), a “copy” of  $M$  containing  $c = 3.2$  in the parameter space for  $c \cos z$  (upper right), a “copy” of  $M$  containing  $c = 2.17 + 1.3i$  in the parameter space for  $c \sin z$  (lower left), and a “copy” of  $M$  containing  $\rho = 0.906 + 0.423i$  in the parameter space for Newton’s method applied to the map  $p_\rho(z) = z(z - 1)(z - \rho)$ .

original Mandelbrot set. The interested reader can look to [22] where it is shown that small Mandelbrot sets are dense in the bifurcation locus for what are called *holomorphic families* of rational maps.

### 1.8. Concluding remarks and new directions

We have investigated the chaos that arises through a number of different complex dynamical systems. We saw how Newton’s method can (and very often must) produce

very chaotic behavior, represented by beautiful fractal images. In order to investigate such chaos in a more general setting, we turned our eyes to iteration of analytic maps that were not necessarily generated as the Newton map of some polynomial. There we found that even in the seemingly simple class  $f_c(z) = z^2 + c$  there was a richness and complexity we could not have imagined. Many of these features were also present in the dynamics of the entire maps  $E_c(z) = ce^z$ ,  $S_c(z) = c \sin z$ , and  $C_c(z) = c \cos z$ , though some new phenomena also appeared. Throughout, an important part of our investigations was to track, if we could, how the behavior of these systems changed when the maps were changed. We did this with the above families by varying the parameter  $c$ . In some sense, however, these were really mild perturbations of the maps since many of the salient features of the maps (such as the super attracting fixed point at  $\infty$  for  $f_c(z) = z^2 + c$  or the essential singularity at  $\infty$  for the transcendental maps) persisted no matter how the  $c$  values were changed.

**1.8.1. Perturbation with a pole.** There are, however, many ways to perturb a map that warrant our attention and can pique our interest in what turns out to also produce very beautiful mathematics. For example, the maps  $F_c(z) = z^d + c/z^m$  with fixed  $d, m \in \mathbb{N}$  are, for  $c \in \mathbb{C} \setminus \{0\}$ , perturbations of the dynamically well understood map  $z \mapsto z^d$ . Unlike the  $f_c(z) = z^2 + c$  perturbations of  $z \mapsto z^2$ , however, these maps  $F_c$  add a whole new dimension to the analysis due to the pole appearing at the origin. In particular, for  $c$  very small, the map  $F_c$  behaves very much like  $z \mapsto z^d$ , but only as long as  $z$  is sufficiently far from the origin. Near the origin the presence of the pole changes the dynamics considerably from  $z \mapsto z^d$ . It turns out that such systems lead to much fascinating mathematics that can sometimes be represented by pictures such as Figure 1.29 showing features not observed in any of the other systems studied in this chapter.

**LARGE PROJECT 1.149.** Investigate the dynamics of the maps of the form  $F_c(z) = z^d + c/z^m$ . You can use the *Parameter Plane and Julia Set Applet* to do this, as well as your own analytic paper and pencil techniques. Note that we have not described how the parameter plane is being drawn. It is up to you to determine this as well as figure out what you can on your own. Out of all the maps mentioned in this chapter, these are the newest and least studied. There is a lot of new territory waiting to be discovered here.

**1.8.2. Random Dynamics.** In each of the examples of perturbed maps throughout this chapter, even though the perturbation could be mild by changing a simple parameter or more severe by adding a pole as in  $F_c$ , there was one fundamental assumption always made regarding the perturbed system – once the map was perturbed, this map was fixed and iterated again and again to create the dynamics. A new way to perturb a system, however, is to allow the map to change at every step in the orbit.

For example, suppose we start with two maps  $f$  and  $g$ . The usual iteration dynamics says we consider the orbit generated by either  $f^n(z_0)$  or by  $g^n(z_0)$ . However, it is natural

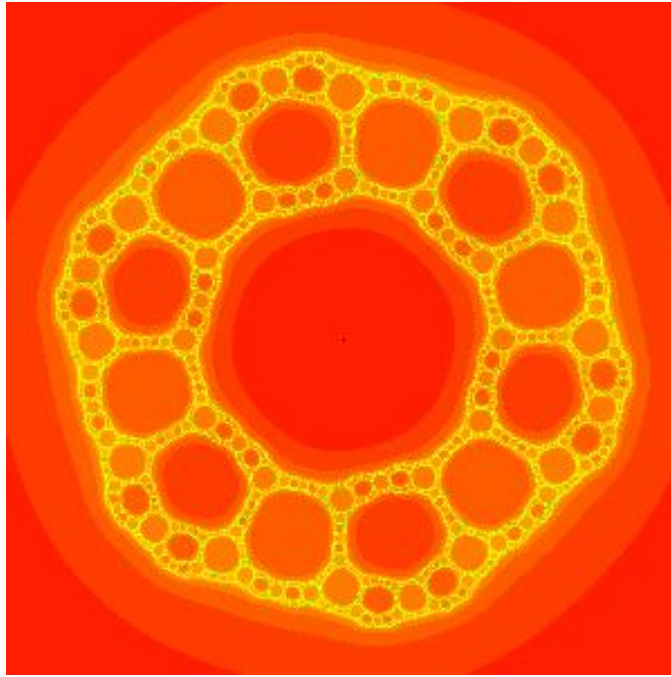


FIGURE 1.29. A Sierpinski curve Julia set for the function  $F(z) = z^3 + 0.13i/z^3$ . The regions of various shades of orange are in  $A_F(\infty)$  and the remaining points in yellow represent  $J(F)$ .

to ask what happens if at each stage of the orbit *either* map  $f$  *or*  $g$  can be applied? In some cases the dynamics can be much more uncivilized (and more fun). Such dynamics investigates the behavior of orbits  $h_{i_1}(z_0), h_{i_2}(h_{i_1}(z_0)), h_{i_3}(h_{i_2}(h_{i_1}(z_0))), \dots$  where the maps  $h_i$  are chosen to be either  $f$  or  $g$ . If one chooses each map  $h_i$  at random at each stage of the orbit, then one enters the research area of so-called *random dynamics*. Such systems are directly connected to the study of what are known as “iterated functions systems” and their attractor sets (see [7]), such as the van Koch curve and Sierpinski triangle.

Instead of investigating such attractor sets, we look in another direction. We investigate what we call a *random basin of attraction* as follows. Fix a point  $z_0 \in \mathbb{C}$  and randomly select the map  $h_1$  to be either  $f$  or  $g$  (each with probability  $1/2$ ). Then set  $z_1 = h_1(z_0)$ . Now randomly select the map  $h_2$  to be either  $f$  or  $g$  and set  $z_2 = h_2(z_1) = h_2(h_1(z_0))$ . Continue in this fashion to produce what we call a **random orbit**  $z_0, z_1, z_2, \dots$ . Now we consider whether or not such a random orbit can have a particular limit, and what the probability is of having that limit.

EXAMPLE 1.150 (Devil’s Staircase). Let  $f(x) = 3x$  and  $g(x) = 3x - 2$  be defined on the real line  $\mathbb{R}$ . Now consider for each  $x_0 \in \mathbb{R}$  generating a random orbit  $x_0, x_1, x_2, \dots$  as described above. Let  $P(x_0)$  denote the probability that this random orbit converges



to  $+\infty$ . Note that here we do distinguish between convergence of this random orbit to  $+\infty$  and  $-\infty$ . It is not hard to believe that if  $x_0 > 1$ , then we must have  $P(x_0) = 1$  since no matter what choices of  $f$  and  $g$  we make at each step of the orbit, we will always have the orbit points growing larger (and positive). Similarly, one can believe that if  $x_0 < 0$ , then we must have  $P(x_0) = 0$  since both maps  $f$  and  $g$  force the orbit points to grow larger (and negative). What happens for  $0 \leq x_0 \leq 1$ , however, is much more interesting, and we show the graph of  $P$ , called the Devil's Staircase, in Figure 1.30.

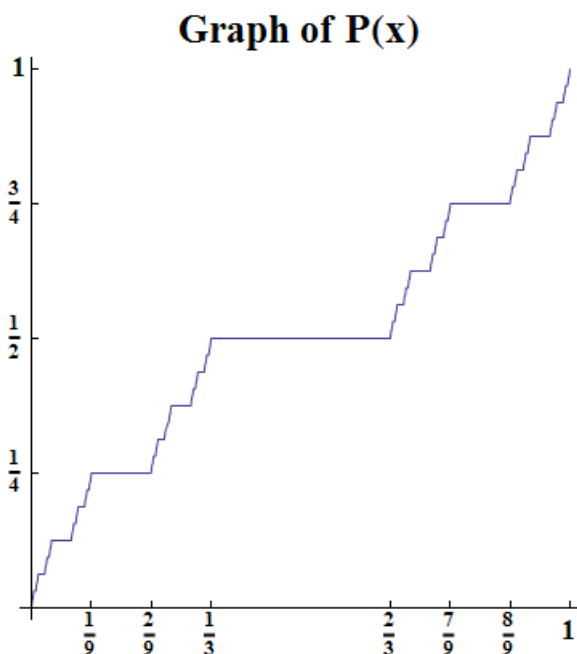


FIGURE 1.30. The “Devil’s Staircase” is the graph of the probability  $P(x)$  that a random orbit generated by the maps  $f(x) = 3x$  and  $g(x) = 3x - 2$  tends to  $+\infty$ .

An interesting property of this graph is that between any two steps (which we define to be the horizontal sections of the graph, i.e., intervals where  $P'(x) = 0$ ), we have infinitely many steps in between. Also, the sum of the lengths of all the steps between 0 and 1 is exactly 1 (for this reason we say that this graph is *almost always* flat, i.e., almost always has  $P'(x) = 0$ ). However, this function is both continuous and increases (not strictly) from  $y = 0$  to  $y = 1$  as  $x$  goes from 0 to 1.

EXERCISE 1.151. Prove the following aspects of the function  $P(x)$ , the Devil’s Staircase function, in Example 1.150.

- (a) Show that  $P(x) = 0$  for  $x < 0$  and  $P(x) = 1$  for  $x > 1$ .
- (b) Show that  $P(0) = 0$  and  $P(1) = 1$ .

- (c) Show that  $P(x)$  is increasing (not strictly), i.e.,  $x < y$  implies  $P(x) \leq P(y)$ .
- (d) Show that on the open interval  $(1/3, 2/3)$  both  $P(x) = 1/2$  and  $P'(x) = 0$ .
- (e) Show that on the open interval  $(1/9, 2/9)$  both  $P(x) = 1/4$  and  $P'(x) = 0$ .
- (f) Find where  $P(x) = 3/4$ .
- (g) In parts (d)-(f), you have located the largest step (corresponding to  $(1/3, 2/3)$ ), and the two next largest steps. Describe the four next largest steps, and then describe the pattern relating all steps.
- (h) Sum the lengths of all the steps to show this sum is 1.
- (i) Show that  $P(x)$  is continuous.

EXAMPLE 1.152 (Devil's Colosseum). The Devil's Colosseum is a higher dimensional analog of the Devil's Staircase, and is also understood through random dynamics. Instead of functions defined on just the real line, we consider the complex valued maps  $g_1(z) = z^2/4$  and  $g_2(z) = z^2 - 1$ , and then using the second iterates of these maps set  $f(z) = g_1^2(z)$  and  $g(z) = g_2^2(z)$ .

We now investigate the *random basin* of attraction for  $\infty$  as follows. Fix a point  $z_0 \in \mathbb{C}$ . Consider the random orbit  $z_0, z_1, z_2, \dots$  generated as described above, and let  $P(z_0)$  be the probability that this random orbit  $z_n$  tends to  $\infty$ . Note that for  $z_0$  large ( $|z_0| > 10$  will do), we have  $P(z_0) = 1$  since no matter what choices of  $f$  or  $g$  we make at each step, the orbit  $z_n$  will go to  $\infty$ . Though it is not as simple, one can also show  $P(z_0) = 0$  for  $z_0$  near zero. In between, however we get some very interesting behavior. In fact, this function  $P(z)$  has a graph given in Figure 1.31 called the Devil's Colosseum, and it has many properties similar to those of the Devil's Staircase. In particular, if you started from the bottom and tried to climb out, you would have to walk a path very much like the Devil's Staircase.

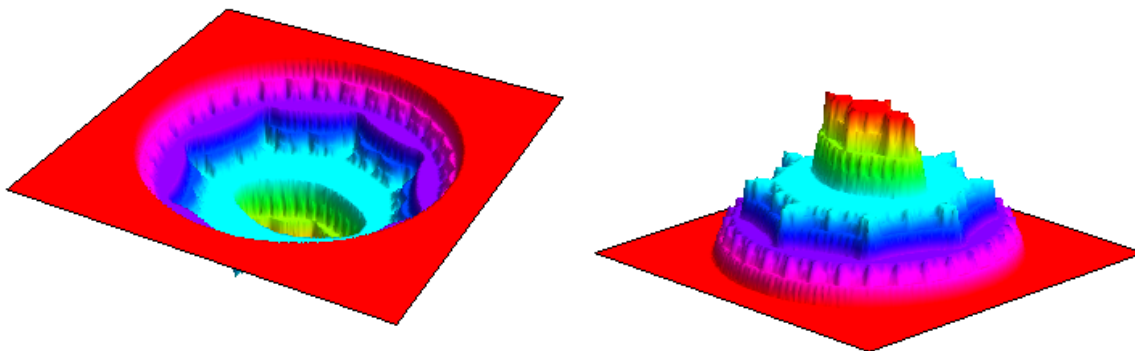


FIGURE 1.31. The left picture shows the Devil's Colosseum, the graph of the probability  $P(z)$  that a random orbit as defined above tends to  $\infty$ . The picture on the right is the inverted Devil's Colosseum, sometimes called a fractal wedding cake. The first pictures of these objects were created and carefully studied by Hiroki Sumi (see [25]).

We can describe the dynamics which underlie the Devil's Colosseum in terms of stability of orbits, and in doing so will introduce the following extensions of the notions of the Fatou and Julia sets. Let  $F(\langle f, g \rangle)$  denote the Fatou set of the random system described above, which we define to be those points  $z_0 \in \mathbb{C}$  such that *every* randomly generated sequence of maps  $h_{i_n}$  produces a stable orbit (in the sense that all nearby seed values will have similar orbits when the sequence of maps  $h_{i_n}$  is used). We then define the Julia set of this random system to be  $J(\langle f, g \rangle) = \overline{\mathbb{C}} \setminus F(\langle f, g \rangle)$ . We can thus describe the oddity of the Devil's Colosseum like so. The function  $P$  is continuous on all of  $\mathbb{C}$ , yet it is constant on each component of the Fatou set, even though the Julia set contains no open set (see [25]). It is these components of the Fatou set which make up the various horizontal *levels* (or steps) you see in Figure 1.31. The Julia set is then the set on which  $P(z)$  varies (since  $P(z)$  does not vary, i.e., it is flat, on  $F(\langle f, g \rangle)$ ). We see this Julia set pictured in Figure 1.32.

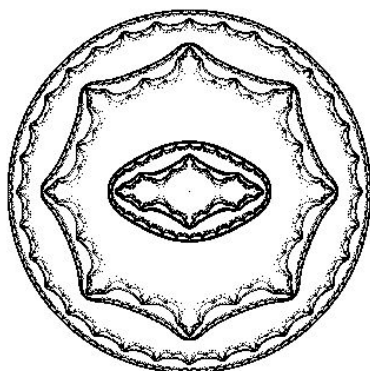


FIGURE 1.32. The Julia set  $J(\langle f, g \rangle)$  in  $\mathbb{C}$  is the the set on which  $P(z)$  varies. This pictured was drawn via Julia 2.0 (see [23]).

REMARK 1.153. We note that the random dynamics displayed in the Devil's Colosseum produced something that cannot happen with the usual iteration dynamics. For example, given a polynomial  $f(z)$ , consider defining a function  $P(z_0)$  to be the probability of an orbit with seed  $z_0$  tending to  $\infty$ . Of course, since there is only one map to choose, there is no randomness involved at all, and so we see that  $P(z_0)$  must be either 0 or 1. In particular, we have  $P(z) = 1$  for  $z \in A_f(\infty)$  and  $P(z) = 0$  for  $z \in K(f)$ . The function  $P$  is then discontinuous at every point  $z \in \partial A_f(\infty) = \partial K(f) = J(f)$ . Thus we see that the random dynamics exhibited by the Devil's Colosseum, where  $P(z)$  is continuous on all of  $\mathbb{C}$ , is a real change from iteration dynamics.

EXERCISE 1.154. The reader is encouraged to investigate such random dynamical systems visually by generating their own pictures similar to the Devil's Colosseum. Sample code is provided in Appendix 1.C.

There is a very large world of chaotic phenomena to explore. Whether you stay only within the confines of the topics mentioned in this book or venture into new areas, there remains an infinite amount of mathematics to discover. We encourage you to go and explore and make your own contributions to mathematics.

## 1.9. Additional Exercises

### Orbits, Examples, and Fixed Points

EXERCISE 1.155. Prove  $f^n(x) \rightarrow +\infty$  for all  $x \in \mathbb{R}$  when  $f(x) = e^x$ . In fact, the advanced reader can actually show that the convergence is *uniform*,<sup>32</sup> i.e., given any  $M > 0$ , there exists an integer  $N > 0$  such that  $n > N$  implies  $f^n(x) > M$  for all  $x \in \mathbb{R}$ .

EXERCISE 1.156. For  $f(x) = \sin x$  where  $x \in \mathbb{R}$  is given in radians prove that  $f^n(x) \rightarrow 0$  for all  $x \in \mathbb{R}$ . Hint: Apply the Mean Value Theorem to show that  $|\sin x| < |x|$  for all  $x \in \mathbb{R} \setminus \{0\}$ . The advanced reader can actually show that the convergence is *uniform*,<sup>32</sup> i.e., given any  $\epsilon > 0$ , there exists an integer  $N > 0$  such that  $n > N$  implies  $|f^n(x) - 0| < \epsilon$  for all  $x \in \mathbb{R}$ .

EXERCISE 1.157. For  $f(x) = \cos x$  where  $x \in \mathbb{R}$  is given in radians prove that  $f^n(x) \rightarrow 0.739085\dots$  for all  $x \in \mathbb{R}$  where  $x^* = 0.739085\dots$  is the number such that  $\cos x^* = x^*$ . Hint: Apply the Mean Value Theorem to show that  $|\cos x - x^*| < |x - x^*|$  for all  $x \in \mathbb{R} \setminus \{x^*\}$ . The advanced reader can actually show that the convergence is *uniform*,<sup>32</sup> i.e., given any  $\epsilon > 0$ , there exists an integer  $N > 0$  such that  $n > N$  implies  $|f^n(x) - x^*| < \epsilon$  for all  $x \in \mathbb{R}$ .

EXERCISE 1.158. For  $g(z) = \sin z$ , show that  $g^n(\pm i\epsilon) \rightarrow \infty$  for any  $\epsilon > 0$ . Hint: First show that  $g(iy)$  is purely imaginary and  $|g(iy)| > |y|$  for each real  $y \neq 0$ .

### Complex Newton's method

EXERCISE 1.159. What Newton's method can "find". Let  $F$  be the Newton map of a polynomial  $f$  of degree two or more.

- (a) Suppose  $F^n(z_0) \rightarrow a$  for some  $z_0 \in \mathbb{C}$  and some *finite* point  $a \in \mathbb{C}$ . Prove  $f(a) = 0$ .
- (b) However, show that we always have  $F(\infty) = \infty$  and so we see that it is necessary that we consider only finite points in part (a).

EXERCISE 1.160. Prove that that the Newton map of  $f(z)/f'(z)$  (as opposed to the Newton map of  $f(z)$ ) always has super attracting fixed points at the roots of  $f$  regardless of the order of the root of  $f$ . Hint: Given a root  $\alpha$  of  $f$  of order  $k$ , determine the order of the root of  $f(z)/f'(z)$ .

EXERCISE 1.161. Construct examples of analytic maps  $f$  to justify the statement that there is no universal  $r^* > 0$  such that  $\Delta(\alpha, r^*) \subseteq A_F(\alpha)$  for *all* analytic maps  $f$  with a root at  $\alpha$ . Here, as usual,  $F$  denotes the Newton map for  $f$ .

EXERCISE 1.162. Radius of Convergence for polynomials.

Let  $p(z) = (z - \alpha)^k(z - \alpha_1) \dots (z - \alpha_s)$  be a polynomial of degree  $n = k + s$ , where the  $\alpha_j$  need not be distinct. Follow the steps below to show that  $r = \frac{d(2k-1)}{2n-1}$  is a radius

---

<sup>32</sup>Uniform convergence is not critical to the development of the text and so may be safely disregarded. However, advanced students should try to understand the concept in the given context.

of convergence for the Newton map  $F$  at  $\alpha$ , where  $d = \min_{j=1, \dots, s} |\alpha - \alpha_j|$  (the distance from  $\alpha$  to the nearest other root of  $p$ ).

- (a) For the Newton map  $F(z) = z - \frac{p(z)}{p'(z)}$ , we wish to show that  $|z - \alpha| < r$  implies  $|F(z) - \alpha| < |z - \alpha|$ . Note that this last inequality says that the action of  $F$  is to move points in the disk  $\Delta(\alpha, r)$  closer to  $\alpha$ . Show that such an inequality then implies that  $F^n(z) \rightarrow \alpha$  as  $n \rightarrow \infty$  when  $|z - \alpha| < r$ .
- (b) Show that  $|F(z) - \alpha| < |z - \alpha|$  is equivalent to  $\frac{|F(z) - \alpha|}{|z - \alpha|} = \left| 1 - \frac{p(z)}{(z - \alpha)p'(z)} \right| < 1$ .
- (c) Show that  $\left| 1 - \frac{1}{w} \right| = \left| \frac{w-1}{w} \right| = \left| \frac{w-1}{w-0} \right| < 1$  holds if and only if  $\operatorname{Re} w > 1/2$ .
- (d) Justify the following. The term  $w = \frac{(z - \alpha)p'(z)}{p(z)} = (z - \alpha) \left[ \frac{k}{z - \alpha} + \sum_{j=1}^s \frac{1}{z - \alpha_j} \right] = k + \sum_{j=1}^s \frac{z - \alpha}{z - \alpha_j}$ . Thus  $\operatorname{Re} w > \frac{1}{2}$  exactly when  $\operatorname{Re} \sum_{j=1}^s \frac{z - \alpha}{z - \alpha_j} > \frac{1}{2} - k$ , which holds, in particular, when  $\sum_{j=1}^s \left| \frac{z - \alpha}{z - \alpha_j} \right| < k - \frac{1}{2}$ .
- (e) Show that if  $|z - \alpha| < r$ , we then have  $|z - \alpha_j| > d - r$ , where  $d = \min_j |\alpha - \alpha_j|$ . Hence  $\sum_{j=1}^s \left| \frac{z - \alpha}{z - \alpha_j} \right| < s \frac{r}{d - r} = (n - k) \frac{r}{d - r}$ .
- (f) Combine all the above to reach the desired conclusion. Also, note that for  $z \in \Delta(\alpha, r)$  we have  $|F(z) - \alpha| < |z - \alpha|$ , which is, in general, a much stronger statement than merely saying that  $\Delta(\alpha, r) \subseteq A_f(\alpha)$ . For this reason, some may call the value  $r = \frac{d(2k-1)}{2n-1}$  a radius of **contraction** for Newton's method at  $\alpha$ .

**SMALL PROJECT 1.163.** Fix an integer  $n \geq 2$  and let  $f(z) = z^n - 1$ . Express the value for  $r$  found in Exercise 1.162 in terms of only  $n$ . See if you can improve upon this value for the radius of *contraction* by carefully investigating the above proof as applied to this select class of maps  $f(z) = z^n - 1$ . You might (or might not) wish to calculate an  $r^* > 0$  such that  $|F'(z)| < 1$  on  $\Delta(\alpha, r^*)$  for each root  $\alpha$  of  $f$ , and then apply the Contraction Lemma 1.136.

**SMALL PROJECT 1.164.** This is an open ended project to investigate whether the value for  $r$  found in Exercise 1.162 can be improved if we know something about the geometry of the roots of  $p$ . See if you can improve upon this value for the radius of *contraction* by carefully investigating the proof in Exercise 1.162 for specific polynomials  $f$  of degree 3 with distinct roots  $\alpha_p, \beta_p, \gamma_p$ . If the roots, all lie on a line, can you squeeze more from that proof? What if the roots form an equilateral triangle? Are there some geometric configurations of the roots that allow for better results than what is given in Exercise 1.162? Can you generalize this to higher degree polynomials? What if you allow for multiple roots of  $f$ ? If a paper and pencil result is too hard, provide a conjecture based on examples you considered with the *Complex Newton Method Applet*. Whether or not you can answer them, come up with some related questions that one might consider. **Remember, asking questions is important, even if you can't answer them.**

Comment: You might (or might not) wish to calculate an  $r^* > 0$  such that  $|F'(z)| < 1$  on  $\Delta(\alpha, r^*)$  for each root  $\alpha$  of  $f$ , and then apply the Contraction Lemma 1.136.

### Global Conjugation

EXERCISE 1.165. Prove that if  $ab \neq 0$ , then the maps  $z \mapsto az$  and  $z \mapsto bz$  are globally conjugate if and only if either  $a = b$  or  $a = 1/b$ .

EXERCISE 1.166. Prove that if  $ab \neq 0$ , then the maps  $z \mapsto z + a$  and  $z \mapsto z + b$  are globally conjugate.

EXERCISE 1.167. Prove that any quadratic map  $f(z) = az^2 + bz + d$  is globally conjugate to one and only one map of the form  $z \mapsto z^2 + c$ .

EXERCISE 1.168. Prove that a rational map  $R$  is globally conjugate to a polynomial if and only if there exists  $w \in \overline{\mathbb{C}}$  with  $R^{-1}(\{w\}) = \{w\}$ .

### Analysis of the Newton map of a cubic polynomial

EXERCISE 1.169. Prove that the attracting basin of an *attracting* fixed point of a rational or entire map is an open set in  $\overline{\mathbb{C}}$ , which, in particular, does not contain any of its boundary points. Hint: Use Theorem 1.18 together with the fact that if  $f$  is a continuous map, then  $f^{-1}(U)$  is open whenever  $U$  is open.

EXERCISE 1.170. Use the *Complex Newton Method Applet* to investigate the behavior of Newton's method applied to  $f_1(z) = z * (z - 1) * (z - 0.908 - 0.423i)$  and  $f_2(z) = z * (z - 1) * (z - 0.913 - 0.424i)$ . Describe the behavior you see, especially for the black seed values where Newton's method fails.

### Iteration of an Analytic Function

EXERCISE 1.171. Dense orbit in  $J(f)$ .

- (a) Show that for the map  $f(z) = z^2$  there is a point  $z_0 \in C(0, 1)$  whose orbit is dense on  $C(0, 1)$ , that is,  $\overline{\{f^n(z_0) : n \in \mathbb{N}\}} = C(0, 1)$ . Hint: Note that on  $C(0, 1)$ , we have  $f(e^{i2\pi\theta}) = e^{i4\pi\theta}$ , that is, the angle  $\theta \in [0, 1)$  is doubled (mod 1). Consider  $\theta_0 \in [0, 1)$  given in binary form as  $\theta_0 = 0.0\ 1\ 00\ 01\ 10\ 11\ 000\ 001\ 010\ 011\ 100\ 101\ 110\ 111\ 0000\ \dots$  where spaces have been included in this binary expansion to help illustrate the pattern.
- (b) Use (a) to justify the second claim in Remark 1.47.
- (c) Notice, however, that due to computer limitations, *any* point you choose on  $C(0, 1)$  will have a *computed* orbit that eventually becomes periodic (although it might take a very large number of orbit points to see this). Justify this statement.

EXERCISE 1.172. In this exercise you are asked to complete the proof of Theorem 1.49.

- (a) Use Schwarz's Lemma (see Theorem A.20 on page 415) to show that an attracting fixed point  $a \in \mathbb{C}$  of an analytic map  $f$  must have  $|f'(a)| < 1$ . Hint: Consider a

small disk  $\Delta(a, r)$  where  $f$  is attracting and then investigate the map  $g : \Delta(0, 1) \rightarrow \Delta(0, 1)$  defined by  $g(z) = \frac{f(rz+a)-a}{r}$ .

- (b) Now suppose  $a \in \mathbb{C}$  is a repelling fixed point of an analytic map  $f$ . Use the fact that  $f$  is locally one-to-one with a locally defined inverse to show  $|f'(a)| > 1$ . Hint: Since  $|f'(a)| \geq 1$  (else  $a$  would be attracting), we must have that  $f$  is locally one-to-one (see Section A.6.1.1 on page 417 regarding the Open Mapping Theorem and the Inverse Function Theorem A.23). Letting  $h$  be  $f^{-1}$  defined on some small disk  $\Delta(a, r)$ , show that  $a$  is an attracting fixed point for  $h$  (since it was repelling for  $f$ ) and then apply part (a) to  $h$ . Then use this to argue for your desired conclusion.

EXERCISE 1.173. Let  $f$  be a map that is analytic at  $\infty$  such that  $f(\infty) = \infty$ . Consider the multiplier  $\lambda = 1/f'(\infty)$ . Prove that if  $|\lambda| < 1$ , then  $\infty$  is an attracting fixed point according to Definition 1.16. Also, prove that if  $|\lambda| > 1$ , then  $\infty$  is a repelling fixed point according to Definition 1.45. Hint: Noting that the map  $k(z) = 1/f(1/z)$  has a fixed point at the origin also with multiplier  $\lambda$  (see Lemma B.19 on page 427), study how the map  $\phi(z) = 1/z$  transfers information about  $k$  at the origin to information about  $f$  at  $\infty$ .

EXERCISE 1.174. Let  $g(z)$  be a polynomial of degree greater than or equal to two (which must then have a super attracting fixed point at  $\infty$ ). Prove that  $\partial A_g(\infty) = \partial K(g)$ , and then note that by Theorem 1.60 we have  $J(g) = \partial A_g(\infty) = \partial K(g)$ .

EXERCISE 1.175. Convergence toward an attracting fixed point depends on the multiplier.

- For  $c = -0.467 + 0.513i$  determine the attracting fixed point  $p_c$  of  $f_c$ .
- Write the multiplier  $\lambda$  for  $p_c$  in polar form.
- Use the *Global Complex Iteration Applet for Polynomials* to iterate a seed  $z_0$  near  $p_c$  one step at a time (use the zoom feature to get a better look) to notice the way in which the orbit approaches  $p_c$ . The way this orbit approaches  $p_c$  is directly related to the multiplier  $\lambda$ . Describe this connection in your own words.
- Use the *Complex Function Iterator Applet* to iterate the map  $z \mapsto \lambda z$  for various seed values near the attracting fixed point at the origin. Describe the convergence.
- Compare (c) and (d), explaining in as much mathematical detail as you can what you find. Hint: Consider the Taylor series of  $f_c$  expanded around the point  $p_c$ .
- Choose various  $c$  in  $K_1$  and then study the convergence of orbits to the attracting fixed point using the applet. Use this picture to approximate the argument of the multiplier. Note: some  $c$  values will be easy to work with here, while others are not as easy.

EXERCISE 1.176. Convergence toward the attracting 2-cycle.

- For  $c = -0.92568 + 0.22512i$  determine the attracting 2-cycle  $\{u_c, v_c\}$  of  $f_c$ .
- Write the multiplier  $\lambda$  for  $\{u_c, v_c\}$  in polar form.
- Use the *Global Complex Iteration Applet for Polynomials* to iterate a seed  $z_0$  near one of the cycle points  $u_c$  one step at a time (use the zoom feature to get a better



look) to notice the way in which every other orbit point approaches  $u_c$ . The way this orbit approaches  $u_c$  is directly related to the multiplier  $\lambda$ . Describe this connection in your own words.

- (d) Use the *Complex Function Iterator Applet* to iterate the map  $z \mapsto \lambda z$  for various seed values near the attracting fixed point at the origin. Describe the convergence.
- (e) Compare (c) and (d), explaining in as much mathematical detail as you can what you find. Hint: Consider the Taylor series of the iterate  $f_c^2$  expanded around the point  $u_c$ .
- (f) Choose any  $c$  in  $K_2$  and then study the convergence of orbits to the attracting 2-cycle using the applet. Use this picture to approximate the argument of the multiplier. Note: some  $c$  values will be easy to work with here, while others are not as easy.

**EXERCISE 1.177.** Multiplier map for attracting 2-cycles of  $f_c$ . Determine the exact form of the multiplier map on  $K_2$ . This function  $\lambda : K_2 \rightarrow \Delta(0, 1)$  maps each  $c \in K_2$  to the multiplier of the attracting 2-cycle of the map  $f_c$ . Also show that this map can be extended to a map  $\lambda : \overline{K_2} \rightarrow \Delta(0, 1)$  which is continuous, one-to-one, and onto.

**EXERCISE 1.178.** Without appealing to Theorem 1.80, prove that if  $f_{c_0}$  has an attracting  $n$ -cycle, then for all  $c$  close to  $c_0$ , the map  $f_c$  also has an attracting  $n$ -cycle. Conclude that  $K_n$  is an open set. Hint: One may use Rouché's Theorem (see [1], p. 294) to prove a general result that if the coefficients of the polynomial  $P$  are sufficiently close to the corresponding coefficients of the polynomial  $Q$  of the same degree, then the roots of  $P$  and the roots of  $Q$  are close. Then apply this result to the polynomials of  $P_1(z) = f_{c_0}^n(z) - z$  and  $Q_1(z) = f_c^n(z) - z$ .

**EXERCISE 1.179.** Mathematically justify Footnote 18 on page 42.

### Critical Points and Critical Orbits

**EXERCISE 1.180.** Let  $f(z) = z^3 - 1$  and let  $F$  denote the corresponding Newton map. Show that  $F$  cannot have an attracting cycle of any order other than the fixed points at the roots of  $f$ . Hint: Check the behavior of each critical point of  $F$  and consider Theorem 1.89.

Note: More can be said about this situation. It is true that Newton's method fails to find a root of  $f$  only for seed values from  $\partial A_F(1) = \partial A_F(e^{2\pi i/3}) = \partial A_F(e^{-2\pi i/3})$ . In fact, we have  $\overline{\mathbb{C}} = A_F(1) \cup A_F(e^{2\pi i/3}) \cup A_F(e^{-2\pi i/3}) \cup \partial A_F(1)$ . The method of proof is along the same lines as above, however, it uses a more powerful set of results. These results imply that if Newton's method fails for all seed values in an open set of points, then there must be a critical point of  $F$  whose orbit does not converge to any of the roots of  $f$ . The key ingredients to this proof are Sullivan's No Wandering Domains Theorem, the Classification of forward invariant components of Fatou sets, and the role of critical points in parabolic domains, Siegel disks, and Herman rings. All of these results can be researched by the interested reader in [1].

EXERCISE 1.181. Show that the periodic points for the map  $f(z) = z^2$  are exactly those points of the form  $e^{i2\pi p/q}$  where  $p, q \in \mathbb{N}$  with  $p/q$  in lowest terms and  $q$  odd. Show that the pre-periodic points have the same form, but for  $q$  even. Hint: Show that if  $p/q = \frac{n}{2^k - 1}$  for some integers  $k \geq 1, n \geq 1$ , then  $e^{i2\pi p/q}$  has a period of  $k$  or some divisor of  $k$ . Then use the fact that every rational number  $p/q$  with  $q$  odd can be expressed in this form (which can be proved by using the fact that the element 2 in the multiplicative group consisting of those elements of  $\mathbb{Z}_q$  which are relatively prime to  $q$  has a finite multiplicative order which we call  $k$ ).

EXERCISE 1.182. Symmetry in  $M$ . One feature of the Mandelbrot set which stands out is that it is symmetric about the  $x$ -axis. Prove this by showing that  $c \in M$  if and only if  $\bar{c} \in M$ . Hint: Compare the critical orbits  $\{f_c^n(0)\}$  and  $\{f_{\bar{c}}^n(0)\}$ .

EXERCISE 1.183. Prove that the Mandelbrot set  $M$  has no “holes” (i.e., its complement  $\overline{\mathbb{C}} \setminus M$  is connected) by appealing directly to its definition. Hint: Suppose that  $U$  is a bounded domain of  $\overline{\mathbb{C}} \setminus M$  such that  $\partial U \subseteq M$ . Now apply the Corollary A.18 on page 415 (a version of the Maximum Modulus Theorem) to the maps  $Q_n$  on  $\bar{U}$  used in the proof of Lemma 1.103.

### Exploring the Mandelbrot Set $M$

EXERCISE 1.184. Let  $P$  be a polynomial of degree  $n \geq 2$ . Show that the Filled-in-Julia set  $K(P)$  has infinitely many points as follows.

- Show that  $P(z)$  has a fixed point  $z_0$  by applying the Fundamental Theorem of Algebra.
- Show that if  $z_0$  is such that  $P^{-1}(\{z_0\}) = \{z_0\}$ , then  $\overline{P(z)} = z_0 + a(z - z_0)^n$  for some  $a \neq 0$  from which it can be shown that  $K(P) = \overline{\Delta(z_0, r)}$  where  $r = |a|^{1/(1-n)}$ .
- Show that if  $P^{-1}(\{z_0\}) \neq \{z_0\}$ , then there exists an infinite sequence of distinct points  $z_{-n}$  such that  $\dots \mapsto z_{-n} \mapsto z_{-n+1} \mapsto \dots \mapsto z_{-2} \mapsto z_{-1} \mapsto z_0$ . Hence,  $\{z_{-n}\} \subseteq K(P)$ .

We note that it is true that  $J(P)$  must contain uncountably many points, but to show this requires considerably more effort (see [1], p. 95).

EXERCISE 1.185. Prove that for all  $c \in \mathbb{C}$ , we have  $z \in A_{f_c}(\infty)$  if and only if  $-z \in A_{f_c}(\infty)$ . Do the same for the sets  $J(f_c)$  and  $K(f_c)$ .

EXERCISE 1.186. Since the root  $c_{p/q}$  of the  $p/q$  bulb in the Mandelbrot set lies on the boundary of two hyperbolic components (namely  $K_1$  and  $B_{p/q}$ ), we see that Theorem 1.80 implies that there are two multiplier maps that are defined at  $c_{p/q}$ . In particular, the map  $\lambda : K_1 \rightarrow \Delta(0, 1)$  can be extended to be defined at  $c_{p/q}$ , but also the map  $\lambda_{p/q} : B_{p/q} \rightarrow \Delta(0, 1)$  can be extended to be defined at  $c_{p/q}$ . Does  $\lambda(c_{p/q}) = \lambda_{p/q}(c_{p/q})$ ? What does it mean if these values are the same? different?

EXERCISE 1.187. Find a  $c$  value in  $B_{5/32}$ . Formal proof is not required.

EXERCISE 1.188. Farey addition.

- (a) Experiment with the *Parameter Plane and Julia Set Applet* to determine what Farey fraction should be used to represent the cusp of the main cardioid  $K_1$  in the Farey procedure for finding child bulbs. Keep in mind that we are to treat the cusp like a Farey parent which is larger than all other bulbs.
- (b) It is true (though not so easy to prove) that starting with Farey parents  $B_{1/2}$  and the cusp one can compute through Farey addition all of the  $p/q$  bulbs attached to the upper half of the main cardioid  $K_1$ . Illustrate this by producing a Farey “family” tree which contains the lineage of  $B_{5/32}$  all the way up to the ancestors  $B_{1/2}$  and the cusp of the main cardioid  $K_1$ .
- (c) Use Exercise 1.118 and part (b) to show that *all* of the  $p/q$  bulbs attached to the main cardioid  $K_1$  can now be identified through Farey addition.

### Other Uni-critical families of polynomials

EXERCISE 1.189. For the maps  $P_c(z) = z^d + c$  with  $d = 2, 3, 4, \dots$  show the following:

- (a) If  $|z| \geq |c|$  and  $|z| > 2$ , then there exists  $\epsilon > 0$  such that  $|P_c(z)| > |z|(1 + \epsilon)$ .
- (b) Use induction to show that if  $|z| \geq |c|$  and  $|z| > 2$ , then  $P_c^n(z) \rightarrow \infty$ .
- (c) Apply (b) to prove  $P_c^n(0) \rightarrow \infty$  (as  $n \rightarrow \infty$ ) if and only if  $|P_c^k(0)| > 2$  for some  $k \in \mathbb{N}$ . In particular,  $M_d \subseteq \overline{\Delta(0, 2)}$ .
- (d) Prove that the filled in Julia set of  $P_c$  is contained in  $\overline{\Delta(0, 2)}$  when  $|c| \leq 2$ . Also show by example that this statement does not necessarily hold when  $|c| > 2$ , i.e., it is not the case that for all  $c$  we have  $P_c^n(z) \rightarrow \infty$  whenever  $|z| > 2$ .

EXERCISE 1.190. Symmetries in the family  $P_c(z) = z^d + c$ .

- (a) Use the *Parameter Plane and Julia Set Applet* to explore the parameter plane for the family  $P_c(z) = z^d + c$ , and then identify and explain the symmetry you see there.
- (b) Use the *Parameter Plane and Julia Set Applet* to explore the Julia sets of maps in the family  $P_c(z) = z^d + c$ , and then identify and explain the symmetry you see there.

EXERCISE 1.191. For fixed integer  $d > 2$ , prove  $M_d$  is the connectedness locus for the family of maps  $P_c(z) = z^d + c$ , i.e., show that  $M_d = \{c \in \mathbb{C} : J(P_c) \text{ is connected}\}$ .

### Transcendental Dynamics

EXERCISE 1.192. Carefully prove that  $E_c^n(z_0) \rightarrow \infty$  if and only if  $\operatorname{Re} E_c^n(z_0) \rightarrow +\infty$ , where  $E_c(z) = ce^z$  and  $c \in \mathbb{C} \setminus \{0\}$ .

LARGE PROJECT 1.193. Accuracy of the Exponential Julia set applet pictures. This large project is open ended and should only be attempted after all of Section 1.6.1 has been covered.

As mentioned in Footnote 26 on p. 67, the algorithm used to illustrate the Exponential Julia set  $J(E_{0.2})$  can color some seed values  $z_0$  non-black (which it does when at least one of the orbit points  $E_{0.2}(z_0), \dots, E_{0.2}^{20}(z_0)$  lands in the set  $\{\operatorname{Re} z > 50\}$ ), but which is actually not in  $J(E_{0.2})$ . For example, consider any point  $z_0$  which maps to  $E_{0.2}(z_0) = 51 + \pi i$ . Such a  $z_0$  will not be left black. However, we see that  $E_{0.2}^2(z_0) = -0.2e^{51} \in H = \{z : \operatorname{Re} z < 1\} \subseteq A_{E_{0.2}}(p)$ , which implies  $z_0 \in A_{E_{0.2}}(p) = F(E_{0.2})$ . The goal of this project is to estimate how close such points like  $z_0$  are to actual points in  $J(E_{0.2})$ . This is in some sense a measure of the error in the algorithm.

One method to approach this problem is to consider an open rectangle  $R$  centered at  $z_0$  and consider its **expanded** image  $E_{0.2}(R)$ . If this expanded image meets some point which truly does have an orbit which tends to  $\infty$ , then there must be a corresponding point in  $R$  which lies in  $J(E_{0.2})$ . So one must consider how much such an  $R$  gets expanded, and how big this expansion needs to be before we are guaranteed that expanded image  $E_{0.2}(R)$  contains some point with an orbit which tends to  $\infty$ . Hint: Consider the open interval  $(q, +\infty)$  and its  $2\pi ik$ -translates where  $q$  is the repelling fixed point for  $E_{0.2}$ .

Also, one should consider what similar estimates one can get if  $w_0$  is a point such that  $\operatorname{Re} E_{0.2}(w_0) < 50$ , but  $E_{0.2}^2(w_0) = 51 + \pi i$ . Thus, such a point  $w_0$  takes two steps before the algorithm gives it a non-black color, as opposed to  $z_0$  above which used only one step. As above,  $w_0$  is also not in  $J(E_{0.2})$ , but there are points nearby which are. Can you estimate how nearby these points are?

Some related questions are: Is there a relationship between the size of the viewing window and the accuracy of our pictures? Can you quantify this either in general or in specific cases? How does this relationship depend on the value 50 that was chosen to determine our escape criterion or on the value 20 that determined how many orbit points might be checked? If we set the **Dynamic plane min iterations** to 2 (which means that a seed value is iterated twice before the escape condition is tested, i.e., a seed  $z_0$  is given a non-black color only if at least one of the points  $z_2, \dots, z_{20}$  has real part greater than 50), do we get a more accurate or less accurate picture?

This is a very technical project. The reader may wish to see [10] where some of these questions are addressed.

EXERCISE 1.194. Contracting and Expanding maps.

- (a) Prove the Contraction Lemma stated on page 69. Hint: Consider the argument made just preceding the statement of the lemma.
- (b) Show that if  $f$  is a one-to-one analytic function such that  $|f'(z)| > \gamma > 1$  for all  $z$  in some domain  $D$ , and  $f(D)$  is convex, then  $f$  is “expanding” on  $D$ , i.e.,  $|f(z) - f(w)| \geq \gamma|z - w|$  for all  $z, w \in D$ . Hint: Consider  $f^{-1}$ , which by the Inverse Function Theorem A.23 on page 417 is analytic.

EXERCISE 1.195. Prove that any two fingers (of any stage) constructed in Example 1.135 are always separated by an infinitely long gap (of black) points in  $A_{E_{0.2}}(p)$ . Hint: Note that the horizontal lines  $K_n = \{z \in \mathbb{C} : \operatorname{Im} z = (2n + 1)\pi\}, n \in \mathbb{N}$  each lie

in  $A_{E_{0.2}}(p)$  and separate the stage 1 fingers. With this show that the inverse image of these lines under  $E_{0.2}$  separate the stage 2 fingers, and then proceed inductively.

**EXERCISE 1.196.** Follow the steps below to prove that the thickness of each stage  $n$  finger is no greater than  $\pi/\gamma^{n-1}$  where  $\gamma = \ln 5 > 1$ .

- (a) Prove that any stage  $n$  finger is contained in the right half plane  $\{\operatorname{Re} z \geq \gamma\}$  by showing  $\operatorname{Re} E_{0.2}(z) \leq |E_{0.2}(z)| < 1$  whenever  $\operatorname{Re} z < \gamma$ .
- (b) Suppose  $E_{0.2}(\Delta(z_0, r)) \subseteq \{\operatorname{Re} z > \gamma\}$  for some  $r < \pi$ . Show that  $E_{0.2}(\Delta(z_0, r)) \supseteq \Delta(E_{0.2}(z_0), \gamma r)$  by filling in the details of the following argument. Define a branch  $L$  of the inverse of  $E_{0.2}$  on the convex set  $\{\operatorname{Re} z > \gamma\}$  such that  $L(E_{0.2}(z_0)) = z_0$  (given by  $L(z) = \operatorname{Log} z + \ln 5 + 2\pi in$  for some  $n \in \mathbb{Z}$ ). For  $|z - z_0| = r$ , we then have  $r = |z - z_0| = |L(E_{0.2}(z)) - L(E_{0.2}(z_0))| \leq (1/\gamma)|E_{0.2}(z) - E_{0.2}(z_0)|$  since  $|L'(z)| = |1/z| < 1/\gamma$  when  $\operatorname{Re} z > \gamma$ . Noting that  $E_{0.2}$  is univalent on  $\Delta(z_0, r)$ , it follows that  $E_{0.2}$  maps the circle  $|z - z_0| = r$  to a simple closed curve  $C$  which encloses  $\Delta(E_{0.2}(z_0), \gamma r)$ .<sup>33</sup> Applying the Maximum Modulus Theorem A.17 on page 415 to  $L(z) - z_0$  on  $E_{0.2}(\Delta(z_0, r))$  we see that  $L(\Delta(E_{0.2}(z_0), \gamma r)) \subseteq \Delta(z_0, r)$ , and the result then follows.
- (c) Use parts (a) and (b) to prove that if  $\Delta(z_0, r)$  is contained in a stage  $n$  finger (for  $n \geq 2$ ), then  $\Delta(E_{0.2}(z_0), \gamma r)$  is contained in some stage  $(n - 1)$  finger.
- (d) Use Exercise 1.139 and induction to complete the proof.

**EXERCISE 1.197.** Prove that the set  $J$  in Proposition 1.140 cannot contain any open set.

**EXERCISE 1.198.** Follow the steps below to construct infinitely many (though not all) of the “hairs” in  $J(E_{0.2})$ . Recall that each hair is the image of some continuous map  $h : [0, \infty) \rightarrow \mathbb{C}$  such that  $h(t) \rightarrow \infty$  as  $t \rightarrow \infty$ .

- (a) Prove that there exists a repelling fixed point  $q \in \mathbb{R}$  such that for any  $x > q$  we have  $E_{0.2}(x) > x$  and therefore  $E_{0.2}^n(x) \rightarrow +\infty$ . Use this to conclude that the interval  $h_0 = [q, +\infty)$  is a hair in  $J(E_{0.2})$  (which we call a straight hair since it extends to  $\infty$  in a straight line).
- (b) Use the  $2\pi i$  periodicity of  $E_{0.2}$  to show that for each  $k \in \mathbb{Z}$  the set  $h_k$  defined to be the  $k2\pi i$  translate of  $h_0$  is also a hair in  $J(E_{0.2})$ . We call each  $h_k$  a stage 1 hair (which could be called the “main” hair in the corresponding stage 1 finger).
- (c) Argue that inside of the stage 1 finger  $C_0$ , there exist infinitely many hairs  $h_{0,k}$  in  $J(E_{0.2})$  such that  $E_{0.2}(h_{0,k}) = h_k$ . Note that no  $h_{0,k}$  is a straight hair (except for  $h_{0,0}$  which equals  $h_0 = [q, +\infty)$ ).
- (d) Use the  $2\pi i$  periodicity of  $E_{0.2}$  again to show that for each  $j, k \in \mathbb{Z}$  the set  $h_{j,k}$  defined to be the  $j2\pi i$  translate of  $h_{0,k}$ , is also a hair in  $J(E_{0.2})$ . We call each  $h_{j,k}$  a stage 2 hair.

<sup>33</sup>At this point one could complete the proof by applying the Argument Principle A.19 on page 415 to see that the number of zeros of  $E_{0.2}(z) - E_{0.2}(a)$  is equal to one for all values  $a$  in the interior of  $C$ .

- (e) Repeat the above arguments to argue that there must exist infinitely many *stages* of hairs in  $J(E_{0.2})$ .
- (f) We remark that if we let  $H_n$  denote all the stage  $n$  hairs generated as above, then  $\bigcup_{n=1}^{\infty} H_n \cup \{\infty\}$  is not quite all of  $J(E_{0.2})$ . However, with a bit of more careful analysis one can show that  $J(E_{0.2}) = \overline{\bigcup_{n=1}^{\infty} H_n \cup \{\infty\}}$  by showing that each point in the hairs described in Section 1.6.2 is a limit of points from the collection of stage  $n$  hairs generated as above.

**EXERCISE 1.199.** Determine the exact real bifurcation value  $c^*$  between  $c = 0.2$  and  $c = 0.5$  for the family of maps  $E_c$ . Also, show that for  $c < c^*$  we have  $\{\operatorname{Re} z < 1\} \subseteq F(E_c)$ , but for  $c > c^*$  we have  $F(E_c) = \emptyset$ .

**EXERCISE 1.200.** For each  $c \in L_1$ , the map  $E_c(z) = ce^z$  has an attracting fixed point with a corresponding multiplier  $\lambda(c)$  (see Figure 1.27). Thus we have a multiplier map  $\lambda : L_1 \rightarrow \Delta(0, 1)$ .

- (a) Find the inverse of the multiplier map.
- (b) Use the inverse of the multiplier map to find the  $c$  value where the 7/13 bulb attaches to the cardioid  $L_1$ . Hint: What kind of fixed point will there be at this  $c$  value.

**EXERCISE 1.201.** Show that orbits under the maps  $S_c(z) = c \sin z$ , and  $C_c(z) = c \cos z$  “escape” to  $\infty$  in the direction of the positive or negative imaginary axis by showing the following.

- (a) Show that  $S_c^n(z) \rightarrow \infty$  if and only if  $|\operatorname{Im} S_c^n(z)| \rightarrow +\infty$ .
- (b) Show that  $C_c^n(z) \rightarrow \infty$  if and only if  $|\operatorname{Im} C_c^n(z)| \rightarrow +\infty$ .

**EXERCISE 1.202.** Show that neither  $S_c(z) = c \sin z$  nor  $C_c(z) = c \cos z$  has a finite asymptotic value by following the steps below.

- (a) Examine  $|\sin(x + iy)|$  to show that if  $S_c$  were to have a finite asymptotic value, then the curve  $\gamma$  (along which  $S_c$  has a finite asymptotic value) would have to be vertically bounded, that is, live in some horizontal strip  $\{|\operatorname{Im} z| \leq M\}$ .
- (b) Show that  $\sin z$  maps the imaginary axis into itself.
- (c) Show that  $\sin z$  maps the vertical line  $\{\pi/2 + iy : y \in \mathbb{R}\}$  into  $[1, +\infty)$ .
- (d) Use the fact that  $\sin z$  is  $2\pi$  periodic along with parts (a), (b) and (c) to show that  $\sin z$  cannot have a finite asymptotic value.
- (e) Show that  $S_c$  cannot have a finite asymptotic value since  $\sin z$  does not.
- (f) Show that  $C_c$  cannot have a finite asymptotic value since  $C_c(z) = S_c(z + \pi/2)$ .

**EXERCISE 1.203.** Trig functions with one critical orbit.

- (a) Explain in what sense  $\{S_c^n(c)\}$  is the only critical orbit of the map  $S_c$ .
- (b) Explain in what sense  $\{C_c^n(c)\}$  is the only critical orbit of the map  $C_c$ .

## Definitions and Properties of the Julia and Fatou sets

EXERCISE 1.204. Let  $a_n$  and  $b_n$  for  $n \geq 0$  be sequences of positive real numbers such that  $1 = a_0 > b_0 > a_1 > b_1 > \dots$  and  $a_n \rightarrow 0$  (which also implies  $b_n \rightarrow 0$ ).

- (a) Construct a strictly increasing function  $g : [0, +\infty) \rightarrow [0, +\infty)$  such that  $g$  is differentiable on  $(0, +\infty)$  and we have  $g(a_n) = a_n$  and  $g(b_n) = b_n$  with  $g'(a_n) = 0$  and  $g'(b_n) = 2$ . Furthermore, construct  $g$  so that  $g$  does not fix any points other than the  $a_n$  and  $b_n$  and 0. Hence each  $a_n$  is a super attracting fixed point of  $g$  and each  $b_n$  is a repelling fixed point of  $g$ . Sketch a graph of such a  $g$  to convince yourself that this can be done. It is not necessary that you produce a formula for this map  $g$ .
- (b) Define a function  $f : \mathbb{C} \rightarrow \mathbb{C}$  given by  $f(re^{i\theta}) = g(r)e^{i\theta}$ . Consider the dynamics of points both on and near the circles  $|z| = a_n$  and  $|z| = b_n$  to see that each “repelling” circle  $|z| = b_n$ , which is fixed by  $f$ , must lie in  $J(f)$ .
- (c) Show that  $0 \in F(f)$ . Hint: Use the fact that  $f(\Delta(0, a_n)) \subseteq \Delta(0, a_n)$  for each  $n \geq 0$ .
- (d) Show that (b) and (c), together with the fact that  $b_n \rightarrow 0$ , implies that 0 is not in the interior of  $F(f)$ .

EXERCISE 1.205. Use the definitions of Fatou and Julia set to prove the statements in Proposition 1.211 parts (a)-(d). Hint: For the complete invariance statements, you can use the fact that, when it is non-constant,  $f$  is an *open map*<sup>34</sup>, i.e., if  $U$  is an open set in the domain of  $f$ , then the image  $f(U)$  is also an open set in  $\overline{\mathbb{C}}$ . For (d), use Montel’s theorem 1.208 and part (c).

EXERCISE 1.206. Show that the set of repelling cycles for the map  $f(z) = z^2$  is dense in  $J(f) = C(0, 1)$  by explicitly solving for the set of  $p$ -periodic points for each  $p \in \mathbb{N}$ .

---

<sup>34</sup>See the Open Mapping Theorem A.22 on page 417.

## 1.A. Appendix - Definitions and Properties of the Julia and Fatou sets

Here we present the formal definitions of the Fatou set and Julia set of a rational or entire map. We also provide the statement of Montel's theorem, a major tool in complex dynamics, along with a proposition stating some of the properties of the Fatou and Julia sets.

Recall that  $\sigma(z, w)$  denotes the spherical distance between the points  $z, w \in \overline{\mathbb{C}}$  (see Appendix Section B.2 on page 421).

**DEFINITION 1.207.** Let  $f$  be a rational or entire map. The Fatou set is the set  $F(f) = \{z \in \overline{\mathbb{C}} : \text{for every } \epsilon > 0 \text{ there exists } \delta > 0 \text{ such that } \sigma(z, w) < \delta \text{ implies } \sigma(f^n(z), f^n(w)) < \epsilon \text{ for all } n \in \mathbb{N}\}$ .

Thus, if  $z \in F(f)$  and  $\epsilon$  is small, then for  $w$  to have an orbit  $\epsilon$ -*similar* to the orbit of  $z$  (by which we mean that corresponding orbit points are never more than  $\epsilon$  apart) we just need to choose  $w$  close enough to  $z$ , i.e., within a distance  $\delta$ . Another way to interpret this definition is to say that  $F(f)$  is the set of points  $z$  such that for any  $\epsilon > 0$  there exists  $\delta > 0$  such that  $f^n(\Delta_\sigma(z, \delta)) \subseteq \Delta_\sigma(f^n(z), \epsilon)$  for all  $n \in \mathbb{N}$ , i.e., a “tiny” neighborhood of  $z$  (of size  $\delta$  measured with the spherical metric) will have an orbit that “stays tiny” (of size no greater than  $\epsilon$  measured with the spherical metric) along the *entire* orbit (see Figure 1.33). The reader should reflect on how this fails to happen with the map  $f(z) = z^2$  for any neighborhood of a point on the unit circle  $C(0, 1)$  and also compare this definition to your own definition given earlier.

A major tool used in dynamics is *Montel's theorem* (see [2], p. 9, where it is stated in terms of the notion of *normal families*), which we state without proof in a setting most easily applied to the dynamics of interest to us here.

**THEOREM 1.208 (Montel's theorem).** Let  $U \subseteq \overline{\mathbb{C}}$  be an open set in the domain set of a rational or entire map  $f$ . If the family of maps  $\{f^n : n \in \mathbb{N}\}$  omits any three given points  $z, w, v \in \overline{\mathbb{C}}$ , i.e.,  $f^n(U) \cap \{z, w, v\} = \emptyset$  for all  $n \in \mathbb{N}$ , then  $U \subseteq F(f)$ . In particular, if  $f(U) \subseteq U$  and  $\overline{\mathbb{C}} \setminus U$  contains three or more points, then  $U \subseteq F(f)$ .

Montel's theorem can be used to make it very quick to show that  $f(z) = z^2$  has  $F(f) = \overline{\mathbb{C}} \setminus C(0, 1) = \Delta(0, 1) \cup (\overline{\mathbb{C}} \setminus \overline{\Delta(0, 1)})$ . Since  $f(\Delta(0, 1)) \subseteq \Delta(0, 1)$ , Montel's theorem gives  $\Delta(0, 1) \subseteq F(f)$ . Similarly, one can show  $\overline{\mathbb{C}} \setminus \overline{\Delta(0, 1)} \subseteq F(f)$ . Also, from our work in Section 1.3.2 or by considering the above definition of Fatou set, we know that  $C(0, 1)$  does not contain any points in the Fatou set  $F(f)$ . Hence, we conclude  $F(f) = \overline{\mathbb{C}} \setminus C(0, 1)$ .

**REMARK 1.209.** Though its proof is too advanced for this text, it is true that if  $f$  is a rational or entire map and  $z_0 \in F(f)$ , then there exists  $r > 0$  such that  $\Delta_\sigma(z_0, r) \subseteq F(f)$ , i.e.,  $F(f)$  is an open set. However, if  $f$  is not rational or entire, then the set  $F(f)$  need not be open. To see this, consider the map  $f(z)$  which is defined to be zero when  $z = x + iy$  with both  $x, y \in \mathbb{Q}$  and  $f(z) = z$  otherwise. In this case



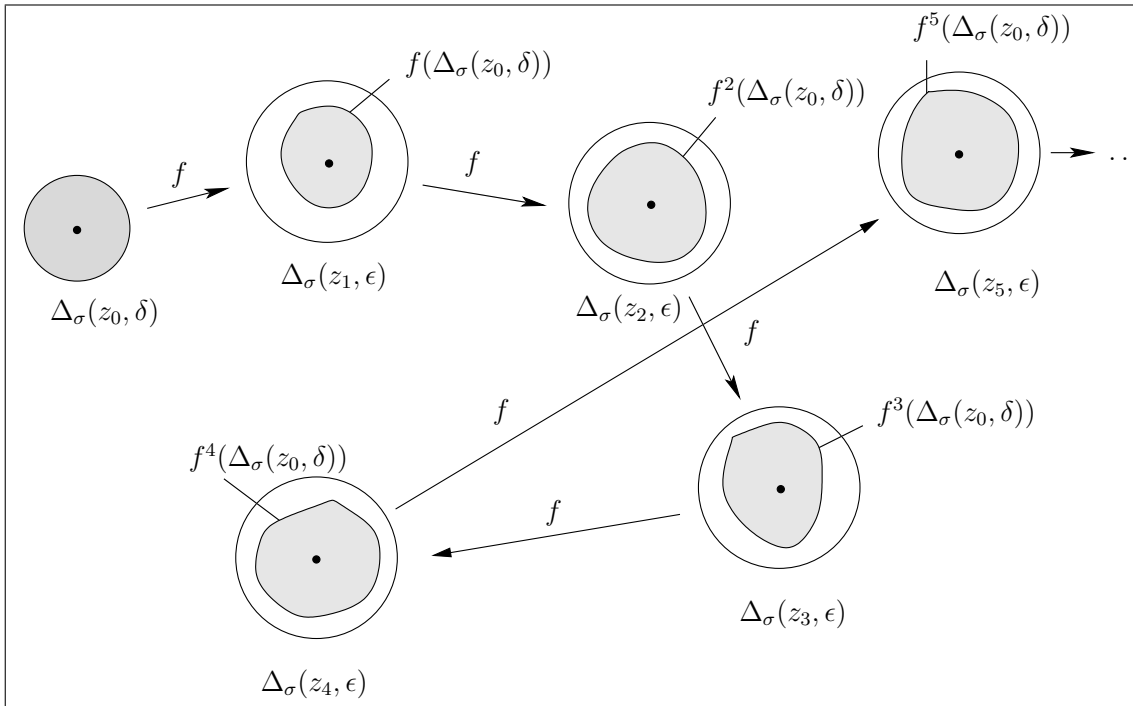


FIGURE 1.33. This picture illustrates how, for a point  $z_0 \in F(f)$ , a tiny neighborhood  $\Delta_\sigma(z_0, \delta)$  has a forward image that stays tiny (within an  $\epsilon$  neighborhood of each orbit point  $z_n$ ) for the entire orbit. We illustrated this up to the fifth iterate, but the reader should take note of the last arrow with the dots indicating that this happens for *all* iterates  $f^n$ .

$f^n = f$  for all  $n \in \mathbb{N}$  and  $F(f) = \{0\}$ . See also Additional Exercise 1.204 for such an example where  $f$  is continuous (but not analytic).

DEFINITION 1.210. The Julia set of a rational or entire map  $f$  is defined to be

$$J(f) = \overline{\mathbb{C}} \setminus F(f).$$

Hence, for a point  $z$  to be in  $J(f)$  there must be points  $w$  which are arbitrarily close to  $z$ , but which fail to have orbits similar to the orbit of  $z$ . More precisely, for a point  $z$  to be in  $J(f)$  there must be some  $\epsilon > 0$  such that for every  $\delta > 0$ , there exists a point  $w$  within a distance  $\delta$  of  $z$  such that the orbit of  $w$  is NOT  $\epsilon$ -similar to the orbit of  $z$ .

Directly from the definitions and discussion above one can show the following properties (a)-(d) (see Additional Exercise 1.205). Properties (e) and (f), however, requires some tools from complex analysis which are a bit beyond the level of this text (see [1], p. 148, and [24], p. 38).

PROPOSITION 1.211 (Properties of the Julia and Fatou sets). Let  $f$  be a rational or entire map. Then we have the following:

- (a)  $F(f)$  is an open set in  $\overline{\mathbb{C}}$  and thus  $J(f)$  is a closed set in  $\overline{\mathbb{C}}$ .
- (b)  $F(f)$  is completely invariant, i.e., if  $f(F(f)) \subseteq F(f)$  and  $f^{-1}(F(f)) \subseteq F(f)$ .
- (c)  $J(f)$  is completely invariant, i.e., if  $f(J(f)) \subseteq J(f)$  and  $f^{-1}(J(f)) \subseteq J(f)$ .
- (d)  $J(f)$  contains an open set if and only if  $J(f) = \overline{\mathbb{C}}$ .
- (e) The set of repelling periodic cycles of  $f$  is dense in  $J(f)$ . That is, each repelling periodic cycle of  $f$  is in  $J(f)$  and for every open set  $U$  which intersects  $J(f)$ , there is a repelling periodic point  $z$  which lies in  $U$ .
- (f) Let  $A$  be the set of  $z$  in  $J(f)$  such that the orbit of  $z$  is *dense* in  $J(f)$  (i.e., for every open set  $U$  which intersects  $J(f)$ , there is an orbit point  $z_n$  which lies in  $U$ ). Then  $A$  is *dense* in  $J(f)$  (i.e., for every open set  $V$  which intersects  $J(f)$ , there is a point  $z \in A$  which lies in  $V$ ).

REMARK 1.212. Additional Exercises 1.206 and 1.171 illustrate properties (e) and (f) explicitly for the map  $f(z) = z^2$ . Reflecting for a moment, we see, both in the  $f(z) = z^2$  example and in general, the Julia set contains a dense set of points which in some sense are the ultimate in regular behavior. These are the periodic points - nothing could be more regular and predictable than to have the orbit follow the same finite set of points over and over again. However, the Julia set also contains points with a dense orbit in  $J(f)$  which means that it never settles into any type of regularity. Thus we see that inside the sensitive dependence which defines chaos (and thus defines the Julia set  $J(f)$ ) there lies a strange interwoven mix of regularity and unpredictability.

## 1.B. Appendix - Global Conjugation and Möbius map dynamics

In this appendix we show that global conjugation (see Section 1.2.6) can be used to quickly classify and understand the dynamics of any Möbius map, i.e., a map of the form  $f(z) = \frac{az+b}{cz+d}$  where  $ad - bc \neq 0$ . The classification depends on the number and type of fixed points of  $f$  and so we begin with the following proposition.

PROPOSITION 1.213. Non identity Möbius maps can only have exactly one or exactly two fixed points in  $\overline{\mathbb{C}}$ .

PROOF. Let  $f(z) = \frac{az+b}{cz+d}$  be a non identity Möbius map. First suppose that  $f(\infty) \neq \infty$ , i.e.,  $c \neq 0$ . Solving for fixed points of  $f$ , i.e., solving the equation  $f(z) = z$ , yields the equation  $cz^2 + (d-a)z - b = 0$ , which has two distinct roots or one double root in  $\mathbb{C}$ . If  $c = 0$ , then  $f$  is a linear map which must have one fixed point at  $\infty$  and possibly a second fixed point in  $\mathbb{C}$ .  $\square$

We now describe the dynamics of a non identity Möbius map  $f$  based on how many fixed points it has.

**Case 1: Suppose  $f(z)$  fixes only  $\infty$ .** Then one can quickly show that  $f$  has the form  $f(z) = z + \beta$  for some  $\beta \in \mathbb{C} \setminus \{0\}$ . Thus  $f^n(z) = z + n\beta$ , and hence  $f^n(z) \rightarrow \infty$

as  $n \rightarrow \infty$  for all  $z \in \overline{\mathbb{C}}$  much in the same way as Example 1.50. We also see that  $J(f) = \{\infty\}$  in this case.

**Case 2: Suppose  $f(z)$  fixes only  $w \in \mathbb{C}$ .** Let  $\psi(z) = \frac{1}{z-w}$  and define  $g(z) = \psi f \psi^{-1}(z)$ , noting that  $g$  is also Möbius. Furthermore, the map  $g(z)$  has only one fixed point at  $\infty$  (see Exercise 1.30). So from Case 1 we see that  $g(z) = z + \alpha$  for some  $\alpha \in \mathbb{C} \setminus \{0\}$  and  $g^n(z) \rightarrow \infty$  for all  $z \in \overline{\mathbb{C}}$ . Hence  $f^n(z) = \psi^{-1} g^n \psi(z) \rightarrow \psi^{-1}(\infty) = w$  for all  $z \in \overline{\mathbb{C}}$ . So, if  $f$  is Möbius with unique fixed point  $w$ , then  $f^n(z) \rightarrow w$  for all  $z \in \overline{\mathbb{C}}$  and  $J(f) = \{w\}$ .

**Case 3: Suppose that  $f$  fixes 0 and  $\infty$ .**

Then  $f(z) = kz$  for some  $k \in \mathbb{C} \setminus \{1\}$  (verify) and thus  $f^n(z) = k^n z$ . We now have the following categories based on  $|k|$ .

- (1) If  $|k| < 1$ , then  $f^n(z) \rightarrow 0$  for all  $z \in \overline{\mathbb{C}} \setminus \{\infty\}$  and  $J(f) = \{\infty\}$ .
- (2) If  $|k| > 1$ , then  $f^n(z) \rightarrow \infty$  for all  $z \in \overline{\mathbb{C}} \setminus \{0\}$  and  $J(f) = \{0\}$ .
- (3) If  $|k| = 1$ , then  $f$  is simply a rotation  $z \mapsto e^{i\theta} z$  for some  $\theta \in (0, 2\pi)$  whose dynamics are easy to understand. In particular,  $F(f) = \overline{\mathbb{C}}$ .

**Case 4: Suppose that  $f$  fixes  $w_1$  and  $w_2$  where  $w_1 \neq w_2$ .** Defining  $\psi(z) = \frac{z-w_1}{z-w_2}$  and setting  $g(z) = \psi f \psi^{-1}(z)$ , we see that  $g$  falls into Case 3. As in Case 2, we can now understand the dynamics of  $f$  as a change of coordinates of the simple dynamics of  $g$  by noting that  $f^n(z) = \psi^{-1} g^n \psi(z)$ . In particular, we have one of the following:

- (1)  $f^n(z) \rightarrow w_1$  for all  $z \in \overline{\mathbb{C}} \setminus \{w_2\}$  and  $J(f) = \{w_2\}$ .
- (2)  $f^n(z) \rightarrow w_2$  for all  $z \in \overline{\mathbb{C}} \setminus \{w_1\}$  and  $J(f) = \{w_1\}$ .
- (3)  $f$  is conjugate to a rotation  $z \mapsto e^{i\theta} z$  for some  $\theta \in (0, 2\pi)$ , and thus  $F(f) = \overline{\mathbb{C}}$ .

REMARK 1.214. In Cases 2 and 4, we see that the Möbius map  $\psi(z)$  was used to move the fixed points of  $f$  to more convenient locations so that the simple dynamics of Cases 1 and 3 could be related to the dynamics of  $f$ . This is one of the great advantages to using global conjugation; it allows us to reposition special points in more convenient places before we do our analysis. Not only can this technique be used to simplify the analysis of Möbius map dynamics, but we can also use it with higher degree maps as well. See Section 1.2.7 where a conjugation of the Newton map of a quadratic function greatly simplifies the analysis. Also see Additional Exercises 1.165–1.168.

### 1.C. Appendix - Code for drawing random dynamics pictures

Because of its complexity, the following computationally heavy algorithm is not well suited for an applet. However, we provide the code for Matlab, which one could use to quickly generate pictures like the Devil's Colosseum in Figure 1.31. These four files `main.m`, `f.m`, `g.m`, and `proced2.m` need to be created separately, but stored in the same folder. When `main.m` is compiled using Matlab, a picture will be generated.

```

% ***** This begins the file main.m *****
% This file requires the files (functions) g.m, f.m, and proced2.m to be
% in the same folder when this file is compiled. Upon compilation
% this file will generate a graph of the probability that a random orbit
% generated by the maps f and g will escape to infinity.

h = 0.1; % Determines step size in mesh of points to be plotted
Maxd = 10; % Determines how many random steps can be taken

cntx = 0; % Counter for x coordinate
clear x1;
for x = -5:h:5
    cntx = cntx + 1;
    cnty = 0; % Counter for y coordinate
    clear y1;
    for y = -5:h:5
        cnty = cnty + 1;
        n = 0;
        x1(cntx) = x;
        y1(cnty) = y;
        [z(cntx,cnty), n] = proced2(x, y, 1, n, Maxd);
    end
end

% % Uncomment the following lines to export/save data sets containing
% % the x(i) coordinates, y(j) coordinates, and z(i,j) values which
% % when plotted make up the graph. These data sets can then be imported
% % into another application (such as Maple or Mathematica) and plotted and
% % otherwise manipulated there.
%
% save DevilDataX3.dat x1 -ASCII;
% save DevilDataY3.dat y1 -ASCII;
% save DevilDataZ3.dat z -ASCII;

figure
surfc(x1, y1, z)
lighting phong
shading interp %flat %interp

clear;
% ***** This ends the file main.m *****

```

```

% ***** This begins the file f.m *****
function z = f(x,y)
z1 = [x*x-y*y-1,2*x*y];
z = [z1(1)*z1(1)-z1(2)*z1(2)-1,2*z1(1)*z1(2)];
% ***** This ends the file f.m *****

% ***** This begins the file g.m *****
function z = g(x,y)
z1 = [(x*x-y*y)/4,x*y/2];
z = [(z1(1)*z1(1)-z1(2)*z1(2))/4,z1(1)*z1(2)/2];
% ***** This ends the file g.m *****

% ***** This begins the file proced2.m *****
% This recursively defined procedure/function will compute the value
% s which for proced2(x, y, 1, n, Maxd) (here I used q=1) represents the
% probability that the point (x,y) will have a random orbit
% escape (have modulus > K) in the first M steps of the orbit.

function [s, n] = proced2(x, y, q, n0, M)
n = n0 + 1;
p = 0.5; % Probability that map f is chosen at each step
K = 10; % Escape radius for random orbit
s = 0.0;
z=f(x,y); % file f.m must be in folder next to this file
w=g(x,y); % file g.m must be in folder next to this file

if n < M % M is the max number of recursion steps allowed
    if z(1)*z(1)+z(2)*z(2) > K*K
        s = s + p*q;
    else
        [d, n] = proced2(z(1), z(2), p*q, n, M);
        s = s + d;
    end

    if w(1)*w(1)+w(2)*w(2) > K*K
        s = s + (1-p)*q;
    else
        [d, n] = proced2(w(1), w(2), (1-p)*q, n, M);
        s = s + d;
    end
end
end
% ***** This ends the file proced2.m *****

```



## Bibliography

- [1] Alan F. Beardon. *Iterations of Rational Functions*. Springer-Verlag, New York, 1991.
- [2] Lennart Carleson and Theodore W. Gamelin. *Complex Dynamics*. Springer-Verlag, New York, 1993.
- [3] Ruel V. Churchill and James Ward Brown. *Complex variables and applications*. McGraw-Hill Book Co., New York, eighth edition, 2009.
- [4] M. Viana da Silva. The differentiability of the hairs of  $\exp(Z)$ . *Proc. Amer. Math. Soc.*, 103(4):1179–1184, 1988.
- [5] R. L. Devaney. Complex exponential dynamics. To appear in Volume 3 of the Handbook of Dynamical Systems.
- [6] R. L. Devaney and M. Moreno Rocha. Geometry of the antennas in the Mandelbrot set. *Fractals*, 10(1):39–46, 2002.
- [7] Robert L. Devaney. *A first course in chaotic dynamical systems*. Addison-Wesley Studies in Non-linearity. Addison-Wesley Publishing Company Advanced Book Program, Reading, MA, 1992. Theory and experiment, With a separately available computer disk.
- [8] Robert L. Devaney. A survey of exponential dynamics. In *Proceedings of the Sixth International Conference on Difference Equations*, pages 105–122, Boca Raton, FL, 2004. CRC.
- [9] Robert L. Devaney and Linda Keen, editors. *Chaos and fractals*, volume 39 of *Proceedings of Symposia in Applied Mathematics*. American Mathematical Society, Providence, RI, 1989. The mathematics behind the computer graphics, Lecture notes prepared for the American Mathematical Society Short Course held in Providence, Rhode Island, August 6–7, 1988, AMS Short Course Lecture Notes.
- [10] Marilyn B. Durkin. The accuracy of computer algorithms in dynamical systems. *Internat. J. Bifur. Chaos Appl. Sci. Engrg.*, 1(3):625–639, 1991.
- [11] K. Falconer. *Fractal geometry - Mathematical Foundations and Applications*. John Wiley & Sons, Chichester, 1990.
- [12] P. Fatou. Sur les équations fonctionnelles. *Bull. Soc. Math. France*, 47:161–271, 1919.
- [13] P. Fatou. Sur les équations fonctionnelles. *Bull. Soc. Math. France*, 48:208–314, 1920.
- [14] P. Fatou. Sur les équations fonctionnelles. *Bull. Soc. Math. France*, 48:33–94, 1920.
- [15] James Gleick. *Chaos*. Penguin Books, New York, 1987. Making a new science.
- [16] John G. Hocking and Gail S. Young. *Topology*. Dover Publications Inc., New York, second edition, 1988.
- [17] Gaston Julia. Mémoire sur l’itération des fonctions rationnelles. *Journal de Math. Pure et Appl.*, pages 47–245, 1918.
- [18] Bogusława Karpińska. Area and Hausdorff dimension of the set of accessible points of the Julia sets of  $\lambda e^z$  and  $\lambda \sin z$ . *Fund. Math.*, 159(3):269–287, 1999.
- [19] Bogusława Karpińska. Hausdorff dimension of the hairs without endpoints for  $\lambda \exp z$ . *C. R. Acad. Sci. Paris Sér. I Math.*, 328(11):1039–1044, 1999.

- [20] Tan Lei. *Ressemblance eintre l'ensemble de Mandelbrot set l'ensemble de Julia au voisinage d'un point de Misiurewicz*, pages 139–152. in Étude dynamique des polynômes complexes. Partie II by A. Douady and J. H. Hubbard.
- [21] John C. Mayer. An explosion point for the set of endpoints of the Julia set of  $\lambda \exp(z)$ . *Ergodic Theory Dynam. Systems*, 10(1):177–183, 1990.
- [22] Curtis T. McMullen. The Mandelbrot set is universal. In *The Mandelbrot set, theme and variations*, volume 274 of *London Math. Soc. Lecture Note Ser.*, pages 1–17. Cambridge Univ. Press, Cambridge, 2000.
- [23] Rich Stankewitz, W. Conatser, T. Butz, B. Dean, Y. Li, and K. Hart. *JULIA 2.0 Fractal Drawing Program*. <http://www.bsu.edu/web/rstankewitz/JuliaHelp2.0/Julia.html>.
- [24] Norbert Steinmetz. *Rational iteration*, volume 16 of *de Gruyter Studies in Mathematics*. Walter de Gruyter & Co., Berlin, 1993. Complex analytic dynamical systems.
- [25] Hiroki Sumi. Random complex dynamics and semigroups of holomorphic maps. *Proc. London. Math. Soc.* 102 (1), 50–112, 2011.